MOLECULAR ORBITAL CALCULATIONS

(on dinitrogen tetroxide and related species)

A thesis presented for the degree of
Doctor of Philosophy in Chemistry
in the University of Canterbury,
Christchurch, New Zealand.

by

R.L. Griffiths

1973

ACKNOWLEDGEMENTS

I should like to thank my supervisor, Professor L.F. Phillips, for his encouragement, interest and guidance throughout the course of this work. I am grateful to Dr R.G.A.R. Maclagan for his helpful suggestions and frequent discussions during the last year.

Special thanks are due to Professor R.D. Brown of Monash University for providing me with the opportunity of spending five weeks in his department, and to the members of his theoretical group, particularly Dr G.R.J. Williams, for making available computer listings of several basic programs.

I wish to thank Mr P.B. Morgan for setting up one of these programs and the staff of the University of Canterbury Computer Centre for their cooperation and help. I am grateful to my parents for giving me the opportunity to pursue this course of study.

I am indebted to I.C.I. (N.Z.) Ltd, for the provision of a research fellowship.

- R.L. Griffiths
March, 1973

CONTENTS

	Page
Acknowledgements	i
List of Figures	v
Introduction and Summary	1
CHAPTER ONE. Molecular Orbital Theory	8
1.1 Introduction	8
1.2 Molecular Orbital Theory for Closed Shell Molecules	8
1.3 Configuration Interaction	15
1.4 The Simplified Ab Initio Method	17
1.5 The Multi-Gaussian Expansion Method	19
1.6 Comparison of the Methods	20
CHAPTER TWO. Review of Nitrogen Dioxide and Dinitrogen Tetroxide	22
2.1 The Structure of Nitrogen Dioxide	22
2.2 An Orbital Correlation Diagram for Nitrogen Dioxide	22
2.3 Qualitative and Semi-Empirical Descriptions of the Bonding in Nitrogen Dioxide	25
2.4 Ab Initio Calculations on Nitrogen Dioxide	30
2.5 The Structure of Dinitrogen Tetroxide	32
2.6 Descriptions of the Bonding in Dinitrogen Tetroxide	36
2.7 Variable Electronegativity SCF Studies of Dinitrogen Tetroxide	42
2.8 The Increased Valence Formula for Dinitrogen Tetroxide	47

Page

CHAPTER THREE. Application of Molecular Orbital Theory to Moderately Large Systems 49

3.1 General Considerations 49

3.2 Construction of a Symmetry Basis 50

3.3 Use of Symmetry in the Calculation of Repulsion Integrals by Gaussian Expansion 54

3.4 Alternative Methods of Solving the SCF Equations 57

3.5 The Method of Steepest Descent 58

3.6 The Method of Conjugate Gradients 60

3.7 Comparison of the Methods 62

CHAPTER FOUR. Open Shell Methods 65

4.1 Introduction 65

4.2 McWeeny's Formulation of the Open Shell Method 66

4.3 Choice of Eigenvectors in the Open Shell Method 69

4.4 Extrapolation Methods 71

4.5 The Unrestricted Hartree-Fock Method 73

CHAPTER FIVE. Interpretation of Calculated Wave Functions 76

5.1 Uncertainties in the Wave Function 76

5.2 Electron Population Analyses 78

5.3 Electron Density Maps 80

5.4 Localized Orbitals 81

5.5 Bond Energy Analysis 84

CHAPTER SIX. Results of Calculations 86

6.1 Introduction 86

6.2 Comparison of the Multi-Gaussian Expansion and Simplified Ab Initio Methods for the Nitrite Ion 88

6.3 Restricted and Unrestricted Hartree-Fock-Roothaan Calculations on Nitrogen Dioxide 93

Page

6.4 The SAI Wave Function for Dinitrogen Tetroxide 98

6.5 The 2G/S Wave Function for Dinitrogen Tetroxide 104

6.6 Comparison of Dinitrogen Tetroxide with Smaller Systems 114

6.7 Comment on the "Pi-Only" Model for N_2O_4 121

6.8 Conclusions 122

APPENDIX I: Character Tables for Point Groups C_{2v} and D_{2h} 126

APPENDIX II: Geometries 127

APPENDIX III: Symmetry Orbitals 130

APPENDIX IV: The Method of Conjugate Gradients 134

APPENDIX V: Localized Orbitals 146

APPENDIX VI: Computer Programs 149

APPENDIX VII: 2G/S Wave Function for N_2O_4 Φ_1 154

2G/S Wave Function for NO_2 $^2A_1$ (N_2O_4 Geometry) 159

REFERENCES 161

LIST OF FIGURES

		Facing Page
2.1	Nitrogen Dioxide	22
2.2	NO_2 Correlation Diagram	22
2.3	Dinitrogen Tetroxide	32
2.4	$ONONO_2$	32
2.5	N_2O_4	32
2.6	N_2O_4	32
2.7	N_2O_4 structures	38
6.1	Sigma density, NO_2, SAI	102
6.2	Sigma density, N_2O_4, SAI	102
6.3	Sigma difference map, SAI	103
6.4	Pi difference map, SAI	103
6.5	NO_2-N_2O_4 Correlation Diagram	104
6.6	Sigma density, NO_2, 2G/S	111
6.7	Sigma density, N_2O_4, 2G/S	111
6.8	Sigma difference map, 2G/S	111
6.9	Pi difference map, 2G/S	111
6.10	Overlap-Bond Energy graph	117
6.11	Localized orbital, HNO	119
6.12	Localized orbital, HNO	119
6.13	Localized orbital, N_2O	119
6.14	Localized orbital, N_2O	119
6.15	Localized orbital, NO_2	120
6.16	Localized orbital, NO_2	120
6.17	Sigma localized orbitals, N_2O_4	121

INTRODUCTION AND SUMMARY

The rapid increase over the last few years in the application of theoretical methods to the study of chemical problems is well known. Although new numerical techniques are being developed and theoretical advances are slowly being made, the major cause of this expansion is a continuing series of improvements in the speed and memory capabilities of digital computers. These advances, as well as improving the accuracy of wavefunctions calculated for small molecules, permit the application of well-established methods to larger molecular systems. Molecular orbital methods which do not use any experimental parameters other than molecular geometry are usually referred to as ab initio methods. This thesis is mainly concerned with the application of two such methods, which incorporate different approximations, to a study of the molecule dinitrogen tetroxide, N_2O_4.

Chapter One outlines the molecular orbital theory necessary for an understanding of these two methods. Most of the calculations were ultimately done using the second method, known as the Multi-Gaussian Expansion technique.

In Chapter Two the structure and bonding of N_2O_4 and of nitrogen dioxide, NO_2, the monomer into which N_2O_4 readily dissociates, are reviewed. Particular emphasis is given to the results of previous molecular orbital calculations on these molecules. An understanding of the nature of the N-N bonding in N_2O_4 is a long-sought goal. The most stable isomer has a planar structure in which the two nitrogen dioxide moieties are joined by a N-N bond that is very much longer than

the normal N-N single bond, such as occurs, for example, in hydrazine, N_2H_4. If O-O interactions were responsible for the long bond the molecule might be expected to adopt a staggered rather than a planar structure. The geometry of the NO_2 moiety is also remarkably similar to that in free NO_2.

Several explanations for these features have been advanced, and the N-N bond has been variously described as (i) a normal sigma bond plus partial pi bond; (ii) a "pi-only" bond in which there is no sigma bond at all between the nitrogen atoms; (iii) a "splayed" single bond which, although of sigma type, requires the molecule to be planar in order to achieve maximum overlap; (iv) a charge transfer configuration; (v) a sigma bond weakened by delocalization of oxygen lone pair electrons into a N-N antibonding orbital with a little pi bonding to account for planarity; and (vi) a normal sigma bond plus a partial pi bond with destabilization coming from 2p orbitals on the nitrogen atoms. These theories were based on calculations which did not include all of the electrons in the molecule and which were semi-empirical to the extent that some experimental parameters were required. To the author's knowledge the calculation described here represents the first non-empirical all-electron treatment of N_2O_4. A brief discussion is given of a type of increased valence formula which may be applied to systems having four electrons in three overlapping atomic orbitals on three atoms. When N_2O_4 is described in terms of these formulae the weak N-N bond results from the fact that the molecule is represented by a resonance between several valence bond structures, some of which lack an N-N bond. In particular, this approach suggests that stability should arise

from reduced net charges on the nitrogen atoms, three centre O-N-N interactions, and long range interactions between the nitrogen atom of one moiety and the oxygen atoms of the other moiety. These suggestions are qualitatively consistent with the present results.

Several problems arose in the application to N_2O_4 of the original versions of the computer programs embodying the methods of Chapter One. These problems are discussed in Chapter Three. Because all forty-six electrons were considered the amount of computer time required for the calculations was very much greater than for smaller systems. The equations must be solved by an iterative procedure, which normally involves the diagonalization of a matrix to find its eigenvalues and eigenvectors. For a large matrix, especially if some of these eigenvalues are very close together, this procedure is a primary source of truncation errors which build up on each iteration. Alternative methods were therefore sought for solving the equations of Chapter One. Most successful of these was a direct minimization procedure called the conjugate gradients method. A much improved rate of convergence to the solution was obtained when this method was used in conjunction with the matrix diagonalization method.

Another major improvement was brought about by making maximum use of the molecule's symmetry. In the approximate molecular orbital theory used here the overall wavefunction is an antisymmetrized product of molecular orbitals, each of which is expressed as a linear combination of basis functions located on the atoms. In exploiting the molecule's symmetry these basis functions are initially combined into symmetry orbitals, whose use in the final iterative procedure results

in less trouble from rounding errors. The effect is that the 30 x 30 matrix which is to be diagonalized is transformed to block diagonal form, each smaller block of which can be diagonalized separately. A further advantage of this method is that it facilitates the selection of the particular electronic state for which the wave function is to be calculated. For the multi-Gaussian expansion method a large number of integrals need to be calculated. Because of the high symmetry of N_2O_4 many small groups of these are equal in magnitude and therefore only one member of each group needs to be calculated. This leads to a drastic reduction in computer time. The method used for organizing the selection and storage of these integrals is discussed in Section 3.3. It should be mentioned here that because dinitrogen trioxide, N_2O_3, for which a similar type of weak N-N bonding has been suggested, has much less symmetry a similar calculation would be correspondingly more difficult.

In order to compare the N_2O_4 wave function with that of its monomer, calculations to the same levels of approximation were required for nitrogen dioxide. Because this species has an unpaired electron the methods of Chapter One are not suitable and wavefunctions were obtained by the two different methods which are described in Chapter Four. Convergence difficulties with these methods are well known. It has been suggested that these result from incorrect choice of eigenvectors on each iteration. This problem was investigated, and a suitable method of choosing the eigenvectors was incorporated into the computer program.

Once wave functions had been obtained it became necessary to interpret them. Methods for doing this are discussed in

Chapter Five. The Mulliken population analysis partitions the density into various atom populations and overlap populations between atoms. The magnitude and sign of this overlap give an indication of the amount of bonding between two atoms. A recently proposed bond energy analysis was also employed. This partitions the total energy of the molecule into contributions from single atoms and from groups of two, three and four atoms. An excellent correlation was found between the two-centre bond energies thus calculated and the Mulliken overlap populations. The population analysis is, however, sensitive to the choice of basis functions. A more complete description of the electron density distribution is therefore obtained from contour plots through various planes in the molecule. For the wave functions computed by the methods of Chapter One the molecular orbitals are not unique, in that particular kinds of transformations of the functions amongst themselves leave the total wavefunction unchanged. One form of transformation leads to localized orbitals which more closely resemble traditional chemical ideas of bonds, inner shells and lone pairs. The method used for this localization is discussed in Section 5.4 and Appendix V.

The results of the calculations are given and discussed in Chapter Six. Results for the nitrite ion, NO_2^-, obtained by the methods of Chapter One are compared with those of an exact ab initio calculation with the same basis functions and molecular geometry, taken from the literature. When the multi-Gaussian expansion wave function for N_2O_4 was examined the following features were apparent. In comparison with NO_2 and its ions NO_2^+ and NO_2^-, all covalent bonding was reduced. The

results indicated that the weakness of the N-N bond was due to the fact that the N-N antibonding orbital was filled and the expected N-N sigma bonding orbital was unoccupied. The major interpretive problem was therefore to understand why the molecule was stable at all since there was very little N-N pi bonding. From the bond energy analysis the stability of this state was found to be due to a lowering of the energy associated with the electrons close to the N atoms, long range N-O interactions, and surprisingly large and negative three centre O-N-N energies. As noted above these three features are important in the increased valence description of N_2O_4. An investigation of the rotational barrier was not attempted because this would require the calculation of a wave function at the perpendicular configuration. This has lower symmetry and in addition to problems from rounding errors would require a much greater amount of computer time to calculate the larger number of unique integrals. Reported calculations with similar size basis sets have produced results for rotational barrier values which are not very good estimates.

Throughout most of this thesis distances are given in atomic units (Bohr radii). For comparison with literature values, however, in Chapter Two distances are given in nanometers.

$$1 \text{ a.u. of length} = 5.29167 \times 10^{-11} \text{ m}$$

Energies are given either in atomic units (Hartrees) or in the SI units of kilojoules per mole:

$$1 \text{ a.u. of energy} = 1 \text{ Hartree}$$
$$= 27.2107 \text{ eV}$$

where 1 eV per particle = 23.061 kcal $mole^{-1}$

= 96.487 kJ $mole^{-1}$.

These values are taken from the tables of Cohen & Du Mond[1]. In the equations all expressions for operators are in corresponding atomic units.

CHAPTER ONE

MOLECULAR ORBITAL THEORY

1.1 Introduction

Recent progress in theoretical chemistry has been well reviewed by many authors[2-7]. The following account will therefore be restricted to a basic description of the molecular orbital (MO) method and to an explanation of the particular methods used in making the calculations described in this thesis. Two methods of differing degrees of approximation were used in the study of dinitrogen tetroxide. Both have been described fully by Williams[8]. Because no experimental parameters apart from molecular geometries are used the methods are usually said to be of ab initio type. Some of the electron repulsion integrals, however, are either neglected or calculated approximately and as noted by Duke[7] the calculated wavefunction therefore does not necessarily satisfy the variation principle[9]. That is to say, it may produce an energy lower than that of an exact, non-empirical calculation. We distinguish the two methods of Williams[8] as the simplified ab initio method, SAI, and the multi-Gaussian expansion method, MGE.

1.2 Molecular Orbital Theory for Closed Shell Molecules

In molecular quantum mechanics the stationary states of the molecular system are described by wave functions obtained as solutions of the time independent Schrödinger equation[10]

$$\hat{H}\,\Psi = E\,\Psi \qquad (1.1)$$

From the wavefunction, Ψ, the electronic structure and properties can in principle be derived. The quantity Ψ is strictly a function of both the electronic and nuclear coordinates. In the Born-Oppenheimer approximation[11] the nuclei are assumed to be fixed point charges, the nuclear and electronic motions are separated, and Ψ becomes a function of electronic coordinates only, the detailed nature of Ψ being dependent on the particular choice of nuclear coordinates. If all interactions which do not arise from purely electrostatic forces are neglected, the electronic Hamiltonian operator, $\hat{H}$, is given in atomic units by

$$\hat{H} = -\tfrac{1}{2} \sum_{i} \nabla^2(i) - \sum_{i,a} \frac{Z_a}{r_{ia}} + \sum_{i>j} \frac{1}{r_{ij}} \qquad (1.2)$$

where Z_a is the charge on nucleus a, r_{ia} is the separation of nucleus a and electron i, r_{ij} the separation of electrons i and j, and $\nabla^2(i)$ the Laplacian operator for electron i. The first term of Equation 1.2 is the kinetic energy operator, the second is the electron-nuclear attraction operator, and the last term is the electron-electron repulsion operator. In the Born-Oppenheimer approximation E in equation (1.1) is the electronic energy corresponding to the state Ψ. The total energy of the molecule is found by adding to E the nuclear repulsion energy, given by $\sum_{a>b} \frac{Z_a Z_b}{r_{ab}}$, where r_{ab} is the separation of nuclei a and b.

In MO theory each electron is assigned to a one-electron spin orbital, ψ_i, delocalized over the whole molecule. The total electronic wave function Ψ may then be approximated as an antisymmetrized product of these N one-electron wave functions. The antisymmetrized product is conveniently written

as a Slater determinant[12]

$$\Psi = (N!)^{-\frac{1}{2}} \begin{vmatrix} \psi_1(1) & \cdots & \psi_N(1) \\ \cdot & & \cdot \\ \cdot & & \cdot \\ \cdot & & \cdot \\ \psi_1(N) & & \psi_N(N) \end{vmatrix} \tag{1.3}$$

$$= (N!)^{-\frac{1}{2}} \det|\psi_1 \ \psi_2 \ \cdots \ \psi_N|$$

where the numbers in parentheses label the N electrons. In this form Ψ satisfies the Pauli principle[13], since it changes sign when two electrons are interchanged; this corresponds to interchanging two rows of the determinant.

Each one-electron molecular spin orbital ψ is composed of a spatial factor ϕ, describing the electron's space coordinates, and a spin factor η. Thus

$$\psi_i(1) = \phi_j(1) \ \eta_k(1). \tag{1.4}$$

Closed shell systems are distinguished by the property that each spatial factor ϕ_j appears twice, once with α spin, ϕ_j, and once with β spin, $\bar{\phi}_j$. In this thesis all ϕ_j are assumed to be real. For a closed shell system the wave function can therefore be written as

$$\Psi = (N!)^{-\frac{1}{2}} \det|\phi_1 \ \bar{\phi}_1 \ \phi_2 \ \cdots \ \phi_{N/2} \ \bar{\phi}_{N/2}|. \tag{1.5}$$

The energy of the state Ψ is given by[14]

$$E = \langle\Psi|\hat{H}|\Psi\rangle$$

$$= 2 \sum_{i}^{N/2} H_i + \sum_{i,j}^{N/2} (2J_{ij} - K_{ij}) \tag{1.6}$$

where $H_i = \langle \phi_i | H | \phi_i \rangle$

$$= \int \phi_i(1)\ H(1)\ \phi_i(1)\ dv_1 \tag{1.7}$$

with the one-electron or "core" Hamiltonian operator given by

$$H(1) = -\tfrac{1}{2}\nabla^2(1) - \sum_a \frac{Z_a}{r_{1a}} \tag{1.8}$$

The Coulomb integrals, J, are given by

$$J_{ij} = \langle \phi_i \phi_j | g | \phi_i \phi_j \rangle \tag{1.9}$$

where

$$\langle \phi_i \phi_k | g | \phi_j \phi_\ell \rangle = \iint \frac{\phi_i(1)\phi_k(2)\phi_j(1)\phi_\ell(2)}{r_{12}}\, dv_1 dv_2 \tag{1.10}$$

and the exchange integrals, K, by

$$K_{ij} = \langle \phi_i \phi_j | g | \phi_j \phi_i \rangle. \tag{1.11}$$

[This notation for the two electron integrals is adhered to throughout this thesis[14]. Here $g = \frac{1}{r_{12}}$. An alternative notation commonly found in the literature is the (11|22) notation given by

$$(\phi_i \phi_j | \phi_k \phi_\ell) = \langle \phi_i \phi_k | g | \phi_j \phi_\ell \rangle. \ ] \tag{1.12}$$

Equation 1.1 is solved in principle by varying the MO's ϕ_i in order to minimize the energy in accordance with the variation principle[9]. The MO's are conveniently taken to form an orthonormal set so that

$$\langle \phi_i | \phi_j \rangle = \int \phi_i(1)\phi_j(1) dv_1$$

$$= \delta_{ij}, \text{ the Kronecker delta} \tag{1.13}$$

and the minimization is performed subject to these constraints. The Hartree-Fock wave function[15,16] is the best possible single-determinant wave function so obtained. In the Unrestricted Hartree-Fock method, which is described more fully in Section 4.5, the MO's corresponding to different spins do not have to have the same spatial factors. The method described above for closed shells does not necessarily produce an absolute minimum in the energy when the restriction of equal spatial factors for opposite spins is removed[17].

Because solution of the Hartree-Fock equations is exceedingly difficult except for the simplest of systems, a further approximation was introduced by Roothaan[18]. In this approximation each MO is expanded as a linear combination of basis functions, which are usually taken as analytical atomic orbitals, χ_μ, centred on the various atoms.

Thus

$$\phi_i = \sum_\mu \chi_\mu C_{\mu i} \qquad (1.14)$$

The coefficients $C_{\mu i}$ are varied to minimize the energy, subject to the orthonormality restraint on the MO's. Roothaan showed that the "best" set of coefficients satisfy the matrix equation

$$\underline{F}\,\underline{C} = \underline{S}\,\underline{C}\,\underline{E} \qquad (1.15)$$

where $\underline{E}$ is a diagonal matrix whose elements are called orbital energies, each corresponding with a particular MO; $\underline{S}$ is the overlap matrix in the atomic orbital basis

$$S_{\mu\nu} = \langle \chi_\mu | \chi_\nu \rangle \ ; \qquad (1.16)$$

and $\underline{F}$, the Hartree-Fock Hamiltonian matrix, is defined by

$$\underline{F} = \underline{H} + \underline{G} \tag{1.17}$$

where $\underline{H}$ is the one-electron core matrix

$$H_{\mu\nu} = \langle \chi_\mu | H | \chi_\nu \rangle, \tag{1.18}$$

with H defined as in equation 1.8. It is convenient to define a density matrix $\underline{R}$ by

$$R_{\mu\nu} = \sum_{i}^{(occ)} C_{\mu i} C_{\nu i} \tag{1.19}$$

where the summation extends over all occupied MO's. The electron interaction matrix $\underline{G}$ is then given as

$$G_{\mu\nu} = \sum_{\lambda\sigma} R_{\sigma\lambda} [2\langle \chi_\mu \chi_\lambda | g | \chi_\nu \chi_\sigma \rangle - \langle \chi_\mu \chi_\lambda | g | \chi_\sigma \chi_\nu \rangle] \tag{1.20}$$

and the electronic energy as

$$E_{el} = \sum_{\mu\nu} R_{\mu\nu} (H_{\mu\nu} + F_{\mu\nu}) \tag{1.21}$$

The solution to the Roothaan equation is found by solving the generalized pseudo-eigenvalue equation

$$(\underline{F} - E_i \underline{S}) \underline{C}_i = 0 \tag{1.22}$$

where $\underline{F}$ and $\underline{S}$ are as given above, and the energies E_i and eigenfunctions $\underline{C}_i$ are to be found. Because $\underline{F}$ depends on $\underline{C}$ through $\underline{G}$, an iterative method of solution is required. An initial guess for the coefficients is used to construct the $\underline{F}$ matrix, the equation is solved as outlined below, and the newly-found coefficients used to form a new $\underline{F}$ matrix for the next iteration. This iterative procedure is continued until the solutions are self-consistent, i.e. the eigenfunctions from

two successive iterations agree to within some specified limits. The whole procedure is called the linear combination of atomic orbitals - molecular orbital - self consistent field (LCAO - MO - SCF) method.

The solution of equation 1.22 is simplified by transforming the basis functions $\underline{\chi}$ to an orthonormal Löwdin basis[19] $\underline{\lambda}$, where

$$\underline{\lambda} = \underline{\chi}\ \underline{S}^{-\frac{1}{2}} \tag{1.23}$$

with $\underline{\lambda}$ and $\underline{\chi}$ row vectors of functions. These orthonormal functions differ least, in a least squares sense, from the non-orthogonal functions $\underline{\chi}$[20]. The other matrices then transform as

$$\underline{C}^{\chi} = \underline{S}^{-\frac{1}{2}}\ \underline{C}^{\lambda}$$

$$\text{and}\quad \underline{F}^{\lambda} = \underline{S}^{-\frac{1}{2}}\ \underline{F}^{\chi}\ \underline{S}^{-\frac{1}{2}} \tag{1.24}$$

$$\text{so that}\quad \underline{F}^{\lambda}\underline{C}^{\lambda} = \underline{C}^{\lambda}\ \underline{E} \tag{1.25}$$

where the basis used is indicated by a superscript. The pseudo-eigenvalue equation in the Löwdin basis is solved by standard diagonalization techniques[21]. Since $\underline{F}^{\lambda}$ is real and symmetric, an orthogonal matrix $\underline{C}^{\lambda}$ can be found such that

$$(\underline{C}^{\lambda})^{T}\ \underline{F}^{\lambda}\ \underline{C}^{\lambda} = \text{diag}\ (\underline{E}) \tag{1.26}$$

In practice a suitable initial choice for $\underline{C}^{\lambda}$ is most easily found by diagonalizing the Löwdin core matrix $\underline{H}^{\lambda}$.

As the form of the basis functions is improved and their number is increased the solution obtained from Roothaan's SCF equations tends to the Hartree-Fock limit. The major error of this Hartree-Fock theory is its failure to treat electron

correlation adequately[14,22]. Since electrons repel each other because of their charge each electron is surrounded by a "Coulomb hole" into which other electrons do not penetrate. In Hartree-Fock theory the antisymmetric wave function ensures that electrons of the same spin have zero probability of being at identical spatial positions. This gives rise to the "Fermi hole". Electrons of opposite spin, on the other hand, are not correlated and this leads to errors in the wave function and energy.

1.3 Configuration Interaction

One way of improving the quality of a single determinant wave function is the method of configuration interaction (CI). The ground state SCF MO wave function of Roothaan's procedure takes the form of a single determinant built from the MO's with the lowest eigenvalues. More generally the total wave function may be expanded as a linear combination of many Slater determinants, Φ[4],

$$\Psi = a_0\Phi_0 + a_1\Phi_1 + \ldots \tag{1.27}$$

If there are n occupied MO's each expressed in terms of m basis functions, the SCF equation produces (m-n) unoccupied MO's which are called virtual orbitals. In the CI method each determinant, Φ_i, is built from a different configuration taken from the set of all the MO's including virtual ones and the coefficients in Equation 1.27 are found by solving a secular equation:

$$\underline{H}\ \underline{a} = E\ \underline{a} \tag{1.28}$$

where $$H_{ij} = \langle\Phi_i|\hat{H}|\Phi_j\rangle \tag{1.29}$$

The matrix elements H_{ij} are obtained with the help of Slater's rules[23,24]. For determinants built from a set of orthonormal molecular spin orbitals, ψ, the only off-diagonal elements (i.e. $i \neq j$) are between determinants which differ by at most two spin orbitals. For exact Hartree-Fock MO's Brillouin's theorem[25,26] states that there is no first order mixing between the ground state determinant and any singly excited determinant. A similar result holds in the LCAO approximation[17]. For the limited CI calculation described in Chapter Six only doubly excited configurations which differed in one molecular orbital ϕ were included. Thus if $\phi_R' \neq \phi_R$ Slater's rules lead to

$$\langle \Phi' | \hat{H} | \Phi \rangle = \langle \phi_R' \phi_R' | g | \phi_R \phi_R \rangle$$

$$= \sum_{\mu\nu\lambda\sigma} C_{\mu R'} C_{\lambda R'} C_{\nu R} C_{\sigma R} \langle \chi_\mu \chi_\lambda | g | \chi_\nu \chi_\sigma \rangle \qquad (1.30)$$

Similarly the diagonal terms are given by

$$\langle \Phi | \hat{H} | \Phi \rangle = 2 \sum_{\mu\nu} R_{\mu\nu} h_{\mu\nu} + \sum_{\mu\nu\lambda\sigma} R_{\mu\nu} R_{\lambda\sigma} [2\langle \chi_\mu \chi_\lambda | g | \chi_\nu \chi_\sigma \rangle$$

$$- \langle \chi_\mu \chi_\lambda | g | \chi_\sigma \chi_\nu \rangle] \qquad (1.31)$$

where each $\underline{R}$ matrix is defined by Equation 1.19 in terms of the orbitals occupied in Φ. The coefficients $\underline{a}$ are found by diagonalizing $\underline{H}$.

An improvement, not used in this work, is the multi-configurational self-consistent field (MC-SCF) method[27,28] in which not only the coefficients but also the individual MO's in each determinant are varied.

1.4 The Simplified Ab Initio Method

In this approximate method[8,29,30] many of the electron repulsion integrals are neglected. The basis set used is a minimal basis of Slater atomic orbitals with 1s, 2s, $2p_x$, $2p_y$, $2p_z$ orbitals on each atom. The real Slater AO's[31] are defined for quantum numbers n,ℓ,m by

$$\chi_{n,\ell,m} = (2\zeta)^{n+\frac{1}{2}}[(2n)!]^{-\frac{1}{2}}\, r^{n-1}\, e^{-\zeta r}\, S_{\ell m}(\theta,\phi) \qquad (1.32)$$

where $S_{\ell m}(\theta,\phi)$ are normalized real spherical harmonics and ζ, the orbital exponent, is approximately Z_{eff}/n. The actual choice of values for ζ will be discussed in Chapter Six.

All one-electron integrals, i.e. overlap, kinetic energy, and nuclear attraction integrals are calculated accurately to 10^{-7} a.u. in the Slater basis $\underline{\chi}$ by standard techniques[32,33]. From these the core matrix $\underline{H}^{\chi}$ is formed exactly in the Slater basis. It is then transformed first to an atomic basis $\underline{\eta}$ and then to an orthonormal Löwdin basis $\underline{\lambda}$. In the atomic basis the 1s and 2s orbitals on each atom are made orthogonal by means of the Gram-Schmidt orthogonalization procedure. The transformation is written

$$\underline{\eta} = \underline{\chi}\ \underline{A} \qquad (1.33)$$

The Löwdin basis is then given by

$$\underline{\lambda} = \underline{\eta}\ \underline{S}_{\eta}^{-\frac{1}{2}} \qquad (1.34)$$

where $\underline{S}_{\eta}$ is the overlap matrix in the atomic basis.

In calculating the $\underline{G}$ matrix, the neglect of diatomic differential overlap (NDDO) approximation[34] is used in the Löwdin basis. This means that only electron repulsion integrals of the form $\langle \lambda_i^A \lambda_k^B | g | \lambda_j^A \lambda_\ell^B \rangle$, where A and B refer to

atomic centres which may be identical, are included in the $\underline{G}$ matrix. These integrals are calculated from the corresponding Slater basis NDDO integrals in the following way:

the NDDO integrals in the atomic basis are

$$\langle \eta_p \eta_r | g | \eta_q \eta_s \rangle = \sum_{C,D}^{\text{atoms}} \sum_{\mu,\nu}^{C} \sum_{\lambda,\sigma}^{D} A_{\mu p} A_{\nu q} \langle \chi_\mu^C \chi_\lambda^D | g | \chi_\nu^C \chi_\sigma^D \rangle . A_{\lambda r} A_{\sigma s} \quad (1.35)$$

Since this transformation involves only a one-centre orthogonalization it requires only the NDDO Slater basis integrals and may be carried out rapidly. These integrals are computed accurately to 10^{-7} a.u. by standard methods[35,36].

The NDDO integrals in the Löwdin basis require all the repulsion integrals in the atomic basis. The transformation is simplified by the use of the Ruedenberg approximation[37] so that non-NDDO integrals are not required and are only implicitly calculated. The transformation is written most simply as

$$\langle \lambda_i^A \lambda_k^B | g | \lambda_j^A \lambda_\ell^B \rangle \approx \tfrac{1}{4} \sum_{C,D}^{\text{atoms}} \Big[\sum_{p,q}^{C} \sum_{r,s}^{D} (U_{ip} X_{qj} + X_{pi} U_{qj}) \cdot \langle \eta_p^C \eta_r^D | g | \eta_q^C \eta_s^D \rangle (U_{kr} X_{s\ell} + X_{rk} U_{s\ell}) \Big] \quad (1.36)$$

where $\underline{X} = \underline{S}_\eta^{-\frac{1}{2}}$ and $\underline{U} = \underline{S}_\eta^{\frac{1}{2}}$.

In this approximation, because so many integrals are neglected, the construction of the $\underline{F}$ matrix is simplified. In N_2O_4, for example, only 4095 integrals out of 108,345 are calculated. The one- and two-centre $\underline{F}$ elements in the Löwdin basis are given by

$$F_{\mu\nu}^{AA} = H_{\mu\nu}^{\lambda} + \sum_{\gamma\delta}^{A} R_{\gamma\delta} [2\langle \lambda_\mu \lambda_\gamma | g | \lambda_\nu \lambda_\delta \rangle - \langle \lambda_\mu \lambda_\gamma | g | \lambda_\delta \lambda_\nu \rangle]$$

$$+ 2 \sum_{\gamma\delta}^{B \neq A} R_{\gamma\delta} \langle \lambda_\mu \lambda_\gamma | g | \lambda_\nu \lambda_\delta \rangle$$

and

$$F^{AB}_{\mu\nu} = H^{\lambda}_{\mu\nu} - \sum_{\delta}^{A}\sum_{\gamma}^{B} R_{\gamma\delta}\langle\lambda_\mu\lambda_\gamma|g|\lambda_\delta\lambda_\nu\rangle \qquad (1.37)$$

The eigenvalue equation in terms of $\underline{F}^{\lambda}$ is then solved in the normal way.

1.5 The Multi-Gaussian Expansion Method

This is a more accurate method in which all integrals are included[8]. The one-electron and two-electron NDDO integrals are calculated exactly in the Slater basis as for the SAI method. In order to save computer time, however, the remaining non-NDDO integrals are calculated approximately by means of the Gaussian expansion technique[38]. Williams[8] has commented that the NDDO integrals should specifically be calculated exactly (to 10^{-7} a.u.) since this can be done rapidly by standard methods, they are not well approximated by Gaussian expansion techniques, and as they have larger magnitude than the other repulsion integrals it is important that they be as accurate as possible.

Normalized Gaussian orbitals[39] have the form

$$\phi_{n\ell m} = 2^{n+\frac{1}{2}}[(2n-1)!!]^{-\frac{1}{2}}(2\pi)^{-\frac{1}{4}}\alpha^{\frac{2n+1}{4}} r^{n-1}\exp(-\alpha r^2).Y_{\ell m}(\theta,\phi) \qquad (1.38)$$

where α is an orbital exponent.

The Gaussian expansion technique[40,41] expresses each Slater basis function as a linear combination of two or more Gaussian functions. A multicentre integral then becomes

$$\langle\chi_\mu(\zeta_\mu)\chi_\lambda(\zeta_\lambda)|g|\chi_\nu(\zeta_\nu)\chi_\sigma(\zeta_\sigma)\rangle = \sum_{ijk\ell}^{n} d_{i\mu}d_{j\nu}\langle\phi_i(\zeta_{i\mu})\phi_k(\zeta_{k\lambda})|g|\phi_j(\zeta_{j\nu})\phi_\ell(\zeta_{\ell\sigma})\rangle d_{k\lambda}d_{\ell\sigma} \qquad (1.39)$$

where n = number of Gaussian type orbitals per Slater type orbital

$\chi_\mu(\zeta_\mu)$ = Slater orbital with exponent ζ_μ

$\phi_i(\zeta_{i\mu})$ = Gaussian orbital with exponent $\zeta_{i\mu} = \zeta_\mu^2 \alpha_{i\mu}$.

The $d_{i\mu}$ and $\alpha_{i\mu}$ are the coefficients and exponents of the Gaussian functions that have been fitted by a least squares procedure to a Slater function χ_μ with unit exponent. Values tabulated by Stewart[42] are used and the multicentre integrals over Gaussian functions are evaluated by standard formulae[40,41]. The $\underline{F}$ matrix is constructed directly in the Slater basis, transformed to a Löwdin basis, and the SCF equations solved by iteration.

1.6 Comparison of the Methods

Gaussian orbitals have both advantages and disadvantages over Slater atomic orbitals[40]. Multicentre integrals are more easily evaluated for the Gaussian functions because the product of two of these functions having different centres A and B is itself a Gaussian function with centre on the line segment AB. As a result four-centre integrals are converted into one- and two-centre Coulomb integrals. The major drawback to using Gaussian functions for approximating atomic orbitals is that they behave poorly for small and large values of r. In particular, because of the exp $(-\alpha r^2)$ dependence, they do not have a cusp at the origin. In order to obtain the same accuracy as from a given Slater basis set many more Gaussian functions are required. As the number of repulsion integrals increases as the fourth power of the size of the basis set, the use of Gaussians involves the calculation, storage and

manipulation of a great many more numbers than is the case with Slater orbitals.

In the Gaussian expansion method the number of integrals stored is reduced, but each Slater repulsion integral requires the calculation of 16 Gaussian repulsion integrals for a two-Gaussian expansion (one Slater orbital approximated by two Gaussians) and 81 integrals for a three-Gaussian expansion.

Williams[8] has compared the SAI and MGE methods with the results of exact ab initio calculations for small molecules. For such systems as H_2O, NH_3, F_2O the two-Gaussian method gave energies typically within 0.2% of the exact Hartree-Fock values. The three-Gaussian method improved the accuracy to within about 0.02%. The SAI method does not give such uniform results, and the agreement is usually not as good, with errors varying from 0.03% for F_2O to 0.7% for NH_3. As discussed in Chapter Five, the quality of a wave function is often not best indicated by its energy. For this reason it is instructive to compare calculated one-electron properties with those derived from exact calculations and from experiment. On the basis of several such comparisons Williams concluded that the M G E method was quite adequate for the calculation of one electron properties.

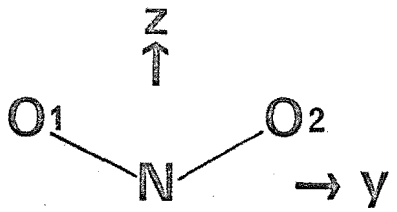
z
O1
O2
N
y

Fig. 2.1

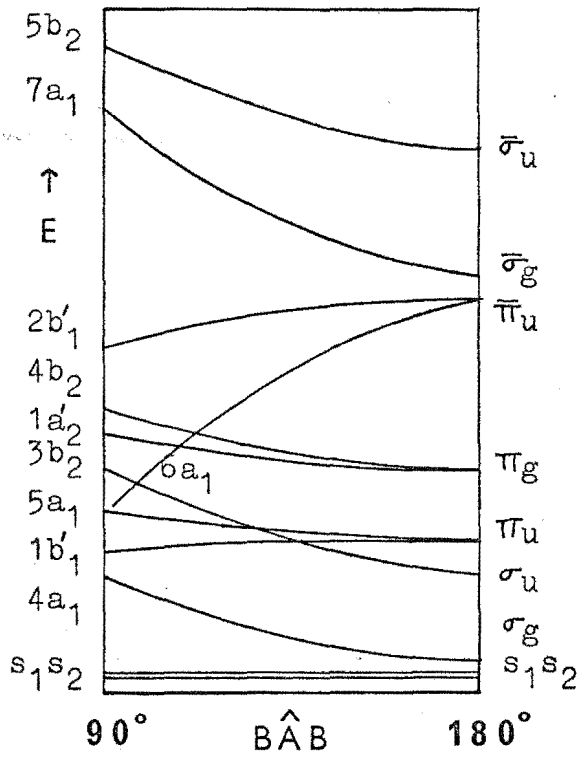
5b2
7a1
E
2b'1
4b2
1a'2
3b2
6a1
5a1
1b'1
4a1
s1s2
σu
σg
πu
πg
πu
σu
σg
s1s2
90°
BÂB
180°

Fig. 2.2

CHAPTER TWO

REVIEW OF NITROGEN DIOXIDE AND DINITROGEN TETROXIDE

2.1 The Structure of Nitrogen Dioxide

A general summary of the chemistry of nitrogen dioxide, NO_2, was given by Mellor[43]. More recently the physical chemistry has been reviewed by Bell[44]. The geometry of NO_2 has been determined by electron diffraction[45], and by infra-red[46] and microwave spectroscopy[47-49]. A structure, derived from microwave data by Laurie & Herschbach[48], has an N-O bond length 0.11967 nm and O-N-O angle $134^{o}15'$. The molecule therefore belongs to the point group C_{2v} whose character table is given in Appendix I. The orientation of the Cartesian axes is shown in Figure 2.1 and is adhered to throughout this thesis.

2.2 An Orbital Correlation Diagram for Nitrogen Dioxide

In the second of his well-known series of papers Walsh[50] gave a qualitative description of the variation with apex angle of the orbitals of symmetric BAB molecules. His correlation diagram is given in Figure 2.2, and the following summary of his results is relevant to a discussion of the electronic structure of NO_2. The diagram is based on extensive spectroscopic data and is rationalized in terms of three rules: (i) in the 90^{o} molecule the 2s orbital on the central atom, s_A, does not mix; (ii) an orbital is more tightly bound if it is built from an s orbital rather than a p orbital; and (iii) if there is no change in A valency an orbital antibonding between the end atoms is more stable in the linear case and one bonding

between the end atoms is more stable bent. The orbitals of the bent BAB molecule are classified according to the irreducible representations a_1, a_2', b_1', b_2 of the point group C_{2v}, where the superscript indicates a pi orbital with a node in the plane of the molecule. In this discussion ls orbitals are not considered. The lowest two molecular orbitals are lone-pair s orbitals delocalized on the B atoms and changing little in energy with apex angle. The orbitals $4a_1$-σ_g and $3b_2$-σ_u are A-B bonding and formed by overlap of pure p orbitals in the bent molecule. Both are more tightly bound in the linear case, the former because it is built from an s orbital on A, and the second because it is B-B antibonding. The doubly-degenerate π_u orbital of the linear molecule is built from in phase overlap of pπ orbitals, mainly localized on the B atoms. It correlates with two orbitals of the bent molecule. The first, a $1b_1'$ orbital, is more tightly bound owing to B-B bonding character but the second, a $5a_1$ orbital, has similar energy because of two counteracting effects. The p atomic orbitals on each B lying at right angles to adjacent A-B bonds provide bonding, but on the other hand, A-B bonding is lost. The doubly degenerate π_g orbital has zero amplitude at A, and is built from p orbitals on B; the p orbitals overlap out of phase. It correlates with separate $1a_2'$ and $4b_2$ orbitals, both having higher energy because of B-B antibonding. The doubly degenerate $\bar{\pi}_u$ orbital is mainly localized on A but there is some out of phase overlap with pπ orbitals on B. It therefore lies higher than the nonbonding π_g. (The bar in the $\bar{\pi}_u$ symbol indicates this A-B antibonding character.) Because of the small B-B bonding character the π orbital with which it correlates, $2b_1'$, is slightly more tightly bound. The other

orbital, $6a_1$, is according to Walsh a pure s orbital on A in the 90^o molecule. It is therefore expected to be much more tightly bound in the bent case, not only as a result of this increased s character, but also because of the absence of the small amount of A-B pπ antibonding in the $\bar{\pi}_u$ orbital. The final two intravalency orbitals are $7\bar{a}_1$-$\bar{\sigma}_g$, constructed mainly from a p_z orbital on A in the bent case and an s orbital on A for the linear molecule, and $5\bar{b}_2$-$\bar{\sigma}_u$ formed from p orbitals overlapping out of phase.

Nitrogen dioxide with twenty-three electrons is a BAB radical stable in the gas phase. Experimental evidence from spectroscopic studies shows that the unpaired electron is in a totally symmetric molecular orbital. Walsh put this electron in the unusual $6a_1$-π_u orbital, thereby giving NO_2 a ground state configuration

$$^2A_1 : [...]^6(3a_1)^2(2b_2)^2(4a_1)^2(1b_1)^2(5a_1)^2(3b_2)^2(1a_2)^2(4b_2)^2(6a_1).$$

For comparison the nitronium ion, NO_2^+, has 16 valency electrons and since all but one of the lowest eight orbitals increase in binding energy for the linear molecule, NO_2^+ is predicted to be linear, in agreement with experiment[51]. The nitronium ion, NO_2^-, with two electrons in the $6a_1$ orbital, is even more bent than NO_2.

An earlier correlation diagram based on a combination of theoretical considerations and empirical evidence was given by Mulliken[52,53]. While it predicted the $^2A_1$ ground state configuration for NO_2, it differed from Walsh's in that the $\bar{\sigma}_g$ orbital was below the $\bar{\pi}_u$ orbital and the $7\bar{a}_1$-$\bar{\sigma}_g$ orbital was more stable in the bent molecule. Accurate single

determinant LCAO calculations for ozone and the azide ion by Peyerimhoff & Buenker[54] were in agreement with Walsh.

Similar calculations on F_2O[55] and some AH_2 molecules[56] have produced some discrepancies with Walsh's diagram, and have led to criticism of his original assumptions. The s orbital on A did hybridize in a 90^o molecule because hybridization of s and p character polarized the charge out of the triangle and reduced electron repulsion. The orbital energy curves for σ_g-$3a_1$ and σ_u-$2b_2$, which corresponded to Walsh's s_1 and s_2, changed markedly with angle for F_2O since both were dominated largely by fluorine s-character. The σ_g-$3a_1$ was strongly FF bonding and therefore was stabilized in the bent molecule. Since σ_u-$2b_2$ was FF antibonding it increased in energy for small FOF angles. An extended Hückel calculation on NO_2 by Burnelle et al.[57] showed the σ_u-$5b_2$ orbital to be more strongly bound in the bent case because the N-O antibonding effect was reduced on bending owing to smaller overlap of p orbitals, and this outweighed the increase in O-O antibonding. Various interpretations of the ordinate of Walsh's diagram can be made and these have been discussed recently by Coulson & Deb[58].

2.3 Qualitative and Semi-Empirical Descriptions of the Bonding in Nitrogen Dioxide

A qualitative account of the bonding in NO_2 was given by Green & Linnett[59] who formulated the following supposition to help in deciding between possible valence bond structures for molecules and ions with an odd number of electrons. "In a molecule containing one or more unpaired electrons, the unpaired electron tends to be localized on one atom if there

is a consequent increase in bond order or if that atom has a high electronegativity relative to the others, otherwise it tends to be delocalized." For NO_2 the structures with highest bond order (3½) are $=\dot{O}\div\dot{N}=O=$ and $=O=\dot{N}\div\dot{O}=$. The small electronegativity difference between N and O is not large enough to offset the fall in bond order in $\equiv O-\dot{N}=O=$ and $=O=\dot{N}-O\equiv$. Pauling[60] attributed the stability of NO_2 relative to N_2O_4 to the three electron bond and found that the odd electron was probably on the nitrogen atom only 65% of the time. Since NO_2 was intermediate between the structures of NO_2^+, $O=\overset{\oplus}{N}=\dot{O}$, and NO_2^-,

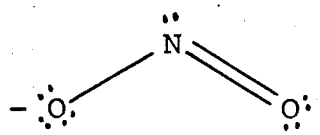

he expected the lone electron to lie in the plane of the molecule. Linnett[61] extended the earlier work by modifying the Lewis-Langmuir Octet Rule so that the octet was considered as a double quartet, one set with positive spin and the other with negative spin. Two possible NO_2 structures, each with seven electrons in the bonding regions were $=O=\overset{\times}{N}\div\overset{\times}{O}=$ and $\overset{\times}{\times}O\div\overset{\times}{N}\overset{\times}{-}\dot{O}=$. Linnett favoured the second, where there was a greater average separation of the electrons, but an unsatisfactory feature of both was that eight electrons of one spin favoured a linear molecule while the other nine favoured a bent molecule.

The electronic structure of NO_2 was considered by Coulson & Duchesne[62] prior to a discussion of the bonding in N_2O_4. Excluding the inner shell orbitals and 2s orbitals on the oxygen atoms there are thirteen valency electrons. Their assignment of these electrons differed from that of Walsh and Mulliken in that there were only three π electrons (defined

relative to the NO_2 plane). Two of these π electrons filled the $1b_1'$-π_u orbital and the unpaired electron went into the non-bonding $1a_2'$-π_g orbital localized entirely on the oxygen atoms. The orbital corresponding to Walsh's $6a_1$-$\bar{\pi}_u$ was a doubly filled nitrogen sigma lone pair, which, while pointing away from the oxygen atoms, had considerable s character and was therefore close to the nitrogen atom. This was important for their subsequent description of the N-N bond of N_2O_4 which is discussed in Section 2.6.

McEwen[63] used the Pariser-Parr-Pople semi-empirical method and calculated the π and σ non-bonding orbitals. She put the single electron in an sp^2 non-bonding orbital on the nitrogen atom, of symmetry a_1, and directed away from the oxygen atoms. In a freely rotating molecule an unpaired s electron produces a hyperfine splitting by interacting with the spin of the nucleus on which it lies. From the fine structure in an electron spin resonance spectrum it is therefore possible to calculate the population of this orbital. Thus if we express the $6a_1$ orbital in the form

$$\psi(6a_1) = a_s(N)2sN - a_{p_z}(N)2p_zN + a_s(O)[2sO + 2sO'] + a_{p_z}(O)[2p_zO + 2p_zO'] + a_{p_y}(O)[2p_yO - 2p_yO']$$

the coefficients can be calculated from experimental data. Resulting values are collected in Table 2.1, together with those from MO calculations including one described in Chapter Six where comparisons are made.

Serre[70] calculated a wave function for NO_2 using the SCF method simplified by the approximations of Parr and Pariser.

Table 2.1: Singly occupied orbital of nitrogen dioxide

Medium	$a_s^2(N)$	$a_{p_z}^2(N)$	$a_{p_x}^2(N)$	$a^2(O)$	Reference
N_2O_4	0.095	0.350	0.040	0.515	64
ice	0.106	0.452	0.019	0.45	65
solution	0.18				66
McEwen	0.098	0.263		0.63	63
Green et al.	0.168	0.222		0.61	67
LCAO	0.167	0.333		0.50	49
Brundle et al.	0.16	0.37		0.48	68
Schaefer et al.	0.17	0.38		0.45	69
RHF 2G/S	0.049	0.495		0.456	Section 6.3

She included only eight electrons, each oxygen contributing one $p\pi$ electron and one $p\sigma$ lone pair and the nitrogen atom contributing two $p\pi$ electrons. The unpaired electron was considered as a core electron localized on the nitrogen atom. This work was extended by Le Goff & Serre[116] in conjunction with an investigation of the bonding in N_2O_4 and will be further discussed in Section 2.6.

An extended Huckel method was used by Green & Linnett[67] to support the orbital assignment of Walsh and Mulliken. They calculated an unpaired charge density of 0.168 for the N 2s orbital in the $6a_1$ level.

A detailed analysis of the fine structure and magnetic coupling of the microwave spectrum of NO_2 by Bird et al.[49] showed that the molecule had a $^2A_1$ ground state, and that the odd electron had 2p character on the nitrogen nucleus, the p orbital being directed along the z axis.

Kato et al.[71] used Hoffmann's extended Huckel method[72] and found their order of orbitals to be consistent with Walsh's diagram, with the odd electron in the $6a_1$ orbital. Their calculation gave considerable differences in electron distributions when compared with the earlier treatments of the pi structure by Tanaka[73] and McEwen[63], using the LCAO SCF method. In their calculation the orbital containing the odd electron had a much greater nitrogen character than McEwen found, and they considered their negative charge on the oxygen atoms, which was almost twice that of Tanaka, to be too large.

Two CNDO/2 calculations have been reported. The first by Pople & Segal[74] used the experimental bond length of Claesson et al.[45] and varied the ONO angle. They predicted an angle for minimum energy of 137.7^{o}, compared with the experimental value of 132^{o}. The other calculation, by Kelkar et al.[75] merely confirmed this result, and was included in a study of several nitrogen oxides only for completeness.

Yonezawa et al.[76] used a semi-empirical unrestricted SCF MO method which included all valence electrons but did not take into account the two-centre sigma-pi type exchange integrals. They reported electron spin densities and an ionization potential of 0.4779 a.u., which can be compared with spectroscopic values of 0.452 a.u. (from Rydberg bands)[77] 0.4032 a.u. (adiabatic)[78], and 0.4126 a.u. (vertical)[68].

Burnelle et al.[57] extended the results of Kato et al.[71] by varying the bond angle in order to make a comparison with Walsh's diagram. In linear NO_2 the σ_u orbital was found to be slightly higher than the π_u orbital. Other discrepancies were mentioned above. The unpaired electron was in the $6a_1$ orbital but when their results were compared with experiment[65] it

was found that there was too great a pile up of charge on the nitrogen atom.

2.4 Ab Initio Calculations on Nitrogen Dioxide

The first non-empirical calculation on NO_2 was done by Burnelle et al.[79], using Roothaan's open shell method[80,81] in the form given by McWeeny[17,82]. This was a single configuration calculation with two different sets of Gaussian orbital basis functions. The smaller set of 33 functions gave an energy of -202.5883 a.u. while the extended basis of 48 functions an energy of -203.6930 a.u. for the ground state $^2A_1$. The $^2A_2$ state ... $(4b_2)^2(1a_2)(6a_1)^2$ was 0.113 a.u. and 0.110 a.u. above the ground state with the respective basis sets. A correlation diagram based on calculated orbital energies was given and compared with that of Walsh.

Fink[83] obtained an energy of -203.729 a.u. for the $^2A_1$ ground state using the LCAO-SCF method with the approximation of Nesbet's symmetry and equivalence restrictions. The basis set was a near Hartree-Fock atomic orbital basis of Gaussian lobe functions and all integrals were computed exactly.

Burnelle & Dressler[84] attempted to calculate a more accurate wave function using a basis set of 72 Gaussian functions. Application of the iterative SCF method, however, resulted in oscillations and the authors decided to contract the basis set to 39 Gaussians. This gave a ground state energy of -203.8857 a.u.

Brundle et al.[68] used a best atom double-zeta Gaussian basis set and obtained an energy of -203.9318 a.u. They gave an extensive discussion of the form of the molecular orbitals and correlated these with an analysis of the photoelectron and

vacuum ultraviolet spectra. They reported a Mulliken population analysis and overlap analysis for the $^2A_1$ ground state.

Schaefer & Rothenberg[69] derived from an ab initio calculation the magnetic hyperfine structure (hfs) parameters of NO_2. In the Hartree-Fock approximation these depend only on the form of the singly occupied $6a_1$ molecular orbital. The results of a population analysis of this orbital are given in Table 2.1. Agreement of the hfs parameters with experiment was very good with respect to the nitrogen nucleus, but the oxygen parameters, while in qualitative agreement, were all too small. Using a Gaussian basis they obtained a $^2A_1$ ground state energy of -203.9468 a.u. which was lowered to -204.0679 a.u. when six d-like functions on each atom were included.

Del Bene[85] used the Orthogonality Constrained Basis Set Expansion method[86] with a minimal basis set formed by expanding a Slater type orbital in terms of three Gaussians. This gave the same configuration as that of Burnelle et al.[79] except for reversal of the $5a_1$ and $1b_1$ orbitals. Her calculations also showed the $^2A_2$ state to lie above the $^2A_1$ ground state by 0.0617 a.u.

Gangi & Burnelle[87] later extended their calculation by a configuration interaction method using up to 180 configurations with their 33 Gaussian basis set. The configurations were chosen under two approximations: only permutations among seven of the molecular orbitals were permitted, and only those configurations with an interaction greater than some cut-off value were considered. Using 44 configurations they reduced the energy of the $^2A_1$ ground state to -202.67317 a.u. A 32 configuration CI treatment of the $^2A_2$ state placed this 0.172 a.u. above the ground state. The calculation using 39

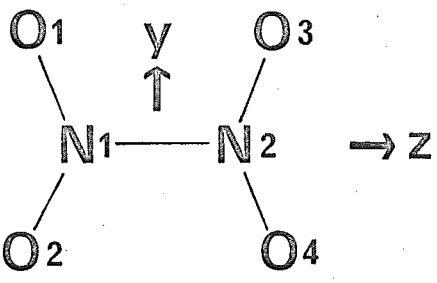

Fig. 2.3

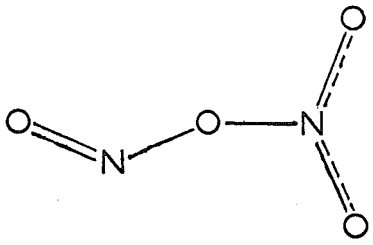

Fig. 2.4

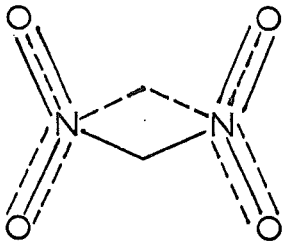

Fig. 2.5

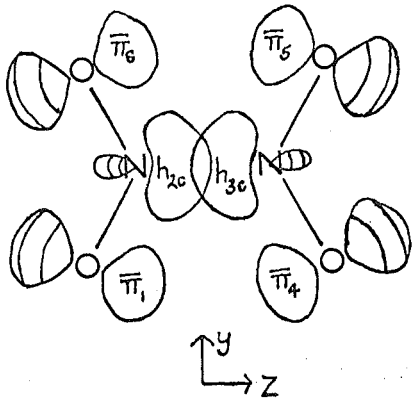

Fig. 2.6

contracted Gaussians[84] was also extended to a CI treatment. 36 configurations led to a ground state energy of -203.94318 a.u. while a 24 configuration calculation on the $^2A_2$ state produced an energy 0.152 a.u. higher.

In order to highlight the variations in the ordering of the orbitals with regard to energy Table 2.2 summarizes the reported ground state configurations. The total energies for the $^2A_1$ ground state are given in Table 2.3. Included in both these tables for comparison are the results for a restricted Hartree-Fock calculation described in Section 6.3. Unfortunately the total energy for the calculation by Del Bene[85], which uses a basis set similar to that of the present calculation but a different method of solution, was not given.

2.5 The Structure of Dinitrogen Tetroxide

As with NO_2, the general chemistry of N_2O_4 has been reviewed by Mellor[43] and by Bell[44]. The structure of N_2O_4 will be seen later to be abnormal; it has therefore been the object of much study. An early X-ray diffraction study[88] found the molecule to have the structure of D_{2h} symmetry shown in Figure 2.3. (This orientation of the molecule with respect to the Cartesian coordinates will be used throughout this thesis.) The NN and NO bond lengths were measured as 0.164 ± 0.003 nm and 0.117 ± 0.003 nm with an ONO angle of 126 ± 1°. Corresponding values for the gaseous molecule, as determined by Smith & Hedberg[89] using electron diffraction were 0.1750 nm, 0.1180 nm and 133.7°. Snyder & Hisatsune[90] showed by analysis of the infrared spectrum that the molecule was planar in the gaseous, liquid and solid states. The planar D_{2h} structure was supported by an infrared study[91] of poly-

Table 2.2

Ground State Configurations of Nitrogen Dioxide

	Reference
$(4a_1)^2(1b_1)^2(5a_1)^2(3b_2)^2(1a_2)^2(4b_2)^2 6a_1$	Walsh[50]
$^2A_2$ $\quad (5a_1)^2(4b_2)^2(6a_1)^2 1a_2$	Coulson[62]
$(4a_1)^2(3b_2)^2(1b_1)^2(1a_2)^2(5a_1)^2(4b_2)^2 6a_1$	McEwen[63]
$(4a_1)^2(3b_2)^2(1b_1)^2(5a_1)^2(1a_2)^2(4b_2)^2 6a_1$	Green[67]
$(4a_1)^2(1b_1)^2(5a_1)^2(3b_2)^2(1a_2)^2(4b_2)^2 6a_1$	Kato[71]
$(4a_1)^2(1b_1)^2(5a_1)^2(3b_2)^2(1a_2)^2(4b_2)^2 6a_1$	Burnelle[57]
$(4a_1)^2(1b_1)^2(5a_1)^2(3b_2)^2(4b_2)^2(1a_2)^2 6a_1$	Burnelle[79]
$(4a_1)^2(5a_1)^2(1b_1)^2(3b_2)^2(1a_2)^2(4b_2)^2 6a_1$	Fink[83]
$(4a_1)^2(3b_2)^2(1b_1)^2(5a_1)^2(1a_2)^2(4b_2)^2 6a_1$	Brundle[68]
$(4a_1)^2(5a_1)^2(1b_1)^2(3b_2)^2(4b_2)^2(1a_2)^2 6a_1$	DelBene[85]
$(4a_1)^2(1b_1)^2(5a_1)^2(3b_2)^2(1a_2)^2(4b_2)^2 6a_1$	2G/S Section 6.3

Table 2.3

Energies of All-Electron Calculations on Nitrogen Dioxide

Description	Energy	Reference
33 Gaussian	-202.5883	79
33 Gaussian with CI	-202.6732	87
RHF 2G/S	-203.0030	Section 6.3
48 Gaussian	-203.6930	79
Gaussian Lobe	-203.729	83
39 Contracted Gaussian	-203.8857	84
Best atom double zeta	-203.9318	68
39 Contracted G. with CI	-203.9432	87
Gaussian	-203.9468	69
Gaussian with d functions	-204.0679	69
Estimate of HF limit	-204.229	79

crystalline films of N_2O_4 at -180° and for the gas, liquid and solid phases by an interpretation of the infrared and raman spectra[92]. Fateley et al.[93] from the infrared spectra of NO_2 and N_2O_4 trapped in argon matrices at liquid helium temperatures found evidence for two other structures as well. One had a staggered structure, formed by rotation of the NO_2 groups about the NN bond, and the other the unsymmetrical structure ONO NO_2 as shown in Figure 2.4. These structures were confirmed by Hisatsune & Devlin[94] and Hisatsune et al.[95], the staggered form having a 90° twist. X-ray structure analyses gave NN bond lengths of 0.175 nm for the compound dinitrogen tetroxide-1,4-dioxan, $N_2O_4.C_4H_8O_2$[96], and for an unstable monoclinic form of N_2O_4[97,98]. NN and NO bond lengths have also been shown to increase by about 0.001 nm per 100° of temperature rise[99]. The most recent structure determination was by gaseous electron diffraction[100]. This gave NN and NO bond lengths, and ONO angle of 0.1782 nm, 0.1190 nm and 135.4°.

Any attempt to understand the bonding in N_2O_4 should take into account several unusual features of the molecular structure. These are now summarized. N_2O_4 is planar, with an exceptionally long NN bond of 0.175 nm. This is 0.027 nm longer than the Schomaker-Stevenson covalent single-bond radius sum and compares with values of 0.147 ± 0.002 nm[101] and 0.1453 ± 0.0005 nm[102] for N_2H_4, 0.1492 ± 0.0007 nm for N_2F_4[103], and the multiple bond values of 0.123 nm for azobenzene[51] and 0.1095 nm for nitrogen[51]. This long bond is consistent with a small force constant of 129 newtons/m[62] and a low dissociation energy that has been calorimetrically measured as 57.3 kJ $mole^{-1}$ [106] and later confirmed by spectroscopic data[104,105]. The corresponding value for N_2H_4

is 250 ± 10 kJ $mole^{-1}$ [107]. If the long bond is due to repulsion between the two NO_2 groups it is then strange that the molecule does not adopt a staggered configuration. The structure with 90° twist has been estimated from experimental data to be 12 kJ $mole^{-1}$ less stable[90]. The planar D_{2h} structure is also more stable than the ONO NO_2 isomer. The geometry of the two NO_2 groups is remarkably similar to that of free NO_2. The ONO angle is wide, 133.7°, and the NO bond length at 0.1180 nm is shorter than the normal NO double bond length of 0.1212 nm for H - N = O[108]. Finally the molecule is diamagnetic[109] and therefore has a singlet ground state.

2.6 Descriptions of the Bonding in Dinitrogen Tetroxide

Chalvet & Daudel[110,111] used simple molecular orbital theory, in which integrals required for the secular equation were obtained from atom electronegativities, to calculate the bond lengths in N_2O_4. They assumed a distribution of electrons where, in addition to five sigma bonds, each oxygen atom furnished two lone pairs and a single pi electron and each nitrogen atom two pi electrons. They described the NN bond as a partial pi bond superimposed on a sigma bond, and attributed its great length to repulsion of partial positive charges on the nitrogen atoms.

Smith & Hedberg[89] proposed an alternative description which was later supported by Coulson & Duchesne[62] who criticized the sigma plus pi model as producing too large a NN bond order, 1.164, and too short a NN distance of 0.158 nm. They suggested the NN bond had no sigma character and that there were only six pi electrons in N_2O_4. Assuming the normal NN single bond energy to be 250 kJ $mole^{-1}$, they obtained a

bond order of 0.4 for N_2O_4. This "pi-only" model followed from their description of NO_2 which was discussed in Section 2.3. The two nitrogen atoms were attracted towards each other by pi electrons but were repelled by the presence of the lone pairs on the nitrogen atoms which were directed towards each other. Since, in their model of NO_2, the unpaired electron was placed in the la_2 pi orbital localized on the oxygen atoms, the major contribution to the bonding would be from the double occupation of the bonding b_{1g} orbital formed by in phase overlap of these two orbitals.

This account was supported by Mason[112] in an interpretation of the visible and near ultraviolet spectrum of dinitrogen trioxide, N_2O_3. Microwave investigations[113] have shown this molecule to have a nitro-nitroso structure, with an even longer NN bond of 0.1864 nm. Because nitrogen and oxygen were known to have large s-p promotion energies, Mason favoured the pi-only bond structure as it had two fewer pi electrons than a sigma plus pi bond structure.

McEwen[63] put the odd electron in NO_2 in an a_1 orbital on the nitrogen atom pointing away from the oxygen atoms, and she suggested that dimerization to N_2O_4 was stabilized by a charge transfer configuration in which one fragment had a doubly occupied a_1 orbital and the other an empty a_1 orbital. A small amount of pi bonding resulted in the planarity of the molecule and accounted for the barrier to internal rotation.

Pauling[60] predicted an NN single sigma bond order of 0.42, and explained the planarity of N_2O_4 as the result of 4% conjugation of two N=O bonds. The bond order was less than unity because the three electron bonds in NO_2 reduced the odd-electron density on the N atoms.

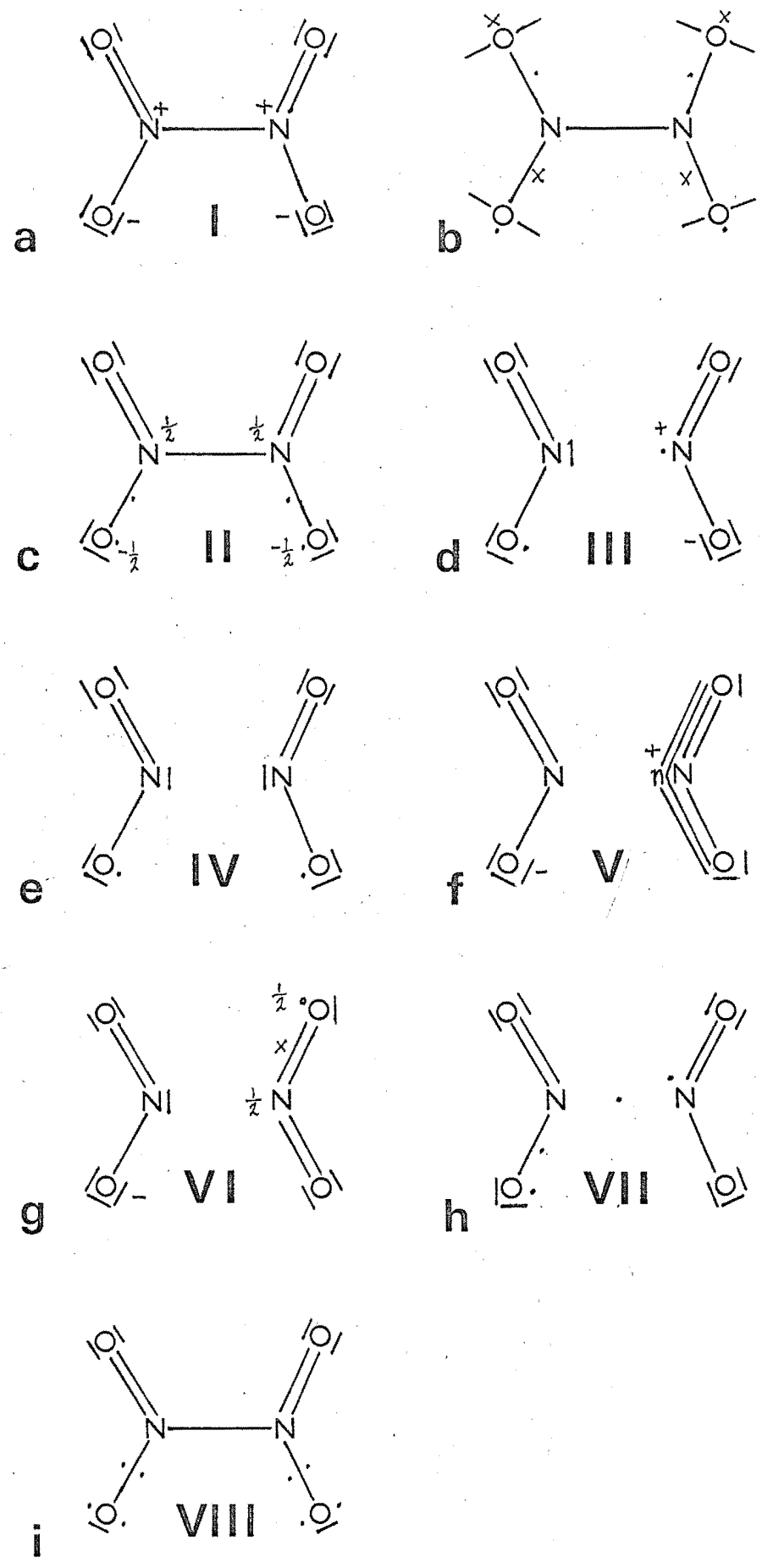

Fig. 2.7

The usual valence bond structure (I) for N_2O_4, which is shown in Figure 2.7a, with a total bond order of 7, was not expected by Green & Linnett[59] to have a large dissociation energy since their bond order for each NO_2 fragment was 3½. Similarly Linnett's description[61] in terms of double quartets of electrons was satisfied by the structure shown in Figure 2.7b for which he noted the electrons of both spin sets favoured the same shape. As will be seen later, however, valence bond structure I has been severely criticized.

On dimerization of NO_2 each of the symmetry orbitals splits, producing two orbitals which transform as irreducible representations of the point group D_{2h}, whose character table is given in Appendix I. The C_{2v} orbital a_1 goes over to b_{1u} and a_g in D_{2h}, and similarly a_2 goes to a_u and b_{1g}, b_1 goes to b_{2g} and b_{3u}, and b_2 goes to b_{3g} and b_{2u}. Herzberg[114] has remarked that in each pair of molecular orbitals, the one without a new nodal plane (a_g, b_{1g}, b_{3u}, b_{2u}) should lie lower than its partner. Green & Linnett[115] compared the energy levels of N_2O_4, calculated by the extended Huckel method, with the values they obtained for the monomer NO_2[67]. Since in this approximation the total energy was equal to the sum of the orbital energies it was easy to investigate the origin of the dissociation energy. No single orbital in particular was found to stabilize the dimer. Thus sigma bonding (a_1 levels) and pi bonding both in the molecular plane (b_2 levels) and out of the plane (b_1 levels) all contributed. The energy of dimerization was found to be very sensitive to small changes in NO_2 geometry. Their first calculation, which used the experimental geometry of N_2O_4[89], gave a dissociation energy of 293 kJ $mole^{-1}$.

A second calculation, assuming no change in NO bond length or ONO angle from NO_2, gave a value of 155 kJ $mole^{-1}$. These were much larger than the experimental value of 57 kJ $mole^{-1}$ [106]. They also calculated the energy of the skew form, having a 90° twist, and found this to be less stable by 218 kJ $mole^{-1}$.

In addition to the eight electron calculation on NO_2 described in Section 2.3, Serre[70] and Le Goff & Serre[116] also made a calculation with only seven electrons, these being a lone pair and pi electron on each oxygen and one pi electron on the nitrogen. This was done in order to test the pi-only bond description of N_2O_4 but did not in itself demonstrate which configuration was valid for NO_2. Using ten atomic orbitals and fourteen electrons (6 pi and 8 oxygen lone pair) they obtained SCF wave functions for N_2O_4 within the approximations of the Parr-Pariser method. According to Coulson & Duchesne[62] the odd electron of NO_2 was in an a_2 orbital. This produced a_u and b_{1g} symmetry orbitals in N_2O_4. Le Goff & Serre calculated energies for the singlet configurations $(a_u)^2$ and $(b_{1g})^2$ and for the singlet and triplet configurations from $(a_u)(b_{1g})$. A configuration interaction treatment was also included and predicted a triplet ground state and only slightly higher singlet and triplet states. These calculations showed the pi-only bond model to be incompatible with the experimental evidence of diamagnetism and absence of colour.

Another calculation using the Parr-Pariser method was carried out by Leroy et al.[117] for eight pi electrons of N_2O_4. This was done in conjunction with calculations on nitrosomethane, CH_3NO, and its cis and trans isomers. The pi bond orders for both NN and NO bonds decreased regularly as the bond length increased. While the double bond character of the

NN bond in the dimers of nitrosomethane was more pronounced than in N_2O_4, this calculation supported Chalvet & Daudel's[110,111] description of the superposition of a normal sigma bond and a partial pi bond.

Bent[118] accounted for most of the structure anomalies in a qualitative fashion by describing the NN bond as a splayed single bond. This description followed from Linnett's double quartet theory; his model is shown in Figure 2.5. Each electron is indicated by a line, the solid lines representing electrons of one spin set and the dotted lines electrons of the opposite spin. Bent suggested that because the normal valence angle opposite a double bond was usually different from 120° the two electrons in the NN bond would be further apart than in a normal, or non-splayed, sigma bond. Maximum overlap in this region therefore required the two nitro groups to be coplanar. A criticism of this description is the uncertainty of the valence angle. His value of 113° in fact leads to coincident NN bonding electrons for the experimental ONO angle of 134°. He made the important suggestion, however, that the NN bond lengthening was caused by delocalization of oxygen atom unshared electrons into the NN sigma antibonding orbital. An example of this effect was given by the length of 0.1736 nm for the C-Cl bond in vinyl chloride, $CH_2=CH-Cl$, compared with 0.1746 nm in acetyl chloride, $O=C(CH_3)-Cl$. Bent claimed that this delocalization also allowed one set of electrons of each spin on each N atom to tend to the arrangement in linear NO_2^+ thus accounting for the large ONO angle.

Moore[119,120] used Hoffmann's extended Huckel method[72] to investigate the internal rotation barrier in N_2O_4. He

calculated a value of 8.83 kJ $mole^{-1}$, compared with the experimental 12 kJ $mole^{-1}$ [90]. By including only positive contributions to the bonds from a population matrix he obtained bond orders for planar N_2O_4 of 0.9821 for NO, 0.4331 for NN sigma, and 0.0057 for NN pi, with no NN pi bonding in the plane of the molecule. This pi bonding, though weak, was strong enough to override pi bonding between non-adjacent atoms which tended to stabilize the staggered form.

Burnelle et al.[57] also applied the extended Huckel method to N_2O_4 and calculated a barrier to internal rotation of 7.36 kJ $mole^{-1}$. They were, however, more concerned with the nature of the NN bond. In contrast to Green & Linnett[115] they found the major contribution to the binding energy to be the $6a_1$ orbital of NO_2. This was indeed overemphasized as their calculation of NO_2 produced too much charge on the N atom in the $6a_1$ orbital. For this reason, too, their computed energy of dimerization was much too large, namely 423 kJ $mole^{-1}$. There was also some pi bonding from the $1b_1$ orbital of NO_2. The b_2 orbitals, on the other hand, all gave rise to a destabilization which appeared to be stronger than a destabilization caused by the $5a_1$ orbital composed mainly of p lone pairs on the oxygen atoms. This was in contrast to the model of Brown & Harcourt[121-124] which is discussed separately in Section 2.7. The picture of a weak pi bond superimposed on a sigma bond with destabilization by $2p_y$ orbitals of the nitrogen atoms was supported by a population analysis.

Extended Huckel and CNDO/2 calculations by Redmond & Wayland[125] suggested that the rotational barrier arose from interactions other than the NN pi bond. The $6a_g$ sigma orbital

of N_2O_4 which was derived from the $6a_1$ orbital of NO_2 was a primary contributor to both the dissociation energy and the rotational barrier. Other sources of the barrier were the dependence of the NO bonding on the dihedral angle (that is, the angle of twist) and the long range Op_z-Op_z sigma interactions.

Kelkar et al.[75] applied the CNDO/2 method to a study of N_2O_4. Although their calculation correctly predicted the molecule to be diamagnetic, the calculated equilibrium bond length was only 0.140 nm with a barrier to internal rotation of 5.78 kJ $mole^{-1}$.

2.7 Variable Electronegativity SCF Studies of Dinitrogen Tetroxide

Considerable work has been done on N_2O_4 by Brown and Harcourt[121-124,126-133] using the variable electronegativity self-consistent field (VESCF) method[134]. While these studies were carried out over a period of several years, they will be discussed together here for the sake of clarity. The method was a semiempirical SCF treatment of pi electrons in which the effective nuclear charge, which was itself a measure of the electronegativity of a $2p\pi$ orbital, was allowed to vary as a function of the pi electron density on that atom. As a result basic integrals became functions of the electron distribution.

After criticizing the classical valency formula[110] as producing too strong an N-N bond, and the "pi-only" structure as predicting paramagnetism and absence of stability in the perpendicular conformation, these authors proposed a new electronic structure[121]. This was a classical sigma plus pi

model with 8π electrons but with lone pair 2p electrons on the oxygen atoms delocalizing into an antibonding σ* orbital between the nitrogen atoms. This delocalization may be compared with that in Bent's[118] description. Pi-only structures then represented doubly excited configurations. The observed diamagnetism[109] was explained by the absence of low-lying triplet states. The details of the calculation were given in subsequent papers[122,123]. They considered eighteen electrons - eight π electrons and ten mobile σ electrons distributed in the six atomic orbitals shown in Figure 2.6. The delocalization with which they were concerned was from the orbital of symmetry b_{1u} constructed from the $\bar{\pi}$ orbitals, namely $\bar{\pi}_1-\bar{\pi}_4-\bar{\pi}_5+\bar{\pi}_6$ into the antibonding orbital of the same symmetry between the two N atoms, i.e. $h_{2c}-h_{3c}$. The following conclusions were elicited from their calculation. If no delocalization took place an NN σ bond order of 1.00 was expected. They found a value of 0.67, together with a π bond order of 0.09, which was assumed to account for the planarity of the molecule. Their total NN bond order of 0.76 was large by comparison with a value 0.46 which had been deduced from a bond order - bond length relationship[126], and values near 0.4 which were suggested by the NN force constant and dissociation energy. Delocalization of other lone-pair σ electrons with larger s character on the oxygen atoms was insignificant. Formal positive charges on the nitrogen atoms were considered not responsible for the NN bond lengthening, as these were also present in $N_2H_6^{2+}$, which had an NN bond length of 0.141 ± 0.001 nm[135], shorter than that in N_2H_4. A change in hybridization from N_2H_4 (sp^3) to N_2O_4 (sp^2) would lead to a

bond length of only 0.150 nm for N_2O_4. A total NO bond order of 2.02 was obtained comprising contributions of 1.00 from the ordinary σ single bond, 0.33 from delocalization of $\bar{\pi}$ orbitals and 0.69 from π-electron out-of-plane bonding. This value was in accord with the observed bondlength, 0.1180 nm[89] which was slightly shorter than the double bond in H-N=O, 0.1212 nm, and the Schomaker-Stevenson double bond, 0.120 nm. Without $\bar{\pi}$ delocalization they would have expected the NO bond to be longer and ONO angle narrower, instead of their being similar to those of NO_2 with a calculated bond order of 2.05. $\bar{\pi}$ delocalization into the σ antibonding NO orbital was also considered but found to be small. Formal charges on oxygen atoms were not considered to be responsible for the large ONO angle since VESCF estimates of these (-0.23e) were smaller than those for NO_2^- (-0.47e) with a bond angle of 115°. They also stressed that, while they were most concerned with the σ orbitals in the plane of the molecule, the σ and π orbitals did not form separate energy groups. The order, in increasing energy, of the highest nine occupied orbitals was

$$a_g(\sigma), b_{3u}(\pi), b_{2g}(\pi), b_{1u}(\sigma), b_{2u}(\sigma), b_{3g}(\sigma), a_u(\pi), b_{1g}(\pi), a_g(\sigma).$$

Brown & Harcourt[124] followed this with a VESCF calculation on the "π-only" model of N_2O_4. In this configuration the σ antibonding orbital, h_{2c}-h_{3c}, between the nitrogen atoms was filled so that any NN bonding had to arise from π electron delocalization. In addition to the ^1A_g ground state they found a $^3B_{1u}$ state which was sufficiently low lying to imply that N_2O_4 should be paramagnetic. Even after an extensive configuration interaction treatment the singlet-triplet separation was still small enough to predict paramagnetism.

This paper concluded with a summary of criticisms of the "π-only" model. The geometries and VESCF NO bond orders for NO_2^-, NO_2^+, NO_2 with 3 and 4 π electrons, and N_2O_4 with 6 and 8 π electrons were compared. The calculated bond orders for NO_2^-, π-only N_2O_4 and three π electron NO_2 were closely similar suggesting similar geometries. NO_2^- was known, however, to have longer bonds and a narrower angle. VESCF bond orders for eight and four π electron N_2O_4 and NO_2 were larger, making them consistent with their shorter bonds. Another criticism was that the "π-only" model ought to be non-planar, as was N_2F_4, owing to repulsion of NN lone pair electrons.

Harcourt[126] used the VESCF method to calculate the contributions of different valency structures to the ground state wave function. He took the ten sigma electrons considered above and constructed the lowest two ^1Ag configurations using antisymmetrized products of D_{2h} symmetry molecular orbitals. The ground state was then approximated by a linear combination of these two determinantal wave functions, the coefficients being found by the VESCF method. As each determinant could be expanded in terms of wave functions describing separate valency structures the contribution of each to the ground state was calculated. Some of these structures are given in Figure 2.7. Different values for the NNσ bond orders were produced by varying the amount of σ delocalization into the NN antibonding orbital. In all cases the most important single structure was II, a covalent structure with one lone-pair electron delocalized from each of two oxygen atoms. Although structure II had nine electrons around each nitrogen atom, its wavefunction could be expanded

in terms of those for I, III and IV each of which did not violate the octet rule.

A later paper[127] gave the results of energy calculations for the various structures. II was found to have the lowest energy and was stabilized by resonance with a charge transfer structure V involving a two-electron three-centre bond. In V, Figure 2.7f, the long lines represent the two π bonds holding four electrons. The one labelled n is NO non-bonding and has an additional node in the vertical symmetry plane along the NN bond.

Structure V was later[128] shown to be very similar to the ionic structure VI, with localized bonds for the NO_2^+ moiety. This was so provided the mobile σ bonds of VI were described by two-centre bond orbitals. While II was the most important structure when a configuration interaction treatment of the lowest two ^1Ag configurations was made, V in fact contributed equally when only the lowest ^1Ag configuration was considered. The wave function for the II $\leftrightarrow$ V resonance hybrid was compared with that for structure VII which had four electrons in different spatial orbitals and was described as a "non-paired spatial orbital" formula. For σ NN bond orders of about the experimental value of 0.4-0.5, VII was much higher in energy than the II $\leftrightarrow$ V resonance hybrid. Both were satisfactory for bond orders of about 0.7. The advantage of VII was that it was a single valency structure. Harcourt accounted for the weak NN bond as follows. On the basis of structure II above he derived an NN bond number of 0.25, the remaining 0.25 nitrogen odd-electron density being used in forming long NO bonds. With this value he predicted an NN bond length of 0.196 nm, which led to an NN σ overlap integral slightly less than that of the

covalent π bonding overlap integral of ethylene. This was taken to indicate there was some covalent bonding between the nitrogen atoms.

2.8 The Increased Valence Formula for Dinitrogen Tetroxide

The consideration of formulae such as II, where the nitrogen atom appeared to violate the octet rule, led Harcourt to suggest a new type of 'increased valence' formula[127-133]. The application to N_2O_4 has been summarized[133]. Increased valence formulae could be applied to all systems which involved a set of four electrons which were distributed amongst three overlapping atomic orbitals on three atoms. A system such as $\ddot{Y}$ A - B could increase its total bond order by delocalizing a Y electron into the antibonding A B orbital to give Y - A · $\dot{B}$, where the Y A bond order was slightly less than unity. The name for this structure was derived from the fact that A had increased its valency. Alternatively the system Y - A $\ddot{B}$ also gave Y - A · $\dot{B}$ by delocalizing a B lone-pair electron into the A B bonding orbital. For N_2O_4 II was derived from I by delocalization of an oxygen σ lone pair electron into the NO bonding orbital vacant in I. The driving force for this was the reduction of the formal nitrogen charges. The NN bond order was thereby reduced because II represented resonance amongst four canonical structures, only one of which had an NN bond. The NO bonding in each NO_2 fragment then resembled that described in Section 2.3 for NO_2[59]; this explained the similarity in the geometry of the two structures (N_2O_4 0.1180 nm, 133.7°; NO_2 0.11934 nm, 134°4'). These structures were also intermediate between those for NO_2^- (0.124 nm, 115°) with six bonding electrons and NO_2^+ (0.115 nm,

180^{o}) with eight bonding electrons. H - N = O (0.1212 nm) was taken to have a normal NO bond order of two. The bond orders in NO_2 and N_2O_4 were made compatible with this value by further delocalizing oxygen pi lone-pair electrons into vacant pi bonding NO orbitals. This is shown in N_2O_4 structure VIII, which summarized sixteen valence bond structures. The NO bond in H - N = O was longer than in free NO (0.1150 nm) because hydrogen, with low electronegativity, was unable to stabilize the one-electron bond formed by delocalization of an oxygen lone pair into an NO bonding orbital.

CHAPTER THREE

APPLICATION OF MOLECULAR ORBITAL THEORY TO MODERATELY LARGE SYSTEMS

3.1 General Considerations

The application of the methods described in Chapter One to the dinitrogen tetroxide system was found to be not straightforward for two basic reasons. The most obvious was the enormous increase in computer time required when the calculations were extended to cope with a thirty-orbital Slater basis set. Several steps in the calculation took a disproportionately longer time. The evaluation of three-centre nuclear attraction integrals, and the application of the Ruedenberg approximation in the SAI method, were sufficiently slow to justify rewriting the major routines in these steps in 'machine language'. Such a procedure is not satisfactory in general, however, because the language is peculiar to each computer, and moreover it is the slowest steps that are most often being improved by the development of better numerical techniques. For example, Williams[136] subsequently obtained nearly comparable accuracy for the three centre nuclear attraction integrals by expanding each Slater orbital in terms of six Gaussian functions in the manner described in Section 1.5. The frequent basis set transformations were noticeably time consuming only for the larger molecule. Routines for manipulating matrices were therefore written with emphasis on execution efficiency. For the MGE method the calculation, storage and rapid manipulation of large numbers of repulsion integrals demanded special attention, as described in Section 3.3. A second problem arose during the iterative solution of

Roothaan's equations. Rounding and truncation errors rapidly accumulated, with the result that the method converged to a wave function which did not have the correct symmetry of the molecule. These difficulties were overcome, as described in the following sections, by making maximum use of molecular symmetry, and by the application of alternative methods of solution of Roothaan's equations.

3.2 Construction of a Symmetry Basis

The use of symmetry and group theory concepts to simplify the solution of the equation $(\underline{F}^{\lambda} - E_i\underline{I})\underline{C}_i^{\lambda} = 0$ has been well described by Cotton[137]. The method will be discussed with particular reference to N_2O_4, which belongs to the molecular point group D_{2h}. The thirty Slater-basis functions can be transformed amongst themselves to form symmetry orbitals, each of which transforms as one of the irreducible representations or symmetry species of D_{2h}. The Hartree-Fock $\underline{F}$ matrix (Equation 1.17) is then formed in this basis. Because the Hartree-Fock Hamiltonian operator F must have the full symmetry of the molecular point group it belongs to the totally symmetric representation. It follows that matrix elements of the form $\langle\psi_i|F|\psi_j\rangle$ are non-zero only if both wave functions ψ_i and ψ_j belong to the same irreducible representation of the point group. When the symmetry orbitals belonging to each irreducible representation are grouped together the $\underline{F}$ matrix in this basis takes block diagonal form:

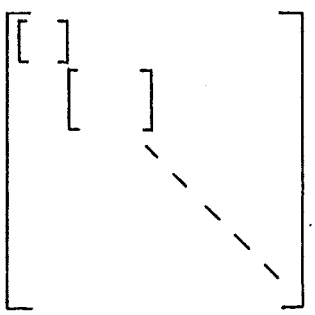

where the elements in each block are non-zero, but all others are zero. The diagonalization of this matrix is then simplified as each block may be separately diagonalized to yield the molecular orbitals belonging to each particular irreducible representation. In choosing the occupied MO's it is normal to take them in order of increasing value of the orbital energy. This may lead to convergence to a configuration which does not have the lowest total energy. The symmetry method overcomes this difficulty because the number of molecular orbitals of each particular symmetry is specified in advance. Different configurations may thus be selected and their total energies compared.

Ideally it would be useful to program the computer to calculate the symmetry orbitals given the molecular point group. The advantage of this would be mainly that of convenience and suggested methods for doing it have recently appeared in the literature[138]. As the results of a calculation on N_2O_4 were the major concern of the present study the symmetry functions were constructed in the following less general manner.

The thirty basis functions form a basis for a reducible representation Γ. The characters of this representation are obtained by acting on each basis function with each of the group symmetry operations in turn. If the function remains unchanged or merely changes sign the contribution to the character is 1 or -1 respectively. Otherwise the contribution is zero. For example, the $2p_x$ orbital on N1 (see Figure 2.3) is left unchanged by I and $\sigma(xz)$ and therefore contributes 1 to the characters of these symmetry operations. Since it is

changed in sign by $\sigma(yz)$ and $C_2(z)$ the corresponding contribution is -1. The characters of the representation Γ for N_2O_4 are given at the foot of the character table for D_{2h} in Appendix I. Γ may be expressed as a linear combination of the eight irreducible representations of D_{2h}. The number of times, a_i, the i^{th} irreducible representation occurs in Γ is calculated from the equation

$$a_i = \frac{1}{h} \sum_R \chi(R)\ \chi_i(R) \tag{3.1}$$

where h is the order of the group (equal to eight for D_{2h}) and $\chi(R)$ and $\chi_i(R)$ are the characters of the reducible and i^{th} irreducible representations corresponding to symmetry operation R. This gives

$$\Gamma = 7A_g + A_u + B_{1g} + 7B_{1u} + 2B_{2g} + 5B_{2u} + 5B_{3g} + 2B_{3u} \tag{3.2}$$

The 30 x 30 $\underline{F}$ matrix is therefore partitioned into blocks of dimensions 7, 1, 1, 7, 2, 5, 5 and 2. A symmetry orbital belonging to the i^{th} irreducible representation is then found by acting on one of the basis functions with a projection operator

$$P_i = \sum_R \chi_i(R)\ \hat{R} \ . \tag{3.3}$$

The resulting unnormalized symmetry orbitals are tabulated in Appendix III. From these the transformation matrix $\underline{X}$ from the Slater basis $\underline{\chi}$ to the symmetry basis $\underline{\sigma}$ is obtained:

$$\underline{\sigma} = \underline{\chi}\ \underline{X} \ . \tag{3.4}$$

The symmetry basis is then transformed to an orthogonal basis designated as a 'Löwdin symmetry' basis $\underline{\lambda}_s$:

$$\underline{\lambda}_s = \underline{\sigma}\ \underline{S}_\sigma^{-\frac{1}{2}}$$

$$= \underline{\chi}\ \underline{B} \tag{3.5}$$

where

$$\underline{B} = \underline{X}\ \underline{S}_\sigma^{-\frac{1}{2}} \tag{3.6}$$

with $\underline{S}_\sigma$ the overlap matrix in the symmetry basis. It follows that

$$\underline{F}^{\lambda_s} = \underline{B}^T\ \underline{F}^{\chi}\ \underline{B} \tag{3.7}$$

and the density matrix $\underline{R}$ transforms as

$$\underline{R}^{\chi} = \underline{B}\ \underline{R}^{\lambda_s}\ \underline{B}^T \tag{3.8}$$

When these two transformations are used in the MGE method, the Hartree-Fock Hamiltonian matrix is formed in the Slater basis and transformed to the Löwdin symmetry basis, which enables each block to be diagonalized separately. The coefficients obtained are used to form a blocked density matrix which is transformed to the Slater basis for use in the next iteration. The accumulation of rounding errors in the non-zero elements is further reduced by writing the whole matrix onto a peripheral disk cartridge and reading it back in such a way that the last few decimal places are truncated. This step is repeated on each iteration.

A complication arose in the SAI method because the repulsion integrals were already calculated in the Löwdin basis; a transformation from that basis to the Löwdin symmetry basis was therefore required. The relationships between the Slater $\underline{\chi}$, atomic $\underline{\eta}$ and Löwdin $\underline{\lambda}$ bases are

$$\underline{\eta} = \underline{\chi}\ \underline{T} \tag{3.9}$$

$$\underline{\lambda} = \underline{\eta}\ \underline{S}_{\eta}^{-\frac{1}{2}} \tag{3.10}$$

Thus

$$\underline{\lambda}_S = \underline{\chi}\ \underline{B} \quad \text{from Equation 3.5}$$

$$= \underline{\lambda}\ \underline{S}_{\eta}^{\frac{1}{2}}\ \underline{T}^{-1}\ \underline{B} \tag{3.11}$$

Using

$$\underline{S}_{\eta} = \underline{T}^{T}\ \underline{S}_{\chi}\ \underline{T} \tag{3.12}$$

gives

$$\underline{S}_{\eta}\ \underline{T}^{-1} = \underline{T}^{T}\ \underline{S}_{\chi} \tag{3.13}$$

so that finally

$$\underline{\lambda}_S = \underline{\lambda}\ \underline{S}_{\eta}^{-\frac{1}{2}}\ \underline{T}^{T}\ \underline{S}_{\chi}\ \underline{B} \tag{3.14}$$

3.3 Use of Symmetry in the Calculation of Repulsion Integrals by Gaussian Expansion

For N basis functions, the total number of two-electron repulsion integrals is N^4. For real orbitals, because the electrons are indistinguishable, the number of unique integrals is reduced to $\frac{1}{4}N(N+1)[\frac{1}{2}N(N+1)+1]$. For example the following eight integrals are equal:

$$\langle\mu\nu|g|\lambda\sigma\rangle,\ \langle\mu\sigma|g|\lambda\nu\rangle,\ \langle\lambda\sigma|g|\mu\nu\rangle,\ \langle\lambda\nu|g|\mu\sigma\rangle,$$

$$\langle\nu\mu|g|\sigma\lambda\rangle,\ \langle\nu\lambda|g|\sigma\mu\rangle,\ \langle\sigma\lambda|g|\nu\mu\rangle,\ \langle\sigma\mu|g|\nu\lambda\rangle \tag{3.15}$$

For N_2O_4 this reduces the total number of repulsion integrals from 810,000 to 108,345; this number may be compared with the number of NDDO integrals, 4095. In a planar molecule such as N_2O_4 the basis functions may be classified as σ or π type depending on their symmetry with respect to the molecular plane. Integrals which involve one or three π functions are identically zero, by symmetry, and this reduces the number of

non-zero integrals which must be evaluated for N_2O_4 to 62,121. The calculation of these integrals would be a formidable undertaking even using an expansion of only two Gaussians per Slater orbital. Fortunately, owing to the symmetry of N_2O_4, small groups of these integrals are equal or differ only in sign. When this symmetry is used the number of integrals actually requiring to be calculated and stored is reduced to 16,093. This procedure has the significant advantage that much less time is used in reading integrals into high speed core during the iterative solution of the SCF equations. Similar considerations apply to the calculation of integrals for nitrogen dioxide, which has fifteen basis functions. The number of integrals found to be non-zero by σ-π symmetry is 4236. This is reduced to 2216 by using the rotation about the $C_2(Z)$ symmetry axis.

The procedure used to sort out the integrals may be described as follows. Each integral $\langle \chi_i \chi_k | g | \chi_j \chi_\ell \rangle$ is distinguished by an integer I formed by combining the subscripts i,j,k,ℓ in order such that $i \leqslant j$, $k \leqslant \ell$, $i < k$. If $i = k$ then $j \leqslant \ell$. Thus each integer I labels at most eight integrals taken from the list 3.15. The molecule is then assumed to be rotated by 180° about each symmetry axis in turn. For example, a rotation about the Z-axis interchanges the orbitals on 01 and 02, and on 03 and 04. The new integral will have the same absolute magnitude but may have a different sign and a different value for the label I. The other two rotations result in two more values for I. Only if the original I is the smallest of these four is the integral calculated and stored.

For the construction of the $\underline{F}$ matrix the integrals are read into high speed core sequentially and used as now described. The subscripts i,j,k,ℓ run over the thirty basis functions in exactly the same order as used in calculating the integrals. Each integral then contributes to the $\underline{F}$ matrix as each of the forms in the list 3.15 which are distinguishable. That is $\langle ik|g|i\ell\rangle$, for instance, also contributes as $\langle i\ell|g|ik\rangle$, $\langle ki|g|\ell i\rangle$, and $\langle \ell i|g|ki\rangle$. The rotations described earlier are then repeated. If the new I value is different the integral will be used again. It may, however, have a different sign and this must first be ascertained. For example a rotation about the z-axis sends $2p_y01$ to $-2p_y02$ so that for this rotation the integral changes sign if there is an odd number of $2p_y$ orbitals.

It should be noted that this sorting procedure is required on every iteration of the SCF scheme. An algorithm designed to avoid this repetition and thereby increase the efficiency of the SCF step has recently appeared in the literature[139].

Several sections in the computer program to calculate the integrals were also rewritten to increase execution speed. The final version of the program calculated the integrals for NO_2, using a two-Gaussian per Slater expansion, in 11 minutes compared with 45 minutes for the original version. The integrals for N_2O_4 were calculated in 90 minutes, compared with an estimate of 11 hours for the original program.

3.4 Alternative Methods of Solving the SCF Equations

It has been pointed out by Sleeman[140] that rounding errors occur in Roothaan's method, not only because of inaccuracies in the atomic integrals, but also as the result of the diagonalization technique. Such errors accumulate at each iteration. Furthermore, for large systems the time taken for each iteration can be significant, and it is therefore expedient to consider methods which converge more rapidly[141,142]. Two methods which will be described in this Chapter are the Steepest Descent method and the method of Conjugate Gradients. Various extrapolation procedures which are designed to assist convergence and have been reported in the literature will be discussed in Section 4.4 in connection with open shell problems.

3.5 The Method of Steepest Descent

This method, proposed by McWeeny[143], has been so fully reviewed elsewhere[144] that only the basic steps will be indicated here.

In the LCAO approximation the Hartree-Fock equation for an orthonormal basis may be written in the form

$$\underline{F}\,\underline{C} = \underline{C}\,\underline{E} \tag{3.16}$$

where the matrices are as defined in Section 1.2. The density matrix takes the form

$$\underline{R} = \underline{C}\,\underline{C}^{T} \tag{3.17}$$

and the total electronic energy

$$E = 2\ \mathrm{tr}\ \underline{R}\,\underline{F} - \mathrm{tr}\ \underline{R}\,\underline{G} \tag{3.18}$$

where the trace of a matrix $\underline{A}$ is defined as tr $\underline{A} = \sum_i A_{ii}$. Since the total energy depends only on $\underline{R}$ the basis of the method is the iterative construction of $\underline{R}$ directly without solving eigenvalue equations to obtain coefficients $\underline{C}$.

The method considers the minimization of ε, the sum of the n lowest eigenvalues,

$$\varepsilon = \text{tr } \underline{E}$$

$$= \text{tr } \underline{R}\ \underline{F} \tag{3.19}$$

subject to the orthonormality restriction

$$\underline{C}^T\ \underline{C} = \underline{1} \tag{3.20}$$

This is equivalent to seeking the unconditional minimum of

$$\varepsilon = \text{tr } \underline{R}\ \underline{F} \tag{3.21}$$

with

$$\underline{R} = \underline{C}'(\underline{C}'^T\ \underline{C}')^{-1}\ \underline{C}'^T \tag{3.22}$$

where $\underline{C}'$ is any matrix with linearly independent but not necessarily orthonormal columns. As

$$\underline{C} \rightarrow \underline{C} + \delta\underline{C} = \underline{C}'$$

then to first order

$$\varepsilon \rightarrow \varepsilon + 2 \text{ tr } \delta\underline{C}^T(\underline{F}\ \underline{C} - \underline{C}\ \varepsilon) \tag{3.23}$$

where matrix $\underline{\varepsilon} = \underline{C}^T\ \underline{F}\ \underline{C}$. (3.24)

Thus ε is reduced most rapidly when the second term in Equation 3.23 has a maximum negative value. This occurs when

$$\delta\underline{C} = -\lambda(\underline{F}\ \underline{C} - \underline{C}\ \varepsilon) \tag{3.25}$$

for some positive λ. It is from this steepest descent that the method derives its name.

The application of the method may be summarized. An approximate $\underline{R}$ is chosen from which are formed the matrices

$$\underline{s} = (\underline{1} - \underline{R})\underline{F}\ \underline{R}$$

$$\underline{I} = \underline{s} + \underline{s}^T$$

and $$\underline{J} = \underline{s} - \underline{s}^T \qquad (3.26)$$

From these a correction to $\underline{R}$ is found according to

$$\delta\underline{R} = -\lambda(\underline{1} + \lambda^2\underline{I}^2)^{-1}(\underline{I} + \lambda\underline{I}\ \underline{J}). \qquad (3.27)$$

λ is determined so that $\delta\underline{R}$ is the best possible correction leading to a minimum in the total energy. Self-consistency is introduced into the method by allowing the matrix $\underline{G}$ to vary continuously as a function of $\underline{R}$. The value of λ can be shown to be

$$\lambda = -a_0/(2b_0 - c_o) \qquad (3.28)$$

where $$a_0 = \text{tr}\ \underline{I}\ \underline{F}$$

$$b_0 = \text{tr}\ \underline{I}\ \underline{J}\ \underline{F}$$

$$c_0 = \text{tr}\ \underline{I}\ \underline{I}'$$

and $$I'_{ab} = \sum_{rs} I_{rs}[2\langle as|g|br\rangle - \langle as|g|rb\rangle] \qquad (3.29)$$

In the present work this method was programmed and checked by a trial calculation on the water molecule. The results converged to a wave function identical with that from Roothaan's method, but took many more iterations - 125 compared with 18. The method was tried for N_2O_4 but here also convergence was too slow, and an alternative method was sought.

3.6 The Method of Conjugate Gradients

As was seen in connection with the steepest descent method, it is possible to express the problem of solving the SCF equations in a form which requires the minimization of the energy as a function of many variables, without any conditional restrictions on these variables. Numerical methods for solving such unconstrained descent problems have been discussed by Kowalik & Osborne[145]. If the function $F(\underline{x})$ is to be minimized with respect to the variables $\underline{x}$ then the application of these methods involves moving from an initial value of $\underline{x}$ to a new value $\underline{y}$ such that F is reduced. Each method uses a different direction vector $\underline{v}$ leading from $\underline{x}$ to $\underline{y}$, and the step length along this vector is found by one-dimensional minimization of $F(\underline{x} + \lambda\underline{v})$ with respect to λ. The steepest descent method uses the negative gradient, $-\nabla F$, as the descent vector at each step. This does not, however, necessarily lead most rapidly to the final minimum. The most powerful direct minimization technique presently available is that of conjugate gradients. The method is described in detail in Appendix IV. It generates at each step descent vectors which are termed conjugate directions. To do this it requires a knowledge of the function and its gradient at any point. The application to the closed shell SCF problem was given by Fletcher[146].

The derivation is simplified by using a slightly different nomenclature from that of Chapter One. The determinantal wave function is the antisymmetrized product of n doubly occupied MO's, $\underline{\phi}$, related to m basis functions, $\underline{\chi}$, by

$$\underline{\phi} = \underline{\chi}\,\underline{C}. \tag{3.30}$$

For nonorthonormal basis functions the orthonormality of the

MO's requires

$$\underline{C}^T \underline{S} \underline{C} = \underline{1} \tag{3.31}$$

where $\underline{S}$ is the overlap matrix for the basis functions. If $\underline{Y}$ is any (m x n) matrix then

$$\underline{C} = \underline{Y}(\underline{Y}^T \underline{S} \underline{Y})^{-\frac{1}{2}} \tag{3.32}$$

satisfies Equation 3.31. $\underline{Y}$ is then varied to find the density matrix $\underline{R} = \underline{C} \underline{C}^T$ which minimizes the electronic energy

$$E = 2\underline{H} : \underline{R} + \underline{R} : \underline{B} : \underline{R} \tag{3.33}$$

where
$$\underline{H} : \underline{R} = \sum_{ij} H_{ij} R_{ij}$$

$$= \text{tr } (\underline{H} \underline{R}^T) \tag{3.34}$$

and

$$B_{ijk\ell} = 2\langle \chi_i \chi_k | g | \chi_j \chi_\ell \rangle - \langle \chi_i \chi_k | g | \chi_\ell \chi_j \rangle. \tag{3.35}$$

An expression for the gradient of E is found as

$$\nabla E = 4(\underline{1} - \underline{S} \underline{R}) \underline{F} \underline{Y} \underline{M} \tag{3.36}$$

where the Hartree-Fock Hamiltonian matrix is

$$\underline{F} = \underline{H} + \underline{B} : \underline{R} \tag{3.37}$$

and

$$\underline{M} = (\underline{Y}^T \underline{S} \underline{Y})^{-1}. \tag{3.38}$$

If the mn elements of $\underline{Y}$ are collected as the vector $\underline{x}$ and the energy gradient corresponding to this $\underline{Y}$ is $g(\underline{x})$ then the conjugate gradient algorithm minimizing the energy $f(\underline{x})$ determines successive values $\underline{x}_0, \underline{x}_1, \ldots$ and is summarized as:

Begin with an arbitrary $\underline{x}_0$.

$$\underline{g}_0 = g(\underline{x}_0); \qquad \underline{p}_0 = -\underline{g}_0 \tag{3.39}$$

Then $$\underline{x}_{i+1} = \underline{x}_i + \alpha_i \underline{p}_i \tag{3.40}$$

where α_i is chosen to minimize $f(\underline{x}_i + \alpha_i \underline{p}_i)$, and

$$\underline{p}_{i+1} = -\underline{g}_{i+1} + \beta_i \underline{p}_i \tag{3.41}$$

where

$$\beta_i = |\underline{g}_{i+1}|^2 / |\underline{g}_i|^2 .$$

Convergence is attained when $\underline{g}_i = \underline{0}$. Since this is unlikely in floating point arithmetic, alternative criteria such as no alteration in $\underline{x}$, or no reduction in $f(\underline{x})$ beyond some tolerance value, must be applied. The basic algorithm was checked by minimizing some analytical functions.

3.7 Comparison of the Methods

Claxton & Smith[147] have compared all three methods in an unrestricted Hartree-Fock calculation on the cyanide radical. They found that the Roothaan method was superior when near the minimum. The best procedure appeared to be to use the conjugate gradients method first, followed by the Roothaan method when about 0.1% from the minimum.

The three methods were tried for N_2O_4 using the approximations of the simplified ab initio method. For comparison purposes the starting density matrix in each case was that obtained after five iterations of Roothaan's method, initialized by diagonalization of the core Hamiltonian matrix. The results for the next three iterations and for the thirtieth iteration are given in Table 3.1. Because of demands on computer time the computations were not carried to convergence and quantitative comparisons are not therefore valid.

Table 3.1 Comparison of Minimization Methods for N_2O_4

Electronic Energies in atomic units

	Roothaan	Steepest Descent	Conjugate Gradients
First approximation	-646.168527	-646.168527	-646.168527
Iteration 1	-646.362805	-646.085551	-647.391199
Iteration 2	-646.772487	-646.663740	-647.527108
Iteration 3	-647.056325	-647.072586	-647.553953
Iteration 30	-648.536895	-648.046541	-648.281080

The comparison was made in order to choose the method which appeared likely to produce a wave function for N_2O_4 most efficiently. The steepest descent and conjugate gradients methods were initially applied in the ordinary Löwdin basis compared with Roothaan's method which used the Löwdin symmetry basis to facilitate diagonalization of the blocked Hartree-Fock Hamiltonian matrix. The steepest descent method was found to converge more slowly than Roothaan's method. However, it appeared, along with the conjugate gradient method, to have much less difficulty with rounding errors than the original Roothaan method in the same basis. These observations are in agreement with the conclusions of Sleeman[140]. It should be pointed out here that at this stage the problem of which configuration to choose had not been investigated; this problem contributed to the large energy differences apparent at the end of thirty iterations in Table 3.1.

The conjugate gradients method can be seen to have produced by far the largest energy decrease on its first application. This method was subsequently used in conjunction

with Roothaan's method, one or two iterations of each being performed alternately. This combined method, using a Löwdin symmetry basis throughout, produced convergence in the total energy after 20 iterations, as compared with 54 for the Roothaan method alone. The execution times for these two methods were comparable because each conjugate gradient iteration took a relatively long time. All the closed shell wave functions given in Chapter Six were calculated by this combined Roothaan-Conjugate Gradients method. A discussion of the convergence criteria appropriate to the different methods and molecular systems is given in Section 6.1.

CHAPTER FOUR

OPEN SHELL METHODS

4.1 Introduction

Extension of the closed shell theory presented in Chapter One to treat the case of open shells where some molecular orbitals are occupied by only one electron leads to some computational difficulties[2,86]. For a determinantal function representing a closed shell state the Hartree-Fock SCF equations may be written in the form[18]

$$F\phi_i = \sum_j \phi_j \, \varepsilon_{ji} \qquad (4.1)$$

where F is the Hartree-Fock Hamiltonian operator, ϕ_i are the doubly occupied molecular orbitals and ε_{ji} are Lagrangian multipliers introduced into the theory to ensure orthonormality of the molecular orbitals. A unitary transformation of the occupied orbitals ϕ_i amongst themselves leaves the total wave function and energy unchanged. For real orbitals this transformation becomes an orthogonal transformation which may be represented by a matrix $\underline{T}$ with the property $\underline{T}^{-1} = \underline{T}^{T}$. The transformation may be chosen to eliminate the off-diagonal ε_{ji} so that the Hartree-Fock-Roothaan equations take the pseudo-eigenvalue form

$$F \, \phi_i = \varepsilon_i \, \phi_i \, . \qquad (4.2)$$

In an open shell system some of the orbitals, the closed shell set, are doubly occupied and others, the open shell set, are singly occupied. A transformation which leaves the operators invariant transforms the orbitals of these two sets within themselves but in general it is not possible to

eliminate rigorously the off-diagonal multipliers coupling the two sets. For particular classes of open shell molecules Roothaan[80] was able to cast the equations into pseudo-eigenvalue form by absorbing the off-diagonal multipliers into coupling operators. The most important class is the half closed-shell system, in which the open shell subset is occupied by electrons with parallel spins. The method is called Restricted Hartree Fock (RHF) because the closed shell is formed by taking each spatial orbital with the two different spin functions. Roothaan showed further that the doubly and singly occupied MO's could be obtained as the solution of a single eigenvalue equation. Walker[148,149] has recently pointed out, however, that errors may arise when there are closed shell orbitals of the same symmetry as an open shell orbital. McWeeny[17,82] has given a mathematically equivalent formulation of the RHF method for half closed-shell systems.

4.2 McWeeny's Formulation of the Open Shell Method

The n_1 MO's of the closed shell and n_2 orbitals of the open shell are expressed as linear combinations of basis functions by the coefficient matrices $\underline{C}_1$ and $\underline{C}_2$ respectively. The theory below pertains to the orthonormal basis functions but it can be modified to accommodate non-orthonormal functions. Density matrices for each shell are defined by

$$\underline{R}_1 = \underline{C}_1 \underline{C}_1^T \quad \text{and} \quad \underline{R}_2 = \underline{C}_2 \underline{C}_2^T. \tag{4.3}$$

The electronic energy can then be written as[150]

$$E = 2 \text{ tr } \underline{R}_1(\underline{H}+\tfrac{1}{2}\underline{G}_1) + \text{tr } \underline{R}_2(\underline{H}+\tfrac{1}{2}\underline{G}_2) \tag{4.4}$$

where $\underline{H}$ is the core Hamiltonian matrix,

$$\underline{G}_1 = 2\underline{G}(\underline{R}_1) + \underline{G}(\underline{R}_2),$$

$$\underline{G}_2 = 2\underline{G}(\underline{R}_1) + \underline{G}'(\underline{R}_2),$$

with

$$\underline{G}(\underline{R}) = \underline{J}(\underline{R}) - \tfrac{1}{2}\underline{K}(\underline{R})$$

and $$\underline{G}'(\underline{R}) = \underline{J}(\underline{R}) - \underline{K}(\underline{R}). \qquad (4.5)$$

The Coulomb and exchange matrices have elements defined in terms of the basis functions by

$$J(\underline{R})_{\mu\nu} = \sum_{\lambda\sigma} R_{\sigma\lambda} \langle \chi_\mu \chi_\lambda | g | \chi_\nu \chi_\sigma \rangle \qquad (4.6)$$

$$K(\underline{R})_{\mu\nu} = \sum_{\lambda\sigma} R_{\sigma\lambda} \langle \chi_\mu \chi_\lambda | g | \chi_\sigma \chi_\nu \rangle \qquad (4.7)$$

The requirement that all the MO's be orthonormal is expressed by conditions on the density matrices as

$$\underline{R}_1^{\,2} = \underline{R}_1, \quad \underline{R}_2^{\,2} = \underline{R}_2 \quad \text{and} \quad \underline{R}_1 \cdot \underline{R}_2 = \underline{0}. \qquad (4.8)$$

The energy is then minimized subject to these constraints. The first order variation in the energy is

$$\delta E = 2 \text{ tr } \underline{h}_1 \, \delta\underline{R}_1 + \text{tr } \underline{h}_2 \, \delta R_2 \qquad (4.9)$$

where

$$\underline{h}_1 = \underline{H} + \underline{G}_1 \quad \text{and} \quad \underline{h}_2 = \underline{H} + \underline{G}_2. \qquad (4.10)$$

The matrices $\underline{R}_1$ and $\underline{R}_2$ are said to define projection operators. Thus if $\underline{t}$ is an arbitrary column matrix $\underline{R}_1\underline{t}$ and $\underline{R}_2\underline{t}$ are the components of $\underline{t}$ lying in the subspaces spanned by the doubly and singly occupied MO's respectively. Similarly $\underline{R}_3 = \underline{1} - \underline{R}_1 - \underline{R}_2$ projects an arbitrary orbital onto the subspace spanned by the vacant MO's.

When the variations in $\underline{R}_1$ and $\underline{R}_2$ are substituted into the orthonormality conditions it is found that the most general

first order variations may be expressed in the form

$$\delta\underline{R}_1 = (\underline{x}_1 + \underline{x}_1^T) + (\underline{x}_0 + \underline{x}_0^T)$$

$$\delta\underline{R}_2 = (\underline{x}_2 + \underline{x}_2^T) - (\underline{x}_0 + \underline{x}_0^T) \qquad (4.11)$$

where $\underline{x}_1 = \underline{R}_1 \underline{X} \underline{R}_3$, $\underline{x}_2 = \underline{R}_2 \underline{Y} \underline{R}_3$, $\underline{x}_0 = \underline{R}_1 \underline{Z} \underline{R}_2$ (4.12)

and $\underline{X}$, $\underline{Y}$ and $\underline{Z}$ are arbitrary symmetric matrices. When the expressions for $\delta\underline{R}_1$ and $\delta\underline{R}_2$ of Equation 4.11 are substituted in Equation 4.9 with $\delta E = 0$ three equations result:

$$\underline{R}_1 \underline{h}_1 \underline{R}_3 = \underline{0}$$

$$\underline{R}_2 \underline{h}_2 \underline{R}_3 = \underline{0}$$

$$\underline{R}_1 (2\underline{h}_1 - \underline{h}_2) \underline{R}_2 = \underline{0}. \qquad (4.13)$$

These conditions may be shown to be equivalent to

$$\underline{\bar{h}}\,\underline{R}_i - \underline{R}_i\,\underline{\bar{h}} = \underline{0} \qquad (i = 1,2) \qquad (4.14)$$

where the effective Hamiltonian $\underline{\bar{h}}$ is

$$\underline{\bar{h}} = a(\underline{1}-\underline{R}_2)\underline{h}_1(\underline{1}-\underline{R}_2) + b(\underline{1}-\underline{R}_1)\underline{h}_2(\underline{1}-\underline{R}_1)$$

$$+ c(\underline{R}_1+\underline{R}_2)(2\underline{h}_1-\underline{h}_2)(\underline{R}_1+\underline{R}_2) \qquad (4.15)$$

for arbitrary non-zero a, b, c. The solution of Equation 4.14 is found by solving the eigenvalue equation

$$\underline{\bar{h}}\,\underline{C} = \underline{C}. \qquad (4.16)$$

At each iteration the matrices $\underline{C}_1$, formed from the first n_1 eigenvectors and $\underline{C}_2$, formed from the next n_2 eigenvectors, are used to create a new $\underline{\bar{h}}$ matrix for the next iteration. Convergence is attained when the density matrices cease changing beyond a small tolerance value.

One of the major computational difficulties of this method is that the solution tends to oscillate and convergence is not easily obtained. It has been suggested[151] that this oscillation may result from incorrect choice of the eigenvectors at each iteration. In the open-shell RHF theory the eigenvalues have no physical significance, so that a selection based on them is not necessarily valid. In the work of this project the eigenvectors were selected using the criterion proposed by Dodds & McWeeny[152] described in the next section.

4.3 Choice of Eigenvectors in the Open Shell Method

For closed shell systems the eigenvalue, or orbital energy, of an occupied MO can be identified with the negative value of the ionization energy for an electron in that orbital. It is here assumed that the positive ion is adequately described in terms of MO's pertaining to the ground state of the parent molecule. This result, known as Koopmans' Theorem[153], does not hold for the open shell case[154], where the eigenvalues depend on the choice of the arbitrary constants a, b, c in Equation 4.15. Dodds & McWeeny[152] considered the problem on the basis of the same assumption for the ionized state. Suppose eigenvectors X, Y and Z are represented by column vectors $\underline{C}_X$, $\underline{C}_Y$ and $\underline{C}_Z$ in the doubly occupied, singly occupied and empty subspaces respectively. Thus, for example

$$\underline{R}_1 = \sum_X \underline{C}_X \, \underline{C}_X^T \qquad (4.17)$$

where the summation is over the doubly occupied orbitals. When an electron is removed from orbital X this orbital becomes an open shell orbital.

Hence

$$\underline{R}_1 \rightarrow \underline{R}_1 - \underline{C}_X \underline{C}_X^T$$

and

$$\underline{R}_2 \rightarrow \underline{R}_2 + \underline{C}_X \underline{C}_X^T \quad . \tag{4.18}$$

The substitution of $\delta\underline{R}_1 = - \underline{C}_X \underline{C}_X^T$ and $\delta\underline{R}_2 = \underline{C}_X \underline{C}_X^T$ into the expression for the first order variation in the energy, Equation 4.9, gives an approximation to the ionization energy from a closed shell orbital as

$$\delta E(X \rightarrow \infty) = -\underline{C}_X^T (2\underline{h}_1 - \underline{h}_2)\underline{C}_X \quad . \tag{4.19}$$

Similar considerations when applied to the open shell lead to the result

$$\delta E(Y \rightarrow \infty) = - \underline{C}_Y^T \underline{h}_2 \underline{C}_Y \quad . \tag{4.20}$$

The energy change for promoting a closed shell electron to an open shell orbital may be obtained by considering a two step process in which the electron is first removed to infinity and then brought back to the open shell. Because, in this second step, the original X orbital now contains only one electron, an extra Coulomb-exchange integral term is required. The result is

$$\delta E(X \rightarrow Y) = - \underline{C}_X^T (2\underline{h}_1 - \underline{h}_2)\underline{C}_X + \underline{C}_Y^T (2\underline{h}_1 - \underline{h}_2)\underline{C}_Y$$

$$- (\langle XY|g|XY\rangle - \langle XY|g|YX\rangle) \tag{4.21}$$

For NO_2, for which the RHF method was used, there is only one open shell orbital. The procedure adopted for selecting the orbitals was as follows. The calculations were performed in the Löwdin symmetry basis, with the orbital configuration specified at the beginning of execution. On each iteration

$\delta E(X \to \infty)$ and $\delta E(Y \to \infty)$ were calculated for each orbital. Within each group of orbitals of a particular symmetry the closed shell orbitals were selected as those having the largest $\delta E(X \to \infty)$; if there was an open shell orbital of that particular symmetry type it was chosen from the remaining orbitals as the one with the largest $\delta E(Y \to \infty)$. At convergence the promotion energy from every closed shell orbital to the open shell orbital was calculated by Equation 4.21. In this way a guide was obtained for choosing the lowest energy configuration. For example, as shown in Section 6.3, when only NDDO repulsion integrals were used the $^2A_1$ state produced a negative value for the promotion energy of an electron from the $1a_2$ closed shell orbital to the singly occupied $6a_1$ orbital. To this level of approximation it was indeed found by a subsequent calculation that the lowest energy configuration was a $^2A_2$ state with the unpaired electron in the $1a_2$ orbital.

Fink[83] gave a similar analysis specifically for the case of NO_2. He obtained the same expression for the open shell ionization energy, but a slightly different closed shell value corresponding to ionization to a hypothetical state neither singlet nor triplet. This value was found by averaging the results for ionization of closed shell α and β electrons and is further discussed in Section 6.3.

4.4 Extrapolation Methods

The solution of the open shell SCF equations by the diagonalization method often does not converge because of oscillations[140]. McWeeny[150] extended his closed shell steepest descent method to treat half-closed shell systems. Although this method does not produce oscillations Sleeman[140]

has pointed out that convergence is slow. The choice of initial density matrices is also considered to have an important effect on the rate of convergence of both these methods[155]. Use of the method of conjugate gradients for an open shell system has been reported for an isolated example[156] but a comparison of the rate of convergence with that obtained by other methods was not made.

In general the convergence of the SCF method is usually improved by using extrapolation formulae which choose a new density matrix by comparing the current matrix with those of the preceeding one or two iterations. These formulae serve only to increase the rate of convergence and unfortunately do not appear to bring about convergence in a divergent case. Well known methods are available[140,157]; the following method was used in this work.

The extrapolation is performed every three iterations for the successive density matrices $\underline{R}_i$, $\underline{R}_{i+1}$, $\underline{R}_{i+2}$ where $\underline{R}_{i+2}$ is the current matrix. In case the matrices are varying too rapidly the ratio

$$T = \frac{R_{i+2} - R_{i+1}}{2R_{i+1} - R_i - R_{i+2}} \tag{4.22}$$

is calculated for each matrix element. No extrapolation is performed if the absolute value of this ratio is greater than 2.0. Otherwise the extrapolated value is obtained as

$$R = R_{i+2} + T(R_{i+2} - R_{i+1}). \tag{4.23}$$

After the extrapolation it is necessary to reorthonormalize the coefficient vectors. This is most easily done by restoring idempotency to the density matrix.

Since $\underline{R} = \underline{C}\,\underline{C}^T$ with $\underline{C}^T\,\underline{C} = \underline{1}$

$$\underline{R}^2 = \underline{C}\,\underline{C}^T\,\underline{C}\,\underline{C}^T$$

$$= \underline{C}\,\underline{C}^T$$

i.e. $$\underline{R}^2 = \underline{R} \qquad (4.24)$$

in which case $\underline{R}$ is said to be idempotent. McWeeny[143] has given a steepest descent method for constructing an idempotent matrix from one which is only approximately so. The formula

$$\underline{R}_{n+1} = \underline{R}_n^{\,2}\,(3\underline{I} - 2\underline{R}_n) \qquad (4.25)$$

gives a sequence $\underline{R}_0$, $\underline{R}_1$, $\underline{R}_2$ ... of increasingly good approximations for $\underline{R}$.

4.5 The Unrestricted Hartree-Fock Method

For comparison purposes, and in order to check some of the integral programs, a calculation was performed on NO_2 using the Unrestricted Hartree-Fock (UHF) method[158,159] with the MGE technique. As the method has been reviewed by Williams[8] only a brief outline will be given here.

The method differs from RHF in that the spatial orbitals associated with α spin are allowed to differ from those with β spin. The number of variational parameters is therefore increased and the method produces a lower energy than the RHF value[160]. A major disadvantage of the method is that the single determinant is no longer an eigenfunction of the total spin operator S^2. It cannot therefore strictly represent a spectroscopic state[17].

The single determinantal wave function for an N electron system with n_α and n_β electrons of α and β spins respectively may be written

$$\Psi = (N!)^{-\frac{1}{2}} \det|\psi_1\psi_2 \cdots \psi_{n_\alpha}\phi_1\phi_2 \cdots \phi_{n_\beta}| \tag{4.26}$$

where ψ_i have α spin and ϕ_i have β spin. The spatial factors of these orbitals are expanded in terms of basis functions $\underline{\chi}$ which are here assumed to be orthonormal.

$$\psi_i = \sum_\mu \chi_\mu \, C^\alpha_{\mu i} \quad \text{and} \quad \phi_i = \sum_\mu \chi_\mu \, c^\beta_{\mu i} \tag{4.27}$$

There result two $\underline{R}$ matrices:

$$\underline{R}^\alpha = \underline{C}^\alpha \, \underline{C}^{\alpha T} \quad \text{and} \quad \underline{R}^\beta = \underline{C}^\beta \, \underline{C}^{\beta T} \tag{4.28}$$

The total energy is given by

$$\begin{aligned} E &= \langle\Psi|\hat{H}|\Psi\rangle \\ &= \tfrac{1}{2} \operatorname{tr} \underline{R}^\alpha(\underline{H}+\underline{F}^\alpha) + \tfrac{1}{2} \operatorname{tr} \underline{R}^\beta(H+\underline{F}^\beta) \end{aligned} \tag{4.29}$$

where $\underline{H}$ is the core Hamiltonian matrix and

$$\begin{aligned} F^\alpha_{\mu\nu} = H_{\mu\nu} &+ \sum_{\lambda\sigma} (R^\alpha_{\sigma\lambda} + R^\beta_{\sigma\lambda}) \langle\chi_\mu\chi_\lambda|g|\chi_\nu\chi_\sigma\rangle \\ &- \sum_{\lambda\sigma} R^\alpha_{\sigma\lambda} \, \langle\chi_\mu\chi_\lambda|g|\chi_\sigma\chi_\nu\rangle \end{aligned} \tag{4.30}$$

and

$$\begin{aligned} F^\beta_{\mu\nu} = H_{\mu\nu} &+ \sum_{\lambda\sigma} (R^\alpha_{\sigma\lambda} + R^\beta_{\sigma\lambda}) \, \langle\chi_\mu\chi_\lambda|g|\chi_\nu\chi_\sigma\rangle \\ &- \sum_{\lambda\sigma} R^\beta_{\sigma\lambda} \, \langle\chi_\mu\chi_\lambda|g|\chi_\sigma\chi_\nu\rangle \, . \end{aligned} \tag{4.31}$$

When the energy is minimized subject to orthonormality constraints two pseudo-eigenvalue equations result:

$$\underline{F}^\alpha \, \underline{C}_i{}^\alpha = \varepsilon_i{}^\alpha \, \underline{C}_i{}^\alpha \tag{4.32}$$

and

$$\underline{F}^\beta \, \underline{C}_i{}^\beta = \varepsilon_i{}^\beta \, \underline{C}_i{}^\beta \tag{4.33}$$

As for the Hartree-Fock-Roothaan closed shell equation, the column vectors $\underline{C}_i$, determined by diagonalization of the $\underline{F}$

matrices, are used to construct $\underline{R}^{\alpha}$ and $\underline{R}^{\beta}$ for the next iteration until self-consistency is achieved. In contrast with the RHF method the eigenvalues ε_i obtained in the UHF method represent orbital energies and approximate to negative ionization potentials in accordance with Koopmans' Theorem.

CHAPTER FIVE

INTERPRETATION OF CALCULATED WAVE FUNCTIONS

5.1 Uncertainties in the Wave Function

Although the methods described in Chapters One, Three and Four all calculate the wave function that gives the lowest energy under the particular set of approximations employed, it does not necessarily follow that the total energy is the best criterion for gauging the quality of a wave function[4,5]. That this is so can be seen from the following analysis, given by Goodisman & Klemperer[161].

Let Φ be an approximation to the exact wave function Ψ, such that

$$\Psi = (1 - \tfrac{1}{2}\varepsilon^2)\Phi + \varepsilon X \qquad (5.1)$$

where X is the correction to Φ and the small quantity ε is a parameter which measures the error in Φ. The factor $(1 - \tfrac{1}{2}\varepsilon^2)$ ensures normalization to fourth order in ε. It is not difficult to show that to second order in ε

$$E_{approx} = \langle\Phi|\hat{H}|\Phi\rangle$$

$$= E_{exact} + \varepsilon^2[\langle X|\hat{H}|X\rangle - E_{exact}]. \qquad (5.2)$$

Thus the energy calculated from any approximate wave function is correct to second order in ε. The energy therefore, is not sensitive to small changes in the wave function; two substantially different functions may give closely similar energies. The expectation value of an operator Q which commutes with the Hamiltonian $\hat{H}$ is also correct to second order in ε because Ψ is then an eigenfunction of Q. That is

$$\langle Q\rangle_{approx} = \langle Q\rangle_{exact} + \varepsilon^2[\langle X|Q|X\rangle - \langle Q\rangle_{exact}] \qquad (5.3)$$

If Q does not commute with $\hat{H}$ the expectation value is correct only to first order and is given by

$$\langle Q\rangle_{approx} = \langle Q\rangle_{exact} - \varepsilon[\langle X|Q|\Psi\rangle + \langle\Psi|Q|X\rangle] + \varepsilon^2[\langle Q\rangle_{exact} + \langle X|Q|X\rangle] \qquad (5.4)$$

If Φ is a single determinant Hartree-Fock wave function for a closed shell system then Brillouin's theorem[25,26] states that the first order correction to Φ (in this case the leading term in X) is orthogonal to Φ in two electronic coordinates. Consequently, if Q is a sum of one-electron operators, then $\langle X|Q|\Phi\rangle$ vanishes and Equation 5.4 simplifies to

$$\langle Q\rangle_{approx} = \langle Q\rangle_{exact} - \varepsilon^2[\langle X|Q|X\rangle - \langle Q\rangle_{exact}] \qquad (5.5)$$

As a result, if the approximate wave function is not near the Hartree-Fock limit, values of one-electron properties such as dipole moment $\langle r\rangle$ or mean square radius for an electron $\langle r^2\rangle$ will have errors tending to first order in ε. In the LCAO MO approximation some one-electron properties should be more accurate than others, depending on the size of the basis set and the type of basis functions used. It is clear that the analysis of properties other than the energy should be used in the evaluation of an approximate method. This analysis was thoroughly done by Williams[8] for the MGE method, as mentioned in Section 1.6. In general the quality of a wave function is best considered with respect to the operator under consideration. For example, the Hartree-Fock wave function, since it is based on the independent-particle model, should give reasonable one electron properties, but would not be

expected to deal with energies very well because of the lack of allowance for electron correlation.

Some of the ways that can be used to interpret numerical wave functions in terms of traditional chemical concepts will be mentioned in the next sections.

5.2 Electron Population Analyses

The most widely used method for analysing a wave function built up from a basis set of atomic orbitals is Mulliken's population analysis[162]. This method is used to partition the electronic charge into atomic and overlap populations according to the following scheme[163].

Each MO, occupied by N_i electrons, is written as

$$\phi_i = \sum_{r_k} \chi_{r_k} C_{r_k i} \tag{5.6}$$

where the subindex k labels the different nuclei. The number of electrons occupying the atomic orbital χ_{r_k} in the MO ϕ_i is $N_i C^2_{r_k i}$. If $\underline{S}$ is the overlap matrix between atomic orbitals, then

$$n(i;r_k,s_\ell) = 2 N_i C_{r_k i} C_{s_\ell i} S_{r_k s_\ell} \tag{5.7}$$

is a measure of the charge associated with the pair of atomic orbitals χ_{r_k} and χ_{s_ℓ}, and is termed a partial overlap population in MO ϕ_i. In the Mulliken analysis this charge is assumed to be divided equally between the two orbitals and the partial gross population in MO ϕ_i and AO χ_{r_k} is accordingly defined as

$$N(i;r_k) = N_i C_{r_k i} (C_{r_k i} + \sum_{s_\ell \neq r_k} C_{s_\ell i} S_{r_k s_\ell}) \tag{5.8}$$

The subtotal gross population in ϕ_i on atom k is

$$N(i;k) = \sum_{r}^{\text{atom } k} N(i;r_k), \tag{5.9}$$

and the gross population on atom k is

$$N(k) = \sum_{i} N(i;k). \tag{5.10}$$

From the last expression the Mulliken atomic charges are calculated as

$$Q(k) = Z_k - N(k) \tag{5.11}$$

where Z_k is the nuclear charge on atom k. For the comparisons given in Chapter Six it will be useful to have a measure of the net population in each atomic orbital χ_{r_k}. This is defined by

$$N(r_k) = \sum_{i} N_i C_{r_k i}\left(C_{r_k i} + \sum_{s}^{\text{atom } k} C_{s_k i} S_{r_k s_k}\right) \tag{5.12}$$

where the second term is necessary for a Slater basis since the 1s and 2s orbitals on the same atom are not orthogonal.

The following overlap populations may also be calculated and used for describing the covalent bonding. The subtotal overlap population in MO ϕ_i between atoms k and ℓ is

$$n(i;k,\ell) = \sum_{r}^{\text{atom } k} \sum_{s}^{\text{atom } \ell} n(i;r_k,s_\ell) \tag{5.13}$$

leading to the subtotal overlap population for the i^{th} MO

$$n(i) = \sum_{k,\ell} n(i;k,\ell) \tag{5.14}$$

The MO is said to be bonding, antibonding or nonbonding according as n(i) is positive, negative or close to zero. The subtotal overlap population between atoms k and ℓ is

$$n(k,\ell) = \sum_{i} n(i;k,\ell) \tag{5.15}$$

and the total overlap population $n = \sum_{i} n(i)$.

The value of this population analysis is limited as can be seen from the following considerations[164]. First, the partitioning obtained is dependent on the choice of basis set. To take an extreme case, it is possible to obtain an accurate wave function from a large basis of functions all centred on one atom. In this situation the Mulliken analysis will apportion the electronic charge of the whole molecule onto this atom. A second criticism results from the assumption of dividing equally the overlap population between two atoms. This is justified only for identical atoms. While other partitioning methods have been suggested[6,163], none is entirely satisfactory and other methods of interpreting the wave function must be considered.

5.3 Electron Density Maps

An important way of displaying the information in a wave function is by using a computer to draw contour maps of the electron density. This is discussed most conveniently in terms of density matrix theory[14].

A spinless electron density function is defined as

$$P(\underline{r}) = \int \rho_1(\underline{x})\, ds \tag{5.16}$$

where $\underline{x}$ stands for both spatial, $\underline{r}$, and spin, s, coordinates. The first order density matrix $\rho_1(\underline{x};\underline{x}')$ for a single determinantal wave function constructed from orthonormal molecular spin orbitals ψ_i takes the form of the Fock-Dirac density matrix:

$$\rho_1(\underline{x};\underline{x}') = \sum_{\substack{i \\ occ}} \psi_i(\underline{x})\ \psi_i^*(\underline{x}') \tag{5.17}$$

$\rho_1(\underline{x})$ in Equation 5.16 is given by

$$\rho_1(\underline{x}) = \rho_1(\underline{x};\underline{x}) \tag{5.18}$$

Integrating Equation 5.16 over the spin coordinates therefore gives

$$P(\underline{r}) = \sum_{\substack{i \\ occ}} |\psi_i(\underline{r})|^2 \tag{5.19}$$

$P(\underline{r})d\underline{r}$ is the probability of finding an electron of either spin in the volume element $d\underline{r}$ at position $\underline{r}$ when the positions of all other electrons are arbitrary.

$P(\underline{r})$ is plotted as a function of $\underline{r}$ to show the electronic distribution in a molecule. This is done by calculating $P(\underline{r})$ at each point of a grid in some specified plane through the molecule. Contours are then drawn by connecting positions of equal $P(\underline{r})$ using linear interpolation between the grid points. The redistribution of electron charge upon molecule formation can be obtained by plotting difference maps in which the density from the component atoms or molecular fragments has been subtracted from the total molecular density. The density may also be plotted for individual orbitals as $|\psi_i(\underline{r})|^2$. While these orbitals are not unique (see the next section) these orbital maps are useful in showing ways in which the total density is built up.

5.4 Localized Orbitals

For a closed shell determinantal wave function the MO's found by diagonalizing the Hartree-Fock matrix are solutions of an eigenvalue equation. They are termed canonical MO's and transform as irreducible representations of the molecular point group. They are not unique, however, and as mentioned in Section 4.1 a unitary transformation of these orbitals amongst themselves leaves the total wave function invariant[18].

In recent years much attention has been given to methods of transforming the canonical orbitals to orbitals which are more easily related to traditional chemical concepts such as bonding, inner shell, and lone pair orbitals. These orbitals have been called localized MO's, in contrast to the canonical orbitals which are delocalized over the whole molecule. Different criteria have been proposed for defining localized orbitals. Their properties and applications as well as the methods for calculating them have recently been reviewed[165-166].

Two widely used methods which generate the localized orbitals directly from the canonical orbitals are due to Foster & Boys[167] and Boys[168] and to Edmiston & Ruedenberg[169]. Both methods are classified as intrinsic as they do not require any specific geometrical features for their calculation; thus the localized orbitals are not necessarily related to the molecular symmetry. The Edmiston-Ruedenberg method is based on maximizing the "sum of orbital self-interaction energies", $\sum_k \langle \phi_k \phi_k | g | \phi_k \phi_k \rangle$ and requires a knowledge of all the two electron integrals. Especially for larger systems, it is more demanding on computer time than the method of Foster and Boys. For this reason, and also because not all the repulsion integrals were available for the SAI wave function, the method of Foster & Boys was used in this project. It may be described as follows.

The localized or exclusive orbitals are defined as those orthonormal linear combinations of the occupied canonical MO's which minimize the function

$$I = \sum_a \langle \phi_a \phi_a | r_{12}^2 | \phi_a \phi_a \rangle \qquad (5.20)$$

This condition may be cast in different forms as follows. Define $\underline{R}_a$, the centroid of the orbital ϕ_a, by

$$\underline{R}_a = \langle \phi_a | \underline{r}_1 | \phi_a \rangle \tag{5.21}$$

and let $$\underline{r}_{1a} = \underline{r}_1 - \underline{R}_a \tag{5.22}$$

Then

$$\begin{aligned} I &= \sum_a \langle \phi_a \phi_a | (\underline{r}_{1a} - \underline{r}_{2a})^2 | \phi_a \phi_a \rangle \\ &= 2 \sum_a \langle \phi_a | r_{1a}^2 | \phi_a \rangle - 2 \sum_a \langle \phi_a \phi_a | (\underline{r}_1 - \underline{R}_a) . (\underline{r}_2 - \underline{R}_a) | \phi_a \phi_a \rangle \\ &= 2 \sum_a \langle \phi_a | r_{1a}^2 | \phi_a \rangle \end{aligned} \tag{5.23}$$

where the second term has vanished because of the definition of $\underline{R}_a$, Equation 5.21. The exclusive orbitals therefore minimize the sum of the quadratic moments of each orbital about its centroid, a result which emphasizes the localized nature of these orbitals. Alternatively

$$\begin{aligned} I &= \sum_a \langle \phi_a \phi_a | (\underline{r}_1 - \underline{r}_2)^2 | \phi_a \phi_a \rangle \\ &= 2 \sum_a \langle \phi_a | r_1^2 | \phi_a \rangle - 2 \sum_a R_a^2 . \end{aligned} \tag{5.24}$$

Since the first term in Equation 5.24 is invariant under a unitary transformation of the orbitals, the exclusive orbitals may be found by maximizing $\sum_a R_a^2$. This is indeed the simplest way of obtaining the orbitals since only the dipole moment matrices are required. The method used for this maximization was derived from Edmiston & Ruedenberg's account[169] and is given in Appendix V.

In conclusion Boys showed that minimization of I is equivalent to maximization of J, the sum of the squares of the distances between the centroids of the orbitals.

$$J = \sum_{ab} (\underline{R}_a - \underline{R}_b)^2$$

$$= 2n \sum_a R_a^2 - 2 \sum_{ab} \underline{R}_a \cdot \underline{R}_b$$

$$= 2n \sum_a R_a^2 - 2[\Sigma_a \langle \phi_a | \underline{r}_1 | \phi_a \rangle]^2 \qquad (5.25)$$

where n is the number of occupied orbitals. Since the second term is invariant under a unitary transformation of the orbitals maximization of J is equivalent to maximization of $\sum_a R_a^2$.

5.5 Bond Energy Analysis

A further aid in interpreting the wave function is a means of partitioning the energy in much the same manner as the Mulliken population analysis partitions electron density. Clementi[27,170-173] has proposed such a bond energy analysis, in which the total energy is divided into one-, two-, three- and four-centre components. This scheme should be useful for rationalizing some features of the wave function, such as the transferability of bond energies. Since the partitioning is essentially arbitrary, in that it assumes basis functions on a given atom are to be associated with the energy contribution of the same atom, and since the values obtained do not correspond to physical observables, its predictive use in a particular problem cannot be guaranteed. Clementi showed that the energy could be further broken down into orbital contributions but this extension was not pursued in this project.

The break-down of the total energy is given by

$$E = \sum_A E_A + \sum_{AB} E_{AB} + \sum_{ABC} E_{ABC} + \sum_{ABCD} E_{ABCD} \qquad (5.26)$$

where A, B, C, D are indices running over the atoms. Each

term is obtained by writing the total energy in terms of integrals over atomic basis functions. For example, the energy for a closed shell system, Equation 1.21, becomes

$$E_{tot} = 2\sum_{\mu\nu} H_{\mu\nu}R_{\mu\nu} + \sum_{\mu\nu\lambda\sigma} [2\langle\chi_\mu\chi_\lambda|g|\chi_\nu\chi_\sigma\rangle - \langle\chi_\mu\chi_\lambda|g|\chi_\sigma\chi_\nu\rangle]R_{\mu\nu}R_{\lambda\sigma} + \sum_{AB}\frac{Z_A Z_B}{r_{AB}} \quad (5.27)$$

The kinetic energy part of $H_{\mu\nu}$, $\langle\chi_\mu|-\frac{1}{2}\nabla^2|\chi_\nu\rangle$ contributes with a coefficient $2R_{\mu\nu}$ to the one- or two-centre energies depending on the atoms on which χ_μ and χ_ν are situated. The nuclear attraction integral $\langle\chi_\mu|-\frac{Z_A}{r_A}|\chi_\nu\rangle$ will contribute to the three-centre energy if χ_μ and χ_ν are on atoms different from A. In practice the easiest way of partitioning the large number of repulsion integrals is to take each in turn so that $\langle\chi_\mu\chi_\lambda|g|\chi_\nu\chi_\sigma\rangle$ contributes with a coefficient $(2R_{\mu\nu}R_{\lambda\sigma} - R_{\mu\sigma}R_{\lambda\nu})$ to any one of the terms depending on the atoms to which the four atomic orbitals belong. The nuclear repulsion term contributes only to the two-centre "bond energy" term. A similar expression is obtained for the RHF energy, Equation 4.4. As shown in Chapter Six, the two-centre bond energies so obtained closely parallel Mulliken overlap populations.

CHAPTER SIX

RESULTS OF CALCULATIONS

6.1 Introduction

The calculations described in this Chapter were carried out by the several methods, at various levels of approximation, as previously outlined. All molecular orbitals were obtained as linear combinations of real Slater-type atomic orbitals. For nitrogen and oxygen the orbital exponents were best atom zetas[174] which optimize the energy of the isolated atoms. The values used are given in Table 6.1.

Table 6.1

Orbital Exponents

N	1s	6.6652
	2s	1.9236
	2p	1.9170
O	1s	7.6580
	2s	2.2461
	2p	2.22625
H	1s	1.0

The atom Cartesian coordinates for all systems are given in Appendix II. Where possible molecular symmetry was used to form symmetry orbitals from the Slater basis functions. The symmetry orbitals, calculated by the method of Section 3.2, are given in Appendix III. In addition the computation of non-NDDO repulsion integrals for the MGE method was

simplified by symmetry as described in Section 3.3 for calculations on N_2O_4, NO_2, NO_2^- and NO_2^+. For systems other than N_2O_4 and NO_2 convergence was considered to be obtained when all coefficients on successive iterations agreed to within 0.0001. For N_2O_4, owing to the much larger amount of time required for each iteration, this convergence criterion was relaxed. For each configuration of N_2O_4 that was calculated the total energy from successive iterations agreed to five decimal places. While most coefficients then did agree to four places, a few differed in the third place. A similar comment applies to the restricted Hartree-Fock calculation on NO_2 where the conjugate gradients method was not used.

The computer programs for calculating one-electron integrals and NDDO two-electron repulsion integrals correctly reproduced values for CO and NH_2 which had been obtained by Williams[136]. Some randomly chosen integrals were also checked against values obtained from closed analytical formulae[31]. The SAI (simplified ab initio) method was tested for CO and produced the same wave function as obtained by Williams[136]. A calculation on H_2O agreed with published results[30] to the quoted three decimal places. The multi-Gaussian expansion program in conjunction with the unrestricted Hartree-Fock method was similarly checked with a calculation on NH_2[136].

The remainder of this Chapter is concerned with a comparison of the various methods, and with a detailed analysis of the wave functions obtained for related chemical species, using a two-Gaussian-per-Slater orbital expansion for the calculation of electron repulsion integrals.

6.2 Comparison of the Multi-Gaussian Expansion and Simplified Ab Initio Methods for the Nitrite Ion

Table 6.2 contains orbital energies and the total energy for various minimal basis set calculations on the closed shell nitrite ion NO_2^-. The results of Mulliken population analyses of these wave functions are collected in Table 6.3. For comparison, the results of an exact ab initio calculation[175] for the experimental geometry and with an identical basis set are given in the first column of each of these tables. For this geometry an expansion of three Gaussians per Slater orbital (3G/S) gives overall better agreement for the orbital and total energies than a 2G/S expansion. The highest occupied orbital is, however, predicted to be the $1a_2$ orbital instead of the $6a_1$ orbital of the exact calculation. In this regard it is worth noting that a more accurate calculation by Bonaccorsi et al.[176], using an improved basis set, lowered all orbital energies by 0.12 to 0.20 atomic units while leaving the order of the levels unchanged; the three highest occupied orbitals were then found to have negative orbital energies.

The 3G/S expansion gives results for the population analysis that are considerably closer to the exact values than are those of the 2G/S expansion. In general the populations for the 3G/S method agree to within 0.04, and for the 2G/S to within 0.2, of the exact values. The direction of improvement does not appear to be predictable. Thus the total gross atomic orbital populations in the 2sN and $2p_xN$ orbitals gain at the expense of $2p_yN$ and $2p_zN$ for the 3G/S expansion when compared with the 2G/S results. Changes in the oxygen orbital populations on the other hand are not as marked.

Table 6.2

Orbital Energies for the Nitrite Ion, NO_2^-

	Expl. geom. Ab-initio[175]	Expl.geom. 3G/S	Expl.geom. 2G/S	N_2O_4 geom. 2G/S	N_2O_4 geom. SAI
Orbital Energies (a.u.)					
$1b_2$	-20.1102	-20.1041	-20.1031	-20.1094	-20.0603
$1a_1$	-20.1102	-20.1042	-20.1029	-20.1092	-20.0592
$2a_1$	-15.3562	-15.3522	-15.2893	-15.3016	-15.2673
$3a_1$	-1.1179	-1.1134	-1.1139	-1.1493	-0.9574
$2b_2$	-0.8947	-0.8792	-0.8890	-0.9289	-0.9340
$4a_1$	-0.4326	-0.4392	-0.4630	-0.4349	-0.8254
$1b_1$	-0.2477	-0.2202	-0.2461	-0.2730	-0.0631
$3b_2$	-0.2180	-0.2115	-0.0922	-0.1316	-0.3591
$5a_1$	-0.2084	-0.2395	-0.2350	-0.2815	-0.1531
$1a_2$	0.0121	0.0697	0.1006	0.0828	0.0055
$4b_2$	0.0574	0.0176	0.1429	0.0785	-0.0470
$6a_1$	0.0713	0.0648	0.1400	0.1949	-0.0190
Total Energy	-203.1737	-203.1701	-202.7481	-202.7955	-204.0673

Table 6.3

Mulliken Population Analysis for the Nitrite Ion, NO_2^-

	Expl.geom. Ab-initio[175]	Expl.geom. 3G/S	Expl.geom. 2G/S	N_2O_4 geom. 2G/S	N_2O_4 geom. SAI
Total gross AO pop.					
1sO	1.999	1.999	2.000	2.000	2.000
2sO	1.873	1.888	1.881	1.873	2.120
$2p_xO$	1.494	1.516	1.593	1.568	1.727
$2p_yO$	1.352	1.325	1.307	1.157	0.682
$2p_zO$	1.736	1.731	1.665	1.865	1.875
1sN	1.998	1.999	2.000	2.000	2.001
2sN	1.644	1.650	1.372	1.311	1.907
$2p_xN$	1.011	0.968	0.813	0.864	0.545
$2p_yN$	0.946	0.976	1.208	1.176	1.143
$2p_zN$	1.493	1.489	1.715	1.722	1.595
Total net atomic and overlap pop.					
Oσ	6.831	6.834	6.722	6.788	7.314
Oπ	1.402	1.423	1.502	1.464	1.635
Nσ	5.755	5.834	6.022	5.997	7.929
Nπ	0.809	0.766	0.616	0.644	0.354
(N-O)σ	0.325	0.279	0.273	0.213	-1.284
(N-O)π	0.202	0.202	0.197	0.220	0.192
(O-O)σ	-0.069	-0.061	-0.012	0.002	0.010
(O-O)π	-0.017	-0.016	-0.014	-0.011	-0.008

In order to compare the results with those for N_2O_4 a calculation was done at the same geometry as that of an NO_2 group in N_2O_4. The most significant change in this calculation is an increase in the $2p_zO$ orbital population at the expense of the $2p_yO$. In N_2O_4 the NO distance is shorter, 2.230 a.u., compared with 2.334 a.u. for NO_2^-, and the ONO angle is larger, 133.7° compared with 115.0°. While comparisons with Walsh's predictions governing orbital energies as discussed in Section 2.2 are not quantitatively valid because of the bond length change, the following observations support the trends in his diagram, Figure 2.2. The $3b_2$, $1a_2$ and $4b_2$ orbitals are less strongly bound at 115°, but the $6a_1$ orbital is more strongly bound. In contrast the $4a_1$ orbital is more strongly bound at the smaller angle, in agreement with calculations on F_2O[55].

An SAI calculation on the nitrite ion at the N_2O_4 geometry gave results that differed markedly from those of the MGE method. Apart from the significant orbital energy differences, the total energy shows the failure of the variation principle for methods using approximations in the calculation of integrals. There are large differences in the total gross AO populations, especially in the 2sN and 2sO values, which are much larger in the SAI case. An examination of the coefficients shows that the $3a_1$ and $4a_1$ MO's are composed mainly of these AO's. Table 6.4 gives these coefficients together with the N-O subtotal overlap population in the MO's.

Table 6.4

Comparison of $3a_1$ and $4a_1$ Molecular Orbitals for the Nitrite Ion

NO_2^- (N_2O_4 geom.)	$3a_1$ 2G/S	$3a_1$ SAI	$4a_1$ 2G/S	$4a_1$ SAI
2sO coefficient	0.42	0.17	0.55	0.61
2sN coefficient	0.43	0.62	-0.64	-1.12
N-O subtotal overlap population	0.38	0.16	-0.18	-0.97

The negative overlap population of the $4a_1$ orbital is at variance with the N - O bonding character predicted for this orbital by Walsh as mentioned in Section 2.2. In particular the large negative value for the SAI method can be seen to be responsible for the unexpected negative N - O σ overlap in Table 6.3. Yet another marked difference is in the pi orbital populations where the SAI method gives a larger contribution from the oxygen atoms.

Williams[8] has also compared the three methods by calculating several properties for small molecules. In summary, the present results parallel his conclusions in that the 3G/S method gives results which agree well with exact ab initio values, and those of the 2G/S expansion, while not giving such good agreement, are much closer than those of the SAI method. The failure of the SAI method to produce satisfactory populations meant that more attention was given to analysing the results for N_2O_4 obtained by the 2G/S method.

6.3 Restricted and Unrestricted Hartree-Fock-Roothaan Calculations on Nitrogen Dioxide

In Table 6.5 are collected some results of calculations on the $^2A_1$ state of NO_2. The columns headed RHF 2G/S give the orbital and total energies obtained using McWeeny's restricted Hartree-Fock method as described in Section 4.2. All integrals were included, with the non-NDDO repulsion integrals being evaluated by a 2G/S expansion. The columns headed by UHF give the results for an unrestricted Hartree-Fock calculation as described in Section 4.5. As in the RHF method all non-NDDO repulsion integrals were calculated by a 2G/S expansion. The wave function in this method is obtained as a Slater determinant with the corresponding MO's of different spin having slightly different spatial factors. Values pertaining to each are accordingly given in columns headed by 'α spin' and 'β spin'. Since the UHF method has fewer constraints than the RHF method it is expected to produce a lower total energy. This observation is borne out in the calculations at the N_2O_4 geometry where the energy difference is 0.0038 atomic units. The column headed SAI contains the results of a calculation using McWeeny's RHF formulation, but in which the NDDO approximation was used in an orthogonal Löwdin basis. This method therefore corresponds to the SAI method described in Section 1.4 for closed shell systems.

The tabulated orbital energies require some explanation. For the UHF method Koopmans' theorem[153] applies and the orbital energies, which are obtained by solution of two independent eigenvalue equations, correspond to negative ionization potentials. An unusual feature of these results is that the $6a_1$ α-spin orbital appears to lie lower than the $4b_2$ β-spin

Table 6.5

Orbital Energies for Nitrogen Dioxide, NO_2, $^2A_1$

	Expl.geom RHF 2G/S	N_2O_4 geom SAI	N_2O_4 geom RHF 2G/S	N_2O_4 geom UHF α spin	N_2O_4 geom UHF β spin	N_2O_4 geom Exchange Integral	N_2O_4 geom RHF-exchange	N_2O_4 geom Fink's defn.	N_2O_4 geom Promotion Energy
Orbitals									
$1b_2$	-20.6812	-20.6547	-20.6822	-20.6894	-20.6831	0.0073	-20.6895	-20.6859	20.3667
$1a_1$	-20.6811	-20.6535	-20.6821	-20.6893	-20.6830	0.0073	-20.6894	-20.6858	20.3666
$2a_1$	-15.9030	-15.7978	-15.9139	-15.9275	-15.9115	0.0141	-15.9280	-15.9210	15.4131
$3a_1$	-1.5863	-1.4027	-1.6070	-1.6463	-1.6069	0.0382	-1.6452	-1.6261	1.3470
$2b_2$	-1.3691	-1.3661	-1.3784	-1.4107	-1.3795	0.0332	-1.4116	-1.3950	1.1416
$4a_1$	-0.8192	-1.2287	-0.8130	-0.9312	-0.8157	0.0995	-0.9125	-0.8628	0.6486
$1b_1$	-0.7118	-0.5133	-0.7250	-0.7440	-0.7230	0.0168	-0.7418	-0.7334	0.4757
$5a_1$	-0.6625	-0.5379	-0.6734	-0.7613	-0.6712	0.0961	-0.7695	-0.7215	0.4953
$3b_2$	-0.5339	-0.8159	-0.5521	-0.6217	-0.5546	0.0602	-0.6123	-0.5822	0.3364
$1a_2$	-0.3561	-0.4477	-0.3563	-0.3631	-0.3628	0.0116	-0.3679	-0.3621	0.1427
$4b_2$	-0.3138	-0.3130	-0.3129	-0.3946	-0.3195	0.0962	-0.4091	-0.3610	0.1627
$6a_1$	-0.3432	-0.5228	-0.3464	-0.3419				-0.3464	
Total Energy (a.u.)	-203.0030	-204.0475	-203.0010	-203.0048					

orbital. For the RHF wave function the orbital energies listed were calculated from the formulae for Koopmans' ionization energies given in section 4.3. The $6a_1$ orbital which is singly occupied has a lower energy than the doubly occupied $4b_2$ MO. These apparent anomalies are resolved by the following considerations. The presence of the unpaired electron means that removal of an electron from a doubly filled orbital will require slightly different energies, depending on whether the electron has α or β spin. By an analysis similar to that of Fink[83], it is found that the orbital energy (or negative ionization potential) of an α electron in a closed shell MO X is lower than the corresponding β electron by the value of the exchange integral $\langle XY|g|YX\rangle$ where Y is the open shell MO. When the closed shell orbital energy formula of Dodds & McWeeny[152] Equation 4.19, is expanded in terms of Coulomb and exchange integrals, it gives the formula for a β closed shell electron. This result is clearly shown in Table 6.5 where the closed shell orbital energies tabulated for the RHF 2G/S calculation at the N_2O_4 geometry differ from the UHF β spin orbital energies by less than 0.007 a.u. The exchange integrals are also listed for each of the closed shell states taken with the open shell $6a_1$ orbital. From the above discussion the RHF orbital energies less the exchange integrals should correspond to the UHF α spin eigenvalues. Inspection of Table 6.5 shows that these do all agree to within 0.02 a.u. In order to have only one orbital energy for the closed shell orbital Fink subtracted only half of the exchange integral. This is equivalent to averaging the values for α and β electrons. The

Table 6.6

Mulliken Population Analysis for Nitrogen Dioxide, NO_2, $^2A_1$

	Expl.geom. RHF 2G/S	N_2O_4 geom. SAI	N_2O_4 geom. RHF 2G/S	N_2O_4 geom. UHF		
				α spin	β spin	total
Total gross AO pop.						
1sO	2.000	2.000	2.000	1.000	1.000	2.000
2sO	1.898	2.101	1.899	0.951	0.948	1.899
$2p_xO$	1.530	1.726	1.527	0.755	0.773	1.528
$2p_yO$	1.103	0.624	1.120	0.526	0.597	1.123
$2p_zO$	1.603	1.486	1.598	0.936	0.656	1.592
1sN	2.000	1.998	2.000	1.000	1.000	2.000
2sN	1.296	1.945	1.281	0.681	0.608	1.289
$2p_xN$	0.939	0.549	0.945	0.489	0.453	0.942
$2p_yN$	1.251	1.130	1.247	0.623	0.627	1.250
$2p_zN$	1.247	1.505	1.240	0.870	0.364	1.234
Total net atomic and overlap pop.						
Oσ	6.463	6.909	6.486	3.393	3.096	6.489
Oπ	1.428	1.634	1.422	0.703	0.721	1.424
Nσ	5.511	7.960	5.502	3.135	2.381	5.516
Nπ	0.723	0.357	0.723	0.378	0.342	0.720
(N-O)σ	0.283	-1.382	0.265	0.038	0.218	0.256
(N-O)π	0.216	0.192	0.222	0.111	0.111	0.222
(O-O)σ	-0.004	-0.014	-0.004	0.004	-0.009	-0.005
(O-O)π	-0.011	-0.008	-0.012	-0.006	-0.006	-0.012

values so obtained are given in the second last column of Table 6.5. When these orbital energies are used the highest doubly occupied MO lies 0.0146 a.u. lower than the singly occupied $6a_1$ MO. The final column in Table 6.5 contains the promotion energies from each closed shell orbital to the $6a_1$ orbital, calculated according to Equation 4.21 in Section 4.3. The promotion energies confirm that the $6a_1$ orbital is indeed higher than the doubly occupied orbitals.

The results of the Mulliken population analysis for the RHF and UHF calculations on NO_2 ($^2A_1$) at the N_2O_4 geometry are tabulated in Table 6.6. Excepting only the nitrogen sigma total net atomic population, these values all agree to better than 0.01. In contrast, the values for the wave function calculated using the SAI approximations give poor agreement. As noted in the NO_2^- calculations, this method seems to give notably different populations in the 2s orbitals. Here also the $2p_y O$ and $2p_x N$ populations are much reduced. The result of this redistribution is that most of the MO's increase in N - O antibonding character. This increase is reflected in the N - O subtotal overlap populations which are compared orbital for orbital in Table 6.7.

Table 6.7

N - O Subtotal overlap populations for NO_2, $^2A_1$, N_2O_4 geometry

	$1a_1$	$2a_1$	$3a_1$	$4a_1$	$5a_1$	$6a_1$
2G/S	0.000	0.001	0.380	-0.277	0.134	-0.151
SAI	0.001	0.003	0.265	-1.072	-0.058	-0.132
	$1a_2$	$1b_1$	$1b_2$	$2b_2$	$3b_2$	$4b_2$
2G/S	0.000	0.222	0.000	0.298	-0.105	-0.015
SAI	0.000	0.192	0.002	-0.141	-0.248	0.000

When the promotion energies were calculated for the SAI $^2A_1$ state it was found that the energy required to promote an electron from the $1a_2$ orbital to the $6a_1$ orbital was -0.0281 atomic units. A new SAI calculation on the $^2A_2$ state of NO_2 was subsequently made with $1a_2$ singly occupied and $6a_1$ doubly occupied. This calculation produced positive promotion energies for all closed shell orbitals, and did indeed give a total energy lower than that of the $^2A_1$ state by 0.0254 a.u. In view of the poor quality of the SAI results, however, these wave functions were not extensively analysed.

A 2G/S RHF calculation was also performed at the experimental geometry of NO_2. This has a slightly larger NO bond (NO_2 2.261 a.u.; N_2O_4 2.230 a.u.) and a fractionally larger ONO angle (NO_2 134.3°; N_2O_4 133.7°). As expected, these slight changes produce only small variations from the values tabulated in Tables 6.5 and 6.6. The partial gross populations in the $6a_1$ MO have previously been given in Table 2.1 for comparison with the results of other calculations and with experimental values. The 2G/S method appears to give too small a population in the 2sN orbital (0.049) even taking into account the fact that the Mulliken population analysis is sensitive to the set of atomic basis functions used. The population in the $2p_zO$ orbitals (0.456) gives better agreement. From this calculation the $6a_1$ orbital energy of -0.3432 a.u. corresponds to a Koopmans' vertical ionization potential of 0.343 a.u. compared with an experimental value of 0.413 a.u.[68].

6.4 The SAI Wave Function for Dinitrogen Tetroxide

The lowest energy state obtained for N_2O_4 by the SAI method is designated N_2O_4(I), with a total energy of -409.0840

a.u. Its configuration and orbital energies are given in Table 6.8. The orbitals correlate with the NO_2 orbitals which are given in parentheses. The state has eight pi electrons occupying the orbitals labelled π in the table. An unexpected feature is that the highest occupied orbital, $6b_{1u}$, derived from the singly occupied orbital of NO_2, is antibonding between the two NO_2 groups. When instead the bonding $6a_g$ orbital was filled at the expense of the $6b_{1u}$ orbital the new state, called N_2O_4(II), converged to an energy of -409.0571 a.u., which is 0.0269 a.u. less stable.

From the population analysis whose results are also given in Table 6.8 the major contributions to the N - N overlap are from the $4b_{1u}$, $4a_g$, $3b_{3g}$, $3b_{2u}$, $5b_{1u}$ and $5a_g$ orbitals, all of which are largely localized on the N atoms. The N - N antibonding orbitals $4b_{1u}$, $3b_{3g}$, and $5b_{1u}$ produce a larger effect than their corresponding N - N bonding counterparts, with the result that the total N - N overlap population is negative, -0.804. Long range O1-O3 interactions are all small and result in a total overlap population of -0.014. The overlap populations for the four pi MO's indicate that there is no pi bonding between the two NO_2 moieties.

In order to examine the nature of the changes on dimerization the results for the two MO's of N_2O_4 which correlate with each NO_2 MO are added together and compared with NO_2 gross atomic populations and N - O overlap populations in Table 6.9. For comparative purposes NO_2 was taken to have the same geometry as N_2O_4 and the $^2A_1$ state was considered. The $3a_1$ and $4a_1$ orbitals in NO_2 are mainly of 2s character. The orbitals formed from the $3a_1$ orbital of NO_2 increase in O atom

Table 6.8

Lowest Energy SAI Wavefunction (I) for N_2O_4 E_{tot} = 409.0840 a.u.

	Orbital Energy, a.u.	Subtotal gross pop. on O	Subtotal gross pop. on N	N1-O1 overlap	N-N overlap	O1-O3 overlap
$(1a_1)$ a_g	-20.6183	0.500	0.001	0.000	0.000	0.000
$(1a_1)$ b_{1u}	-20.6182	0.500	0.001	0.000	0.000	0.000
$(1b_2)$ b_{3g}	-20.6173	0.500	0.001	0.000	0.000	0.000
$(1b_2)$ b_{2u}	-20.6171	0.500	0.000	0.000	0.000	0.000
$(2a_1)$ a_g	-15.7614	0.001	0.998	0.002	0.000	0.000
$(2a_1)$ b_{1u}	-15.7530	0.001	0.998	0.002	0.000	0.000
$(3a_1)$ b_{1u}	-1.4397	0.429	0.142	0.098	-0.056	-0.007
$(2b_2)$ b_{3g}	-1.4009	0.560	-0.120	-0.315	-0.028	-0.012
$(2b_2)$ b_{2u}	-1.3974	0.560	-0.119	-0.295	0.025	0.012
$(3a_1)$ a_g	-1.3967	0.553	-0.106	-0.158	0.002	0.010
$(4a_1)$ b_{1u}	-1.3388	0.159	0.682	-0.501	-0.296	-0.004
$(4a_1)$ a_g	-1.2658	0.049	0.903	-0.231	0.099	0.001
$(3b_2)$ b_{3g}	-0.9619	0.095	0.809	0.012	-0.122	0.000
$(3b_2)$ b_{2u}	-0.8329	0.136	0.727	0.042	0.091	0.000
$(5a_1)$ b_{1u}	-0.6124	0.006	0.989	-0.037	-0.986	0.000
$(5a_1)$ a_g	-0.5368	-0.004	1.007	-0.043	0.489	0.000
$\pi(1a_2)$ a_u	-0.4954	0.500	0.0	0.0	0.0	-0.002
$\pi(1a_2)$ b_{1g}	-0.4922	0.500	0.0	0.0	0.0	0.002
$\pi(1b_1)$ b_{2g}	-0.4879	0.483	0.035	0.027	-0.001	-0.002
$\pi(1b_1)$ b_{3u}	-0.4792	0.498	0.004	0.004	0.000	0.002
$(4b_2)$ b_{3g}	-0.4162	0.500	-0.001	-0.002	0.000	-0.013
$(4b_2)$ b_{2u}	-0.3715	0.500	0.000	0.000	0.000	0.014
$(6a_1)$ b_{1u}	-0.3483	0.511	-0.022	-0.060	-0.020	-0.013

Table 6.9

Mulliken Population Analysis for SAI Wave functions of NO_2 and N_2O_4

	Subtotal Gross Population on O			Subtotal Gross Population on N			N1-O1 Overlap Populations		
NO_2 MO's	N_2O_4(I)	N_2O_4(II)	$NO_2\ ^2A_1$	N_2O_4(I)	N_2O_4(II)	$NO_2\ ^2A_1$	N_2O_4(I)	N_2O_4(II)	$NO_2\ ^2A_1$
$1a_1$	1.000	1.000	1.000	0.002	0.002	0.001	0.000	0.000	0.001
$2a_1$	0.002	0.002	0.001	1.996	1.996	1.997	0.004	0.004	0.003
$3a_1$	0.982	0.964	0.795	0.036	0.071	0.411	-0.060	-0.030	0.265
$4a_1$	0.208	0.226	0.345	1.585	1.549	1.309	-0.732	-0.760	-1.072
$5a_1$	0.002	0.006	0.228	1.996	1.988	1.543	-0.080	-0.040	-0.058
$6a_1$	0.511	0.511	0.407	-0.022	-0.021	0.187	-0.060	-0.048	-0.132
$1a_2$	1.000	1.000	1.000	0.0	0.0	0.0	0.0	0.0	0.0
$1b_1$	0.981	0.978	0.726	0.039	0.045	0.549	0.031	0.035	0.192
$1b_2$	1.000	1.000	0.999	0.001	0.001	0.002	0.000	0.000	0.002
$2b_2$	1.120	1.120	1.059	-0.239	-0.240	-0.118	-0.610	-0.606	-0.141
$3b_2$	0.231	0.231	0.377	1.536	1.538	1.246	0.054	0.052	-0.248
$4b_2$	1.000	1.000	1.000	-0.001	-0.001	0.000	-0.002	-0.001	0.000
Atom Charge	-0.036	-0.036	0.063	0.072	0.072	-0.127			

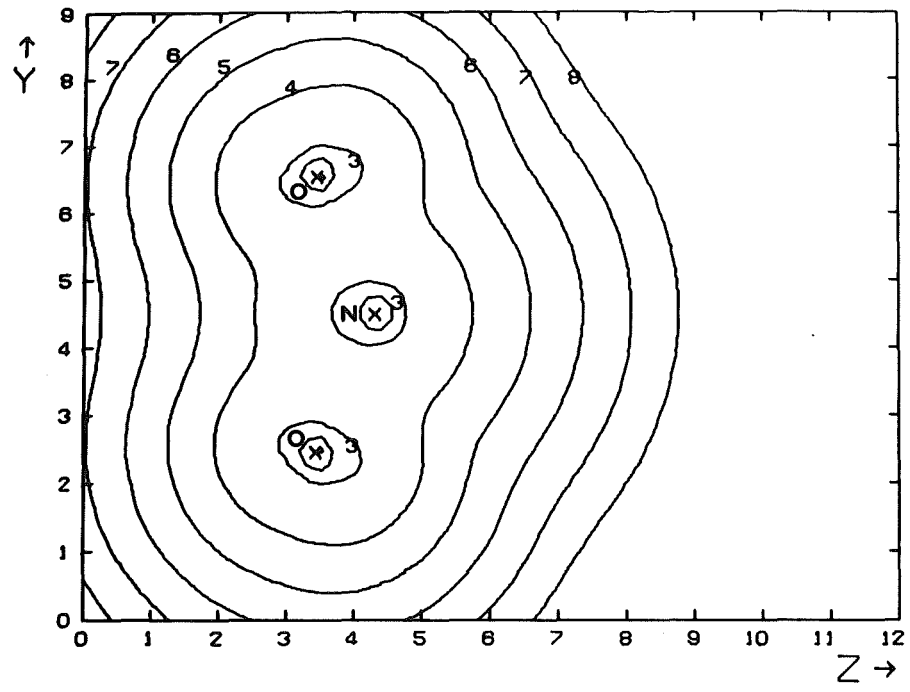

Fig. 6.1 NO_2 SAI

Max Dens. 114.

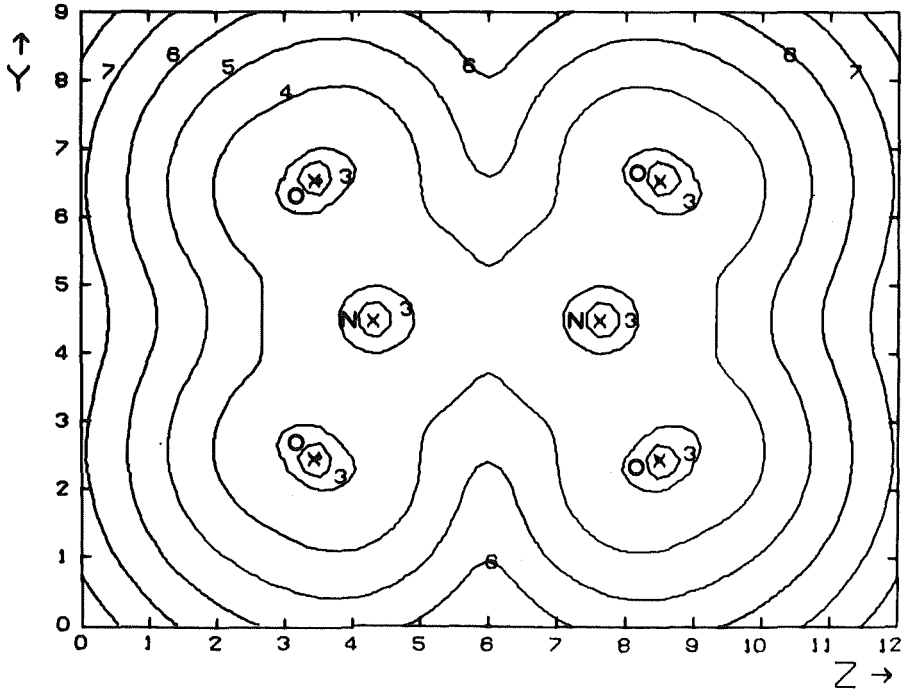

Fig. 6.2 N_2O_4 SAI

Max Dens. 114.

population in N_2O_4 and net N - O antibonding results. At the same time, the $4a_1$ orbital becomes more localized on the N atom and this leads to the significant N - N overlap previously noted. The $5a_1$ orbital in NO_2 has a small contribution from the oxygen atoms, mainly from the $2p_x$ and $2p_y$ orbitals. This contribution vanishes in N_2O_4 where the $5a_g$ and $5b_{1u}$ orbitals are composed almost entirely of $2p_z$ on the N atoms, with resulting large N - N interaction. Brown & Harcourt[123], as discussed in Section 2.7, have attributed the weakness of the N - N bond to this delocalization of the lone pair oxygen density on dimerization. The nitrogen atom population in the $6a_1$ orbital of NO_2 vanishes in N_2O_4. For this reason there is little difference between the two states of N_2O_4 given in Table 6.9. Other noticeable changes that occur on dimerization are in the $2b_2$ and $3b_2$ orbitals. For instance, in NO_2 the $3b_2$ orbital is composed mainly of $2p_y$ orbitals located on the nitrogen atom. This orbital is, however, N - O antibonding because of a small contribution from $2p_yO$ orbitals. In N_2O_4 it is more localized on the nitrogen atoms and becomes N - O nonbonding.

Figures 6.1 and 6.2 show the electron density in the molecular planes for NO_2 and N_2O_4(I). In all the contour diagrams distances are given in atomic units. Under each map the maximum electron density in the given plane is recorded in atomic units so that integration of the density over all space gives the number of electrons. In each case the innermost contour, labelled '1', has a value equal to the largest power of ten that is less than the maximum density. Successive contours, labelled '2', '3' ... etc, show a decrease by a factor of ten in the density. Much more detail is obtained

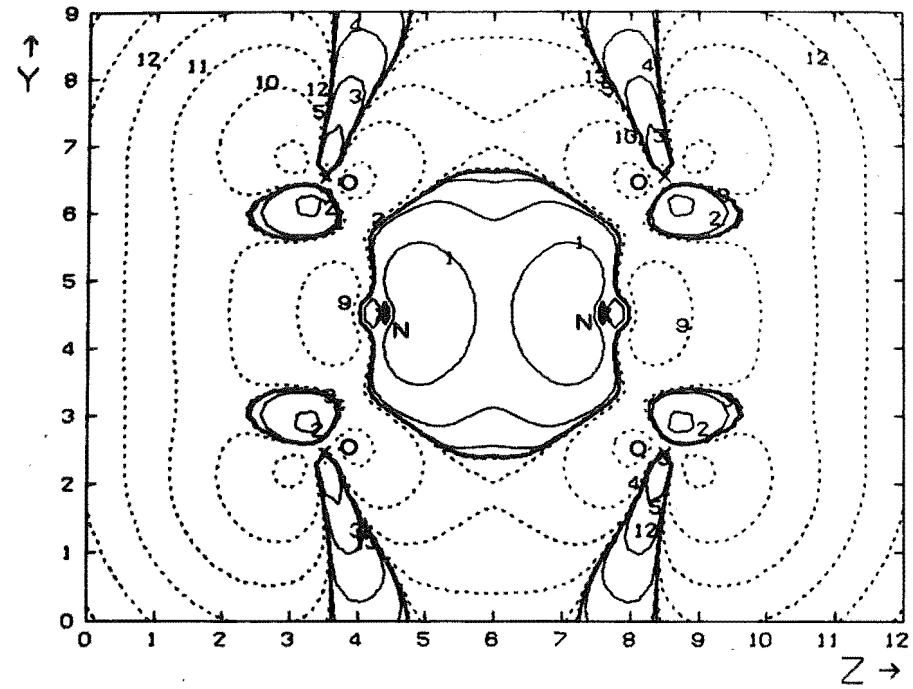

Fig. 6.3 N_2O_4 - 2 NO_2 SAI

Max Dens. +0.513 , - 0.194

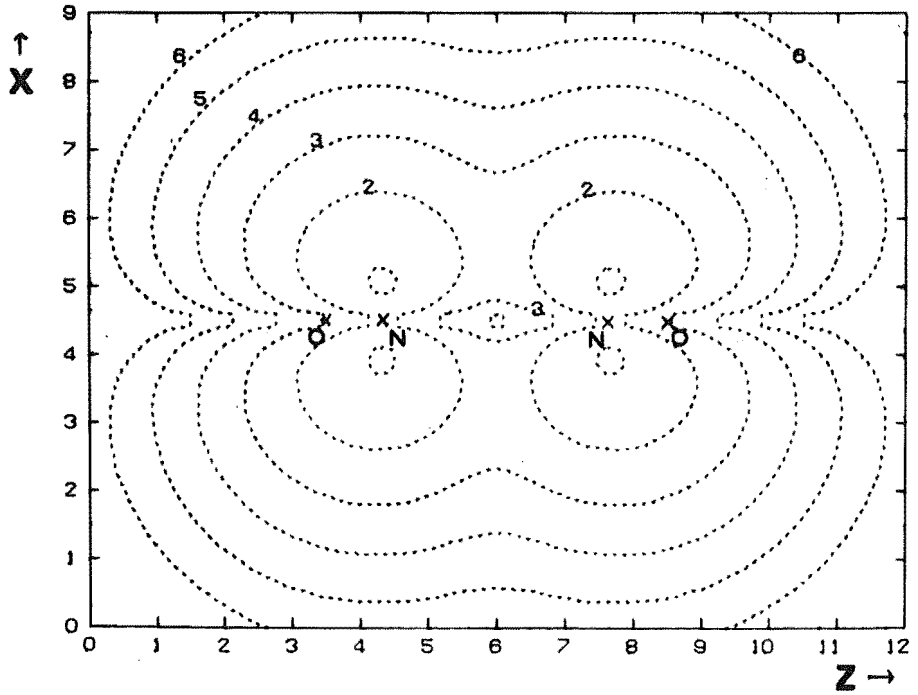

Fig. 6.4 N_2O_4 - 2 NO_2 SAI

Max Dens. -0.113

in the electron density difference map of Figure 6.3. This plot is obtained by subtracting the density due to two NO_2 molecules from the N_2O_4 density. The dashed lines are for 'negative' densities where there is less density in N_2O_4 than there is in two separate NO_2 molecules. These negative values are labelled in the same manner as described earlier except they begin with the next available integer. Examination of Figure 6.3 shows that there is more density between the two nitrogen atoms in N_2O_4, but that this is of an antibonding character. The atom charges given in Table 6.9 show that there is a net increase in electronic charge on the oxygen atoms in N_2O_4. From Figure 6.3 the extra negative charge is seen to be taken from the nitrogen atom in the triangle formed by the two N - O bonds. Figure 6.4 is the corresponding difference map for π electrons in the xz-plane which contains the nitrogen atoms. The negative contours are consistent with the fall in gross population on the nitrogen atom in the $1b_1$ orbital from 0.549 in NO_2 to 0.039 in N_2O_4.

We may conclude that at this level of approximation significant changes occur in several MO's upon dimerization. The a_1 orbitals contribute most to the N - N interaction. Long range O - O and N - O interactions are negligible, and no N - N π bonding is significant. An unsatisfactory feature of these results has already been mentioned in connection with the nitrite ion. This is the N - O overlap population, which here again is negative.

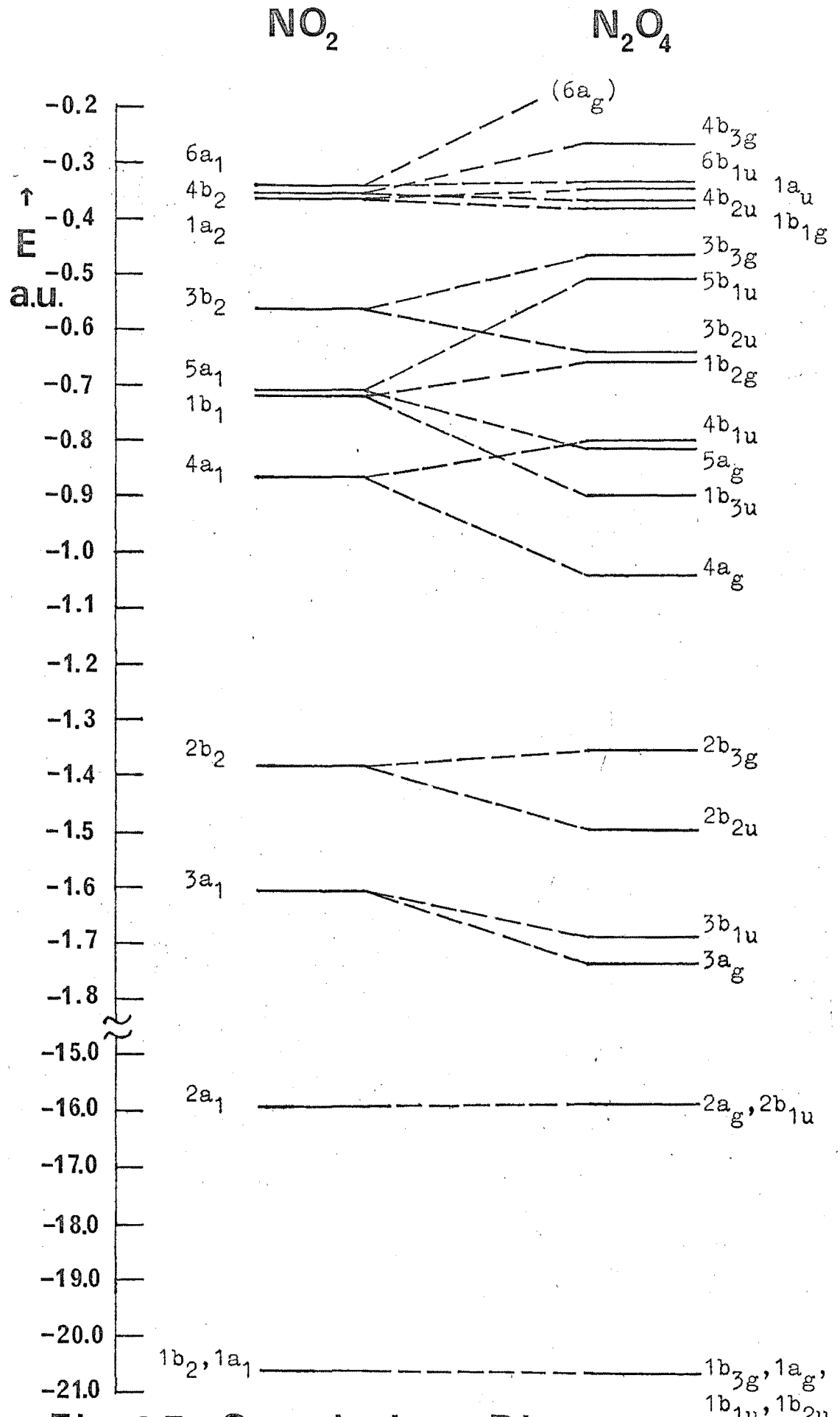

Fig. 6.5 Correlation Diagram

6.5 The 2G/S Wave Function for Dinitrogen Tetroxide

The lowest energy state found for N_2O_4 using the 2G/S expansion approximation is designated Φ_1, with a total energy of -405.9277 a.u. Its configuration and orbital energies are given in Table 6.10 together with some of the results of a population analysis. As was the case with the SAI lowest energy state, there are eight pi electrons and the N - N anti-bonding $6b_{1u}$ orbital is occupied.

A correlation diagram is given in Figure 6.5 for the orbital energies of Φ_1 and the energies found from Fink's definition for the experimental geometry of NO_2. Both wave functions are calculated with the 2G/S expansion. As noted by Brown & Harcourt[121], the sigma and pi orbitals are not energetically separable. The rule quoted by Herzberg[114] that of the newly formed orbitals the ones which are symmetric with respect to the new plane of symmetry (i.e. a_g, b_{1g}, b_{3u} and b_{2u}) lie lower than the corresponding antisymmetric orbitals (b_{1u}, a_u, b_{2g}, b_{3g}) is obeyed in all cases except for the $6a_1$ orbital of NO_2 where the virtual $6a_g$ has an energy 0.2733 a.u. compared with the $6b_{1u}$ orbital energy of -0.3335 a.u.

A limited configuration interaction calculation was done with this state and six other doubly excited singlet configurations as outlined in Section 1.3. The results of this calculation are given in Table 6.11. The CI was done using the virtual orbitals from Φ_1, with the result that the total energy was reduced to -405.9638 a.u. In addition Φ_2, Φ_3 and Φ_4 were separately taken to convergence and the energies obtained for these states are given in Table 6.11. Φ_1 contributes over 95% of the CI wave function. Φ_2, which is

Table 6.10

Lowest Energy 2G/S Wavefunction Φ_1 for N_2O_4 E_{tot} = -405.9277

	Orbital Energy	Subtotal gross pop. on O	Subtotal gross pop. on N	N1-01 overlap	N-N overlap	01-03 overlap
$(1b_2)b_{2u}$	-20.6940	0.500	0.000	0.000	0.000	0.000
$(1a_1)b_{1u}$	-20.6940	0.500	0.000	0.000	0.000	0.000
$(1a_1)a_g$	-20.6940	0.500	0.000	0.000	0.000	0.000
$(1b_2)b_{3g}$	-20.6939	0.500	0.000	0.000	0.000	0.000
$(2a_1)a_g$	-15.8703	0.001	0.999	0.001	0.000	0.000
$(2a_1)b_{1u}$	-15.8696	0.000	0.999	0.001	0.000	0.000
$(3a_1)a_g$	-1.7380	0.324	0.351	0.132	0.092	0.005
$(3a_1)b_{1u}$	-1.6903	0.278	0.443	0.198	0.002	-0.002
$(2b_2)b_{2u}$	-1.4963	0.305	0.389	0.159	0.030	0.005
$(2b_2)b_{3g}$	-1.3549	0.403	0.194	0.122	-0.012	-0.005
$(4a_1)a_g$	-1.0408	0.359	0.281	-0.015	0.166	0.000
$\pi(1b_1)b_{3u}$	-0.9007	0.235	0.530	0.107	0.056	0.001
$(5a_1)a_g$	-0.8131	0.420	0.161	-0.054	0.000	0.012
$(4a_1)b_{1u}$	-0.7994	0.384	0.231	-0.190	-0.156	-0.005
$\pi(1b_1)b_{2g}$	-0.6610	0.329	0.342	0.108	-0.036	-0.001
$(3b_2)b_{2u}$	-0.6460	0.402	0.196	-0.070	0.035	0.001
$(5a_1)b_{1u}$	-0.5079	0.215	0.570	0.110	-0.615	-0.005
$(3b_2)b_{3g}$	-0.4705	0.253	0.495	-0.099	-0.090	-0.002
$\pi(1a_2)b_{1g}$	-0.3817	0.500	0.0	0.0	0.0	0.002
$(4b_2)b_{2u}$	-0.3697	0.440	0.120	-0.011	0.018	0.010
$\pi(1a_2)a_u$	-0.3457	0.500	0.0	0.0	0.0	-0.002
$(6a_1)b_{1u}$	-0.3335	0.301	0.399	-0.220	-0.546	-0.007
$(4b_2)b_{3g}$	-0.2696	0.500	0.000	-0.001	0.000	-0.015

Table 6.11

Configuration Interaction for Dinitrogen Tetroxide

Configuration	Energy (a.u.)	No. of π electrons	Coefficient in CI expansion	% Contribution to CI Wavefunction
$\Phi_1 .. (1b_{1g})^2(4b_{2u})^2(1a_u)^2(6b_{1u})^2(4b_{3g})^2$	-405.9277	8	0.977	95.45
$\Phi_2 .. (1b_{1g})^2(4b_{2u})^2(1a_u)^2(4b_{3g})^2(6a_g)^2$	-405.3018	8	-0.170	2.89
$\Phi_3 .. (4b_{2u})^2(4b_{3g})^2(6b_{1u})^2(1b_{1g})^2(6a_g)^2$	-405.2826	6	-0.003	0.00
$\Phi_4 .. (1b_{1g})^2(1a_u)^2(4b_{2u})^2(4b_{3g})^2(2b_{3u})^2$	-405.5243	10	-0.015	0.02
$\Phi_5 .. (1b_{1g})^2(4b_{2u})^2(1a_u)^2(2b_{3u})^2(6b_{1u})^2$	-	10	-0.007	0.00
$\Phi_6 .. (1b_{1g})^2(4b_{2u})^2(1a_u)^2(6b_{1u})^2(6a_g)^2$	-	8	-0.054	0.29
$\Phi_7 .. (1b_{1g})^2(4b_{2u})^2(6b_{1u})^2(4b_{3g})^2(2b_{3u})^2$	-	8	-0.116	1.35

formed by occupying the bonding $6a_g$ orbital and depopulating $6b_{1u}$ has the next highest contribution, although it is higher in energy than the ten pi electron configuration Φ_4. The $2b_{3u}$ orbital which is filled in Φ_4 has coefficients of 0.4 and -0.5 for the $2p_x$ orbitals on the oxygen and nitrogen atoms respectively. Thus while the orbital is N - O antibonding it contributes more to the N - N pi bonding than does $1b_{3u}$. This is shown from their respective N - N overlap populations of 0.082 for $2b_{3u}$, compared with 0.063 for $1b_{3u}$. It is interesting to note that the six pi electron configuration Φ_3, corresponding to the model of Coulson & Duchesne[62], has both a higher energy and a smaller contribution than even the ten pi electron Φ_4. It will be further considered in Section 6.7. Discussion in the remainder of the present section will therefore be confined to the two configurations Φ_1 and Φ_2.

The set of coefficients for N_2O_4 Φ_1 and for the RHF 2G/S calculation on NO_2, $^2A_1$, at the same geometry as N_2O_4 are given in Appendix VII. Contributions to the N - N interaction in N_2O_4 Φ_1 can be seen from an examination of Table 6.10 which shows that the $3a_g$ and $3b_{1u}$ orbitals give some N - N bonding, and the pair $4a_g$, $4b_{1u}$ gives a small net contribution to bonding. In contrast to results obtained by the SAI method the results here indicate that the $5a_g$ orbital is N - N non-bonding while the $5b_{1u}$ and $6b_{1u}$ orbitals are strongly anti-bonding. The $2b_{2u}$, $2b_{3g}$ and $4b_{2u}$, $4b_{3g}$ pairs give a small net bonding effect as opposed to the $3b_{3g}$ orbital which is N - N antibonding.

The orbitals of the two N_2O_4 states Φ_1 and Φ_2 are compared with NO_2 orbitals in Table 6.12, which contains the results of

Mulliken population analyses for these systems. A notable difference is in the $5a_1$ orbital, which has a greater nitrogen population in Φ_1 and a smaller population in Φ_2 than in NO_2. Inspection of the wave functions in Appendix VII shows that the nitrogen contribution is pure $2p_z$ in NO_2 but has some 2s character in N_2O_4. The $5a_1$ N - O bonding is thereby reduced. The 2s nitrogen orbital has a different sign in the $5b_{1u}$ and $5a_g$ orbitals. This leads to more electron density extending out from the N atom in the $5b_{1u}$ orbital and this accounts for the large net N - N antibonding contribution of this pair. There is very little delocalization from the oxygen atoms. These conclusions can be seen in another way. Once the wave functions for N_2O_4 and NO_2 with the same geometry have been obtained as LCAO MO's, it is possible to expand each N_2O_4 MO in terms of all the MO's of NO_2, including the virtual orbitals, obtained by diagonalization of the effective Hamiltonian in Section 4.2, Equation 4.15. This was done for N_2O_4 Φ_1; the resulting coefficients after normalization are given in Table 6.13. While the lower orbitals are built entirely from their corresponding orbitals in NO_2 (eg. $1a_g$ and $1b_{1u}$ from $1a_1$ of NO_2) this is not the case for the higher MO's. In particular the $5a_g$ and $5b_{1u}$ orbitals have a large but opposite contribution from the $4a_1$ orbital. It is because this orbital has a large 2sN content that the $5b_{1u}$ and $5a_g$ orbitals are so different and have the large splitting in orbital energy shown in Figure 6.5.

The $6a_1$ orbital of NO_2 has a large $2p_zN$ contribution which is still present in the N_2O_4 states Φ_1 and Φ_2. As a result the $6b_{1u}$ orbital is strongly N - N antibonding and the $6a_g$ is strongly bonding. The expansion of the $6b_{1u}$ orbital in

Table 6.12

Mulliken Population Analysis for 2G/S Wavefunctions of NO_2 and N_2O_4

	Subtotal Gross Population on O			Subtotal Gross Population on N			N1-O1 Overlap Populations		
NO_2 MO's	N_2O_4 (Φ_1)	N_2O_4 (Φ_2)	NO_2 $^2A_1$	N_2O_4 (Φ_1)	N_2O_4 (Φ_2)	NO_2 $^2A_1$	N_2O_4 (Φ_1)	N_2O_4 (Φ_2)	NO_2 $^2A_1$
$1a_1$	1.000	1.000	1.000	0.000	0.000	0.000	0.000	0.000	0.000
$2a_1$	0.001	0.001	0.001	1.998	1.998	1.999	0.002	0.001	0.001
$3a_1$	0.602	0.564	0.620	0.794	0.873	0.761	0.330	0.339	0.380
$4a_1$	0.743	0.745	0.705	0.512	0.511	0.591	-0.206	-0.238	-0.277
$5a_1$	0.635	0.806	0.684	0.731	0.387	0.633	0.055	0.005	0.134
$6a_1$	0.301	0.246	0.231	0.399	0.509	0.538	-0.220	-0.113	-0.151
$1a_2$	1.000	1.000	1.000	0.0	0.0	0.0	0.0	0.0	0.0
$1b_1$	0.564	0.523	0.527	0.872	0.954	0.945	0.215	0.218	0.222
$1b_2$	1.000	1.000	1.000	0.000	0.000	0.000	0.000	0.000	0.000
$2b_2$	0.708	0.693	0.726	0.583	0.614	0.547	0.281	0.288	0.298
$3b_2$	0.655	0.644	0.664	0.691	0.712	0.672	-0.169	-0.194	-0.105
$4b_2$	0.940	0.936	0.986	0.120	0.129	0.028	-0.012	-0.050	-0.015
Atom Charge	-0.150	-0.157	-0.144	0.300	0.314	0.288			

Expansion of N_2O_4 Φ_1 MO'S in terms of NO_2 MOS at the same geometry

N_2O_4 MOS \ NO_2 MOS	$1a_1$	$2a_1$	$3a_1$	$4a_1$	$5a_1$	$6a_1$	$7a_1$*
$1a_g$, $1b_{1u}$	1.00						
$1a_g$, $2b_{1u}$		1.00					
$3a_g$		0.01	0.96	-0.16	0.19	0.05	-0.14
$3b_{1u}$			0.98	0.08	-0.16	-0.11	0.06
$4a_g$		-0.01	0.33	0.82	-0.47	0.07	
$4b_{1u}$		0.01	-0.05	0.96	0.27	-0.03	-0.02
$5a_g$			-0.08	0.53	0.83	-0.11	0.01
$5b_{1u}$		-0.02	0.24	-0.34	0.88	0.23	0.06
$6b_{1u}$		-0.02	0.15	-0.05	-0.06	0.98	-0.14

N_2O_4 MOS \ NO_2 MOS	$1b_2$	$2b_2$	$3b_2$	$4b_2$	$5b_2$*
$1b_{2u}$, $1b_{3g}$	1.00				
$2b_{2u}$		1.00	0.08	0.09	0.06
$2b_{3g}$		1.00	-0.13	-0.03	0.01
$3b_{2u}$		0.14	0.92	0.38	0.03
$3b_{3g}$		-0.13	0.92	-0.35	0.09
$4b_{2u}$		0.06	-0.38	0.92	0.03
$4b_{3g}$		-0.09	0.36	0.92	-0.10

N_2O_4 MOS \ NO_2 MOS	$1a_2$	$1b_1$	$2b_1$*
$1a_u$, $1b_{1g}$	1.00		
$1b_{3u}$		1.00	0.04
$1b_{2g}$		1.00	0.12

* Virtual Orbital

terms of NO_2 MO's, as given in Table 6.13, shows that this orbital is built almost entirely from the $6a_1$ orbital of the monomer. In all three cases, i.e. $6a_1$, $6a_g$ and $6b_{1u}$, the orbital is N - O antibonding as expected from Walsh's description given in Section 2.2. It is interesting to contrast the changes in the Mulliken atomic charges, defined by Equation 5.11, on dimerization with those found with the SAI method. In both cases the nitrogen atomic charge increases on dimerization. This increase is much greater for the SAI approximation, from -0.127 in NO_2 to 0.072 in N_2O_4(I), compared with the 2G/S method where the corresponding change is from 0.288 to 0.300 in N_2O_4 Φ_1.

The total overlap populations may conveniently be compared according to symmetry, so that the contribution of each type (a_1,a_2,b_1 or b_2) to the bonding can be ascertained. Here only the important features will be mentioned. The N - O bonding is significantly reduced in Φ_1 and Φ_2 compared with NO_2 (Φ_1 0.276, Φ_2 0.257, NO_2 0.487). The major decrease is in the a_1 and b_2 symmetries since the pi bonding is reasonably constant at 0.22. Φ_1 has a large negative N - N overlap (-1.056) arising mainly from the $6b_{1u}$ orbital. It may be compared with the positive overlap (0.319) in Φ_2. In both these states the N - N pi bonding is constant but small at 0.019. The O1-O3 long range overlap is very small and negative (-0.009) for Φ_1. The long range N1-O3 overlaps are particularly interesting: Φ_1 has a small bonding overlap of 0.032 compared with an anti-bonding effect of -0.018 in Φ_2. This difference, which arises from the a_1 orbitals, may help to stabilize Φ_1. (The same trend was apparent in the SAI results but there the interaction

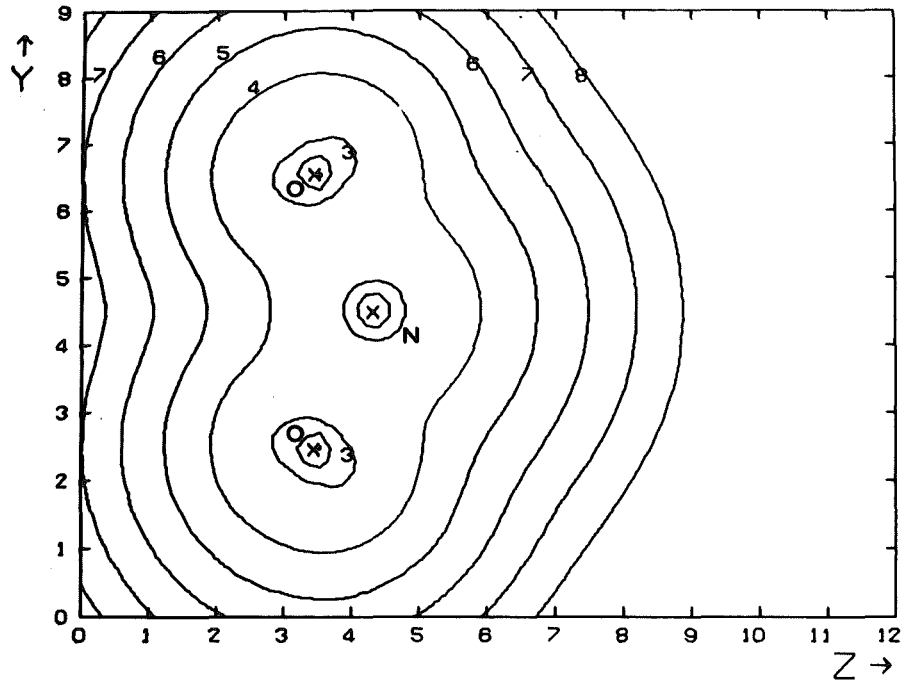

Fig. 6.6 NO_2 2G/S

Max Dens. 114.

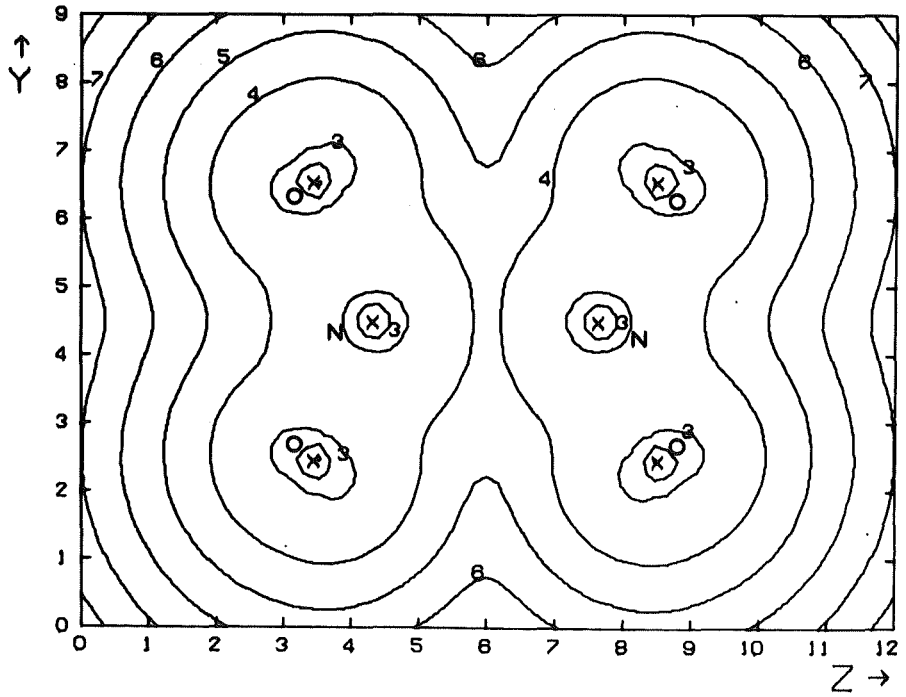

Fig. 6.7 N_2O_4 2G/S

Max Dens. 114.

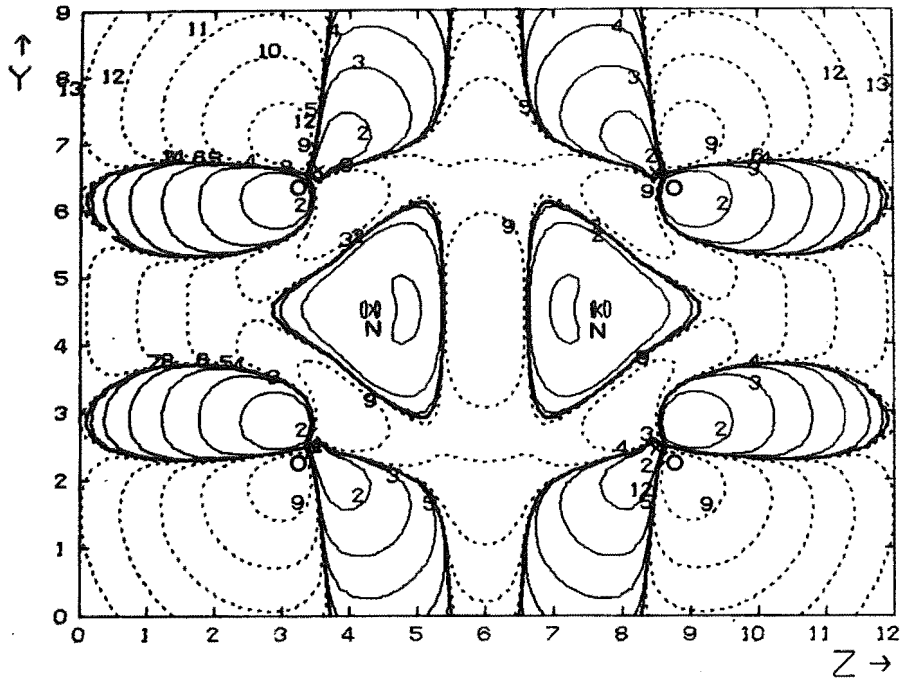

Fig. 6.8 N_2O_4 - 2 NO_2 2 G/S

Max Dens. + 0.128, - 0.0882

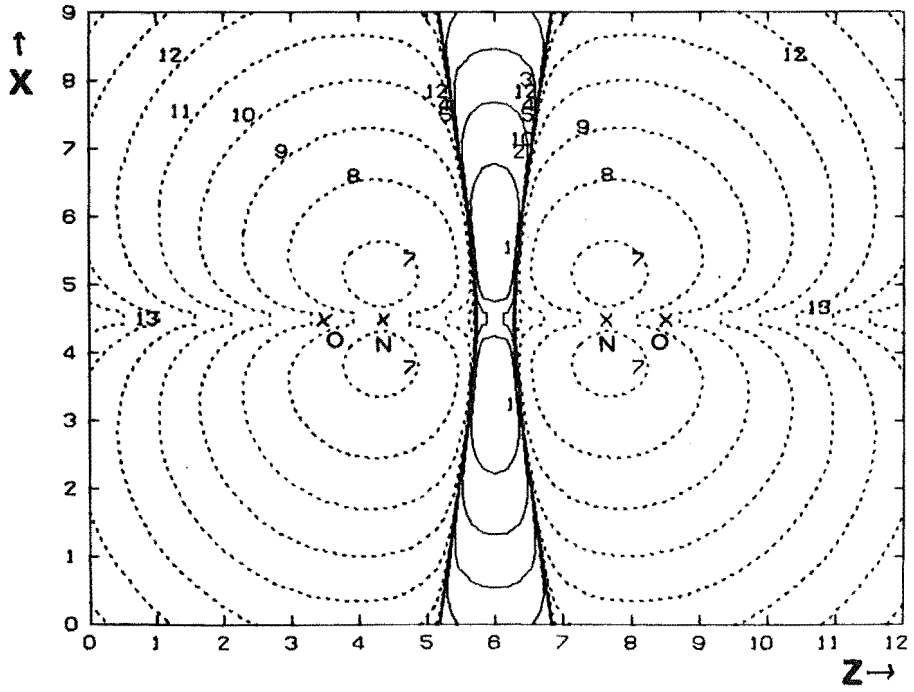

Fig. 6.9 N_2O_4 - 2 NO_2 2 G/S

Max Dens. + 0.000573, - 0.0221

was smaller, with the overlap population being of the same order as the long range O1-O3 overlap.) The N1-O3 overlap for Φ_1 has in fact a larger magnitude than the negative N - N overlap resulting from b_2 orbitals (-0.019) which has been suggested[57] to be responsible for the weak N - N bond as mentioned in Section 2.6.

Figures 6.6 and 6.7 give the total density in the molecular plane for NO_2 and N_2O_4 Φ_1. From these densities the difference map shown in Figure 6.8 was constructed as described for the SAI wave functions in Section 6.4. The strong antibonding character of the N - N interaction is apparent. There is an increase in electron density around the nitrogen atoms in N_2O_4, which is reflected in the net atomic populations of 6.917 in N_2O_4 Φ_1 and 6.289 in NO_2. The difference is not as marked for the oxygen atoms, where the net atomic populations are 7.992 in Φ_1 and 7.908 in NO_2. The density difference map shows a different distribution of charge on the oxygen atoms but the coefficients indicate that this is not attributable to any one MO in particular. The region between the two nitrogen atoms in Figure 6.8 appears different from that in Figure 6.3, because the SAI wave function for NO_2 has very little density directed away from the nitrogen atom, with the result that a smaller amount of density is subtracted from this region. Figure 6.9 shows the pi electron density difference map in the xz-plane which contains the two nitrogen atoms. Here, as opposed to the SAI result of Figure 6.4, the small amount of pi bonding expected from the overlap population of 0.019 is apparent.

Table 6.14 contains the results of the bond energy analysis of Section 5.5 for N_2O_4 and NO_2. The numbers in

Table 6.14

Bond Energy Analysis for N_2O_4 and NO_2

	N_2O_4 Φ_1	N_2O_4 Φ_2	NO_2
One Centre Energies			
(4) O1	-74.4293	-74.4780	-74.3515
(2) N1	-53.3911	-52.9790	-53.0691
Two Centre Energies			
(2) O1-O2	-0.0497	-0.0557	0.0365
(4) O1-N1	-0.3399	-0.3645	-0.6997
(4) N1-O3	-0.1448	0.0396	
(2) O1-O3	0.0400	-0.0075	
(2) O1-O4	-0.0114	-0.0199	
(1) N1-N2	1.0011	-0.5008	
Three Centre Energies			
(2) O1-O2-N1	0.0535	0.0435	0.1338
(2) O1-O2-N2	-0.0349	0.0192	
(4) O1-N1-N2	-0.1326	0.0493	
(4) O1-O2-O3	0.0104	-0.0027	
(4) O1-N1-O3	-0.0070	0.0164	
(4) O2-N1-O3	-0.0148	0.0199	
Four Centre Energies			
(2) O1-O2-N1-N2	-0.0020	0.0005	
(4) O1-O2-N1-O3	0.0000	0.0000	
(4) O1-O2-N2-O3	0.0013	0.0011	
(2) O1-N1-N2-O3	0.0222	0.0193	
(2) O2-N1-N2-O3	0.0226	0.0167	
(1) O1-O2-O3-O4	0.0001	0.0000	
Total Energies			
One Centre	-404.4995	-403.8698	-201.7720
Two Centre	-0.9799	-1.9668	-1.3628
Three Centre	-0.5389	0.4572	0.1338
Four Centre	0.0906	0.0776	
Total	-405.9277	-405.3018	-203.0010

parentheses in the first column are the number of times each of the various terms occurs in the expression for the total energy of N_2O_4. Thus the total energy for Φ_1 and Φ_2 is found by multiplying each entry by the appropriate factor and summing. In general the results parallel those from the Mulliken population analyses. The lowest nitrogen atom one-centre energy is found for Φ_1, where the electron density is increased around this atom. The net nitrogen atom population is 6.917 for Φ_1 and 6.289 for Φ_2. The two centre N1-O1 energy is not as low in N_2O_4, which is in accord with the smaller overlap population. The N1-N2 energy is more positive in Φ_1 than in Φ_2, as expected from the antibonding nature of Φ_1. The O1-O3 energy is stabilizing in Φ_2 but is positive in Φ_1. This trend is also in accord with the total O1-O3 overlap of -0.009 for Φ_1 as mentioned earlier. A major stabilizing factor for Φ_1 is the N1-O3 term, which is lower than in Φ_2. While the three and four centre energies are generally smaller, the O1-N1-N2 term in Φ_1 gives a marked stabilization. This value of -0.1326 is lower than that in any other calculation made, the next lowest being -0.0697 for an H - N - H term in hydrazine. Overall, the increase in energy in Φ_1 caused by the N - N antibonding character is offset by lower nitrogen atom one-centre energies and long range N - O and O - N - N terms.

Further features of the bonding in this wave function will be discussed in the next section, in comparison with results for some smaller species.

6.6 Comparison of Dinitrogen Tetroxide with Smaller Systems

In addition to the calculations on NO_2^- and NO_2 previously discussed in Sections 6.2 and 6.3, computations were also done for NO_2^+, N_2, N_2H_4, HNO and N_2O, for the configurations given in Table 6.15. The total energies quoted were obtained at the experimental geometries given in Appendix II. Table 6.16 compares the results of Mulliken and Bond Energy analyses for NO_2^+, NO_2 and NO_2^- at experimental and N_2O_4 geometries. For both sets all the gross AO populations show NO_2 to be intermediate between NO_2^+ and NO_2^-. In going from NO_2^+ through NO_2 to NO_2^- the N - O bond becomes longer, the N - O overlap smaller, and the two-centre N - O bond energy less negative. When an electron is added to NO_2^+ there is a marked increase in population in the $2p_zO$ and $2p_zN$ orbitals. This is consistent with the electron's being placed in the $6a_1$ orbital, and there is a further increase in these same populations when another electron is added to give NO_2^-. These changes are reflected in the atomic charges, where about one third of the electron's charge is added to each atom. The $6a_1$ orbital is antibonding, with the result that the σ(N - O) overlap population decreases from NO_2^+ to NO_2^- but the π(N - O) overlap is fairly constant. The last column of Table 6.16 gives the results for the N_2O_4 state Φ_1. Comparisons with NO_2^+, NO_2 and NO_2^- all at the N_2O_4 geometry lead to the following conclusions. The populations in the $2p_z$ orbitals of N_2O_4 are closest to those of NO_2, but the N_2O_4 population in the $2p_x$ π orbitals and the (N - O) π overlap are closer to those of NO_2^- while the populations in the 2sN and $2p_yN$ orbitals are more similar to NO_2^+. The (N - O) σ overlap is very much smaller than in NO_2^+, NO_2 or NO_2^- and this feature

Table 6.15

Configurations for smaller systems

Species	Orbital Configuration	Total Energy
NO_2^+	$^1\Sigma_g^+(1\sigma_u)^2(1\sigma_g)^2(2\sigma_g)^2(3\sigma_g)^2(2\sigma_u)^2(4\sigma_g)^2(1\pi_u)^4$ $(3\sigma_u)^2(\pi_g)^4$	-202.8292
N_2O	$^1\Sigma_g^+(1\sigma)^2(2\sigma)^2(3\sigma)^2(4\sigma)^2(5\sigma)^2(6\sigma)^2(1\pi)^4(7\sigma)^2(2\pi)^4$	-182.8761
HNO	$^1A_1(1a')^2(2a')^2(3a')^2(4a')^2(5a')^2(1a'')^2(6a')^2(7a')^2$	-129.2763
N_2	$^1\Sigma_g^+(1\sigma_g)^2(1\sigma_u)^2(2\sigma_g)^2(2\sigma_u)^2(\pi_u)^4(3\sigma_g)^2$	-108.5878
N_2H_4	$^1A_1(1a)^2(1b)^2(2a)^2(2b)^2(3a)^2(3b)^2(4a)^2(4b)^2(5a)^2$	-110.8713

Table 6.16

Comparison of NO_2, NO_2^-, NO_2^+ and N_2O_4

	Experimental Geometry			N_2O_4 Geometry			
	NO_2^+	NO_2	NO_2^-	NO_2^+	NO_2	NO_2^-	N_2O_4 Φ_1
Gross AO pop.							
1sO	2.000	2.000	2.000	2.000	2.000	2.000	2.000
2sO	1.912	1.989	1.881	1.924	1.899	1.873	1.898
$2p_xO$	1.501	1.530	1.593	1.513	1.527	1.568	1.564
$2p_yO$	0.875	1.103	1.307	1.119	1.120	1.157	1.102
$2p_zO$	1.501	1.603	1.665	1.248	1.598	1.865	1.586
1sN	2.000	2.000	2.000	2.000	2.000	2.000	2.000
2sN	1.141	1.296	1.372	1.271	1.281	1.311	1.204
$2p_xN$	0.998	0.939	0.813	0.974	0.945	0.864	0.872
$2p_yN$	1.284	1.251	1.208	1.288	1.247	1.176	1.394
$2p_zN$	0.998	1.247	1.715	0.860	1.240	1.722	1.230
Atomic Charges							
O	0.211	-0.133	-0.446	0.197	-0.144	-0.463	-0.150
N	0.578	0.266	-0.109	0.607	0.288	-0.073	0.300
Subtotal overlap							
(N-O)σ	0.100	0.283	0.273	0.327	0.265	0.213	0.063
(N-O)π	0.469	0.216	0.197	0.223	0.222	0.220	0.215
Total (N-O) overlap	0.569	0.499	0.470	0.550	0.487	0.433	0.278
Bond Energy Analysis							
One centre O	-74.251	-74.328	-74.315	-74.244	-74.352	-74.336	-74.429
One centre N	-52.650	-53.065	-53.236	-52.721	-53.069	-53.282	-53.391
Two centre N-O	-0.834	-0.722	-0.597	-0.816	-0.700	-0.543	-0.340
Internuclear Distance	2.173	2.261	2.334	2.230	2.230	2.230	2.230

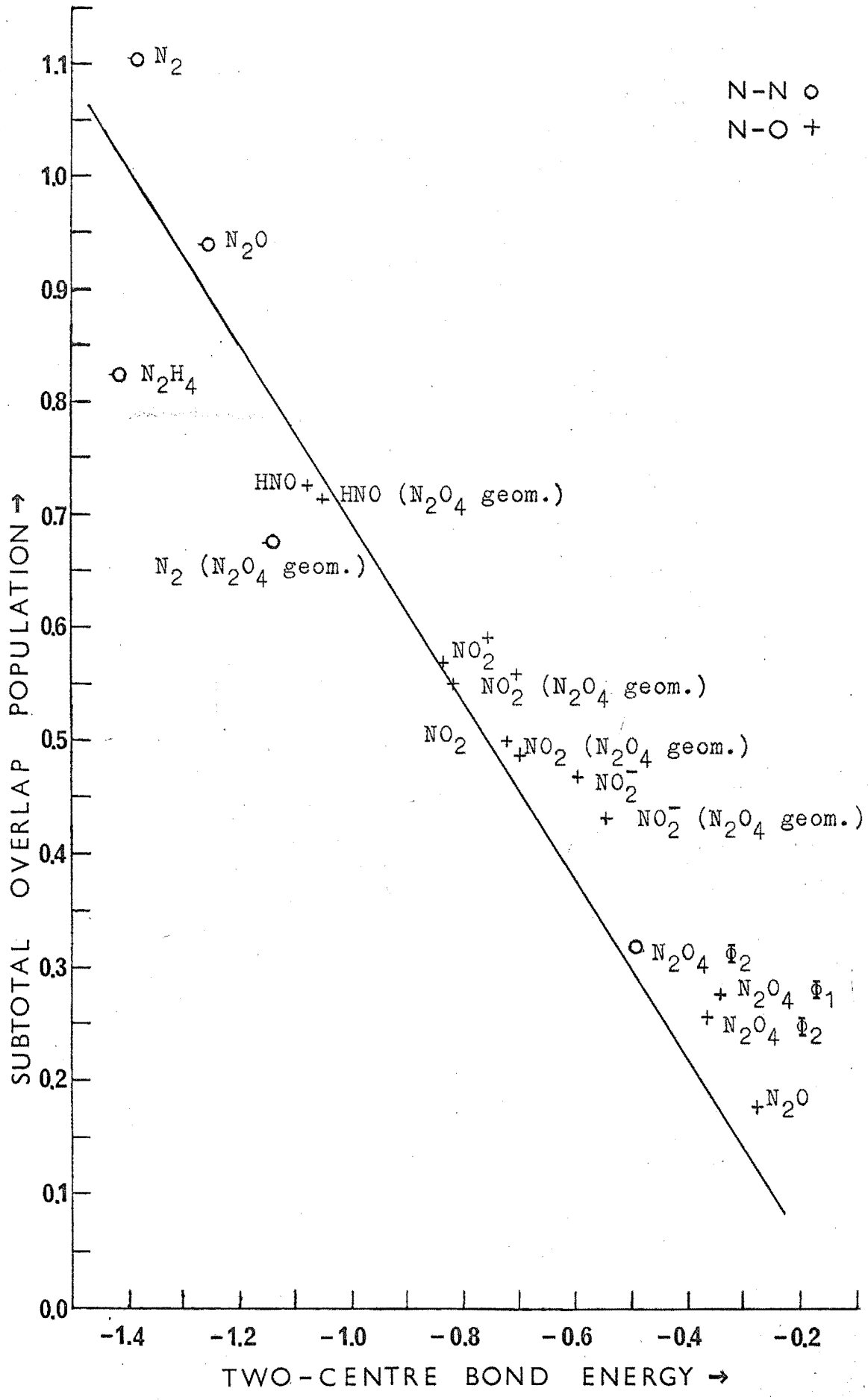
N-N o
N-O +
o N2
o N2O
o N2H4
HNO + HNO (N2O4 geom.)
o N2 (N2O4 geom.)
+ NO2+
+ NO2+ (N2O4 geom.)
NO2 + NO2 (N2O4 geom.)
+ NO2−
+ NO2− (N2O4 geom.)
o N2O4 Φ2
+ N2O4 Φ1
+ N2O4 Φ2
+ N2O
SUBTOTAL OVERLAP POPULATION →
1.1
1.0
0.9
0.8
0.7
0.6
0.5
0.4
0.3
0.2
0.1
0.0
−1.4
−1.2
−1.0
−0.8
−0.6
−0.4
−0.2
TWO-CENTRE BOND ENERGY →

Fig. 6.10

is reflected in a less negative N - O two-centre bond energy. The oxygen and nitrogen one-centre bond energies are lower for N_2O_4 and, as noted in the previous section, are important for the stabilization of this state.

The two-centre bond energies and subtotal overlap populations for the different species are compared in Tables 6.17 and 6.18. In Figure 6.10 these two quantities are plotted and a least squares line is fitted using all the points including that for the N - N bond of N_2O_4 Φ_1 which does not appear on the graph. The correlation coefficient for this data is -0.978 which demonstrates ($\rho < 0.001$) that a relationship exists[177]. The two points which deviate most are for N_2 at the very large N_2O_4 separation and for N_2H_4 which has an unusually low bond energy. Examination of the wave function for hydrazine shows that the 2a orbital (composed mainly of 2sN) and 4a orbital (composed mainly of $2p_yN$) contribute to the N - N bonding. When the canonical orbitals were localized using the method of section 5.4 there resulted a sigma N - N bond, two inner shell orbitals on the nitrogen atoms, four N - H bonding orbitals, and a lone pair orbital on each nitrogen atom. This is entirely consistent with the usual description of the bonding in hydrazine as resulting from sp^3 hybridization on the nitrogen atoms. The trend in the N - N overlap population for N_2, N_2O, N_2H_4 and N_2O_4 shows a decrease in the order given, and this is consistent with the increasing bond length from 2.068 a.u. in N_2 to 3.307 a.u. in N_2O_4.

The correlation between bond length and overlap population for the N - O bonds is not, however, well defined. Thus HNO has the largest overlap population, but also the second longest bond of those considered. Its localized orbitals consist of

Table 6.17

Comparison of N-O bonds

	Two centre bond energy	σ overlap pop.	π overlap pop.	Subtotal overlap pop.	Bond length (a.u.)
NO_2^+	-0.8340	0.100	0.469	0.569	2.1730
N_2O_4 Φ_1	-0.3399	0.063	0.215	0.278	2.2298
N_2O_4 Φ_2	-0.3645	0.039	0.218	0.257	2.2298
NO_2^+ (N_2O_4 geom.)	-0.8157	0.327	0.223	0.550	2.2298
NO_2 (N_2O_4 geom.)	-0.6997	0.265	0.222	0.487	2.2298
NO_2^- (N_2O_4 geom.)	-0.5430	0.213	0.220	0.433	2.2298
HNO (N_2O_4 geom.)	-1.0480	0.377	0.338	0.715	2.2298
N_2O	-0.2731	-0.043	0.220	0.177	2.2418
NO_2	-0.7224	0.283	0.216	0.499	2.2613
HNO	-1.0754	0.407	0.319	0.726	2.2884
NO_2^-	-0.5430	0.273	0.197	0.470	2.3341

Table 6.18

Comparison of N-N bonds

	Two centre bond energy	σ overlap pop.	π overlap pop.	Subtotal overlap pop.	Bond length (a.u.)
N_2	-1.3903	0.199	0.905	1.104	2.068
N_2O	-1.2674	0.178	0.760	0.938	2.1273
N_2H_4	-1.4268	-	-	0.825	2.7401
N_2O_4 Φ_1	1.0011	-1.075	0.019	-1.056	3.307
N_2O_4 Φ_2	-0.5008	0.301	0.019	0.320	3.307
N_2 (N_2O_4 geom.)	-1.1487	0.406	0.266	0.672	3.307

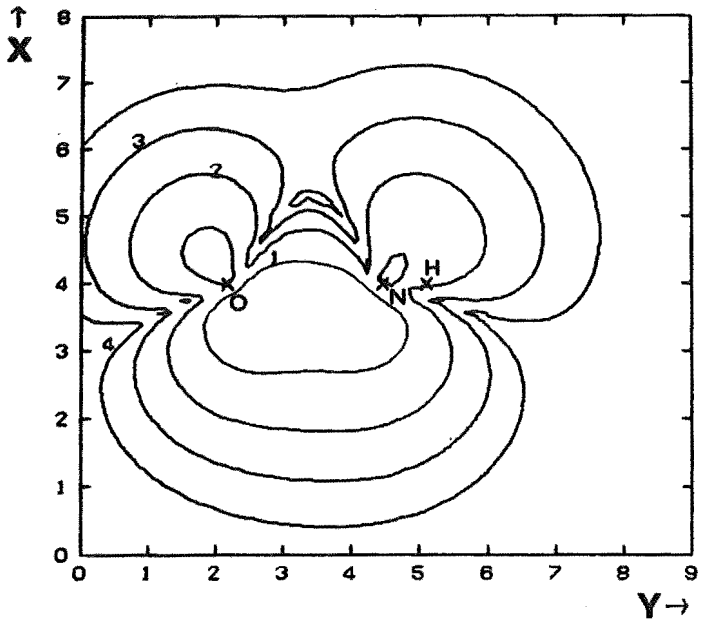

Fig. 6.11 HNO

Max Dens. 0.539

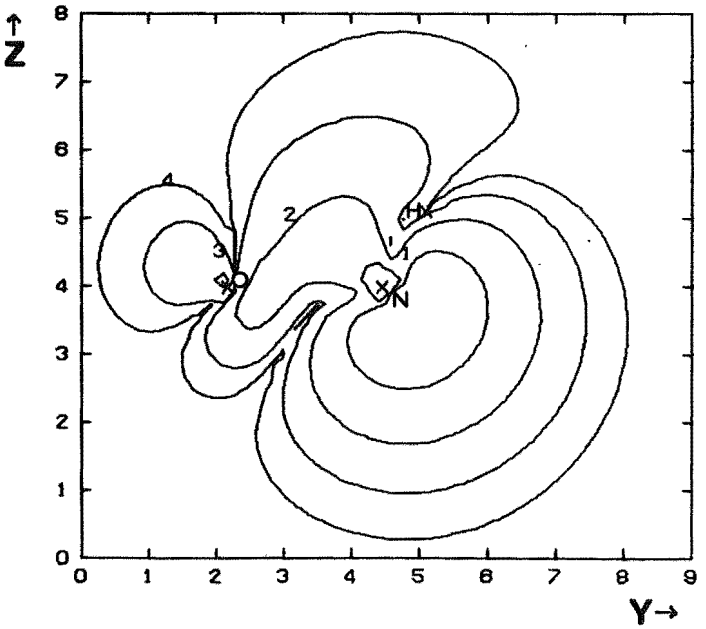

Fig. 6.12 HNO

Max Dens. 0.713

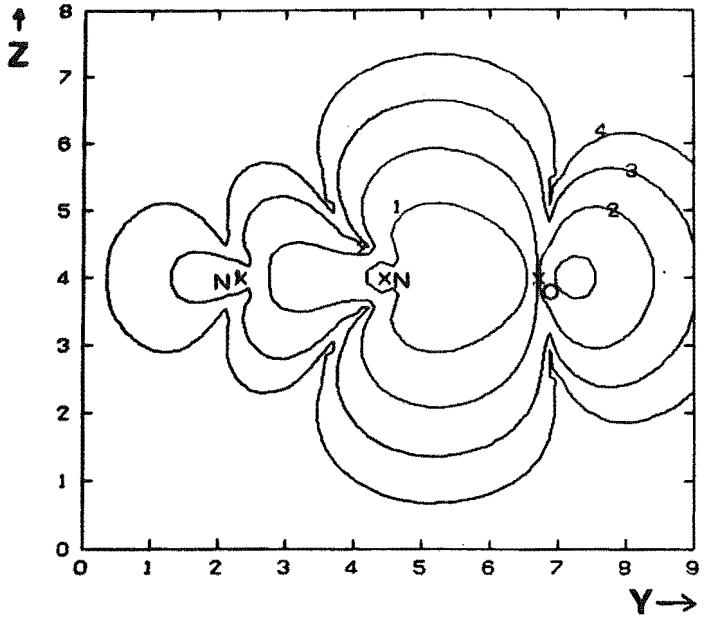

Fig. 6.13 N_2O

Max Dens. 0.513

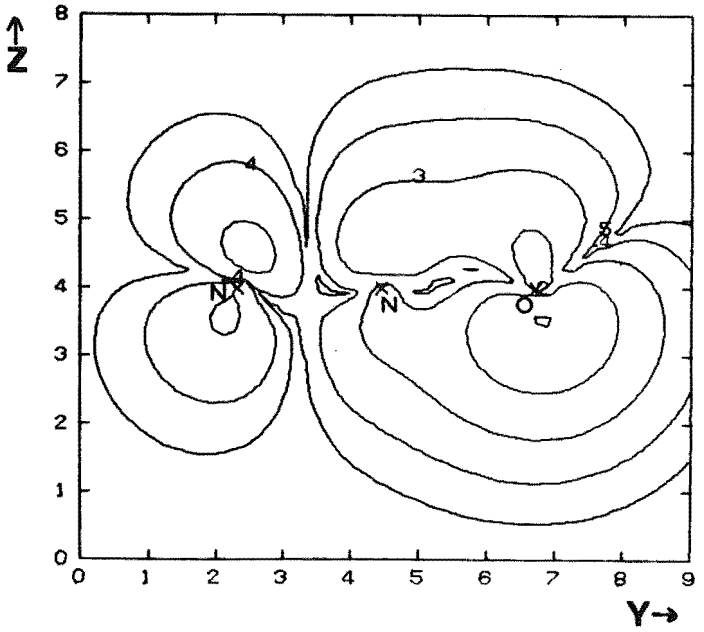

Fig. 6.14 N_2O

Max Dens. 1.05

inner shell orbitals on N and on O, an N - H sigma bond and two 'banana' N - O bonds in a plane perpendicular to the molecular plane. One of these is shown in Figure 6.11. In this, as for all the localized orbitals which are shown in succeeding Figures, the lowest electron density contour drawn has the value 1.00×10^{-4} a.u. Since all the diagrams are drawn to the same scale the relative diffuseness of the orbitals from different molecules is highlighted. In addition to the orbitals just described for HNO there are two lone pairs on the oxygen atom and one on the nitrogen atom. These all contribute a small amount of N - O sigma bonding. The lone pair on the nitrogen atom is plotted in Figure 6.12.

The present calculations do not give a very clear picture of the bonding in N_2O. The N - O bond in N_2O shows only a small amount of overlap (0.177), yet it is shorter than in NO_2. The localized orbitals comprise three inner shells, three N - N 'banana bonds', a nitrogen atom lone pair, three oxygen atom lone pairs, and a weak N - O sigma bond which is localized mainly on the nitrogen atom. This last orbital is plotted in Figure 6.13 where the larger nitrogen contribution is apparent. As can be seen from the overlap populations, most of the N - O bonding is of pi type derived from small delocalizations of the oxygen atom lone pairs. Figure 6.14 is a plot of one of the lone pairs with its maximum density in the plane of the diagram. Thus the usual resonance formulation[60] for N_2O

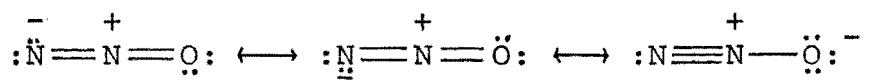

of a normal sigma bond plus some pi bonding is not well reproduced.

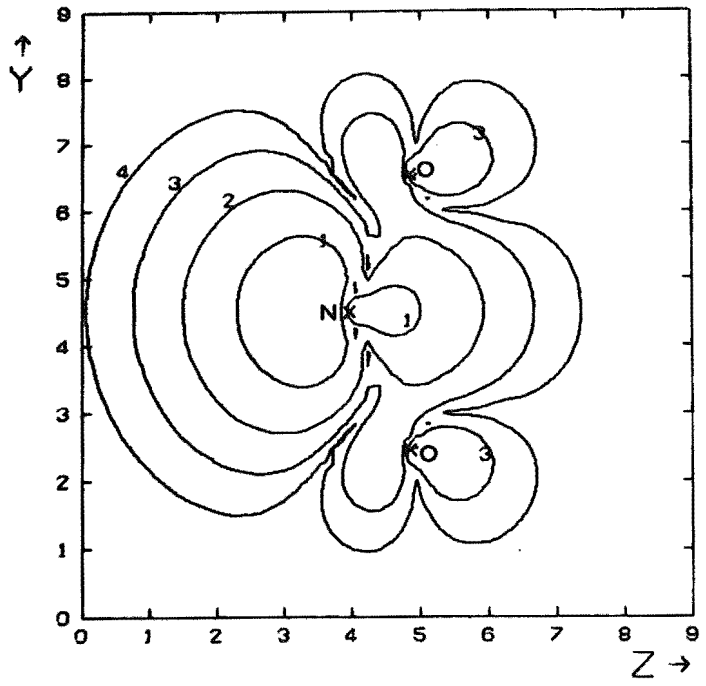

Fig. 6.15 NO_2

Max Dens. 0.772

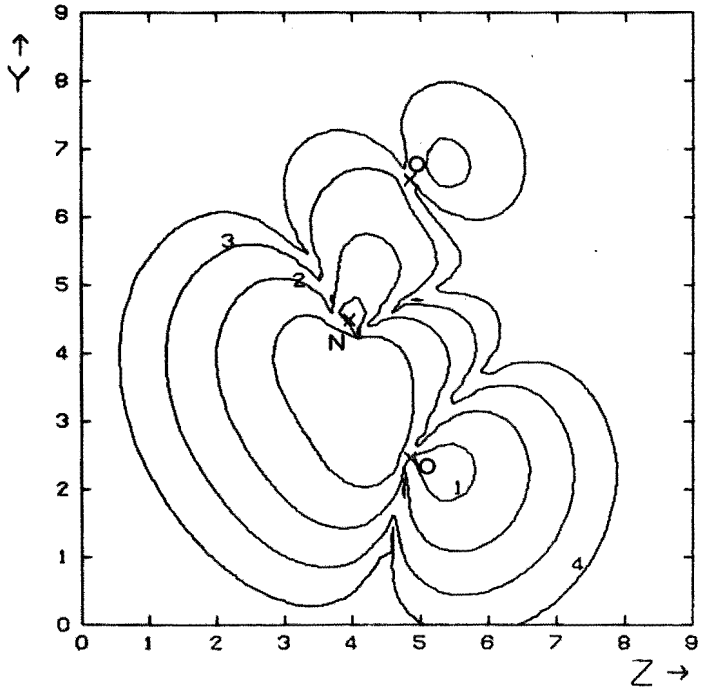

Fig. 6.16 NO_2

Max Dens. 0.520

Localized orbitals for NO_2 were obtained by separately localizing the α and β spin MO's resulting from the UHF calculation with the 2G/S approximation at the N_2O_4 geometry. At this same geometry the localized orbitals for NO_2^- (24 electrons) and NO_2^+ (22 electrons) had the same form as those for the 12α and 11β orbitals of NO_2. The extra α orbital is in the form of a lone pair on the nitrogen atom. The electron density for this orbital, shown in Figure 6.15, was calculated assuming for the sake of comparison with other molecules an occupancy of two electrons. For the α orbitals of NO_2 there are two lone pairs on each oxygen atom and two N - O banana bonds. These bonds have a higher oxygen contribution than in HNO and this may explain the smaller N - O overlap in NO_2^- and NO_2 (HNO 0.726, NO_2^- 0.470, NO_2 0.499). The NO_2 β orbitals do not localize into such well defined bonds. Three banana bonds are formed to each oxygen atom. One of these is in the plane of the molecule and is plotted in Figure 6.16 again assuming an occupancy of two electrons. It has a very much larger nitrogen contribution than the other two, one of which is above and one below the molecular plane. These three bonds account for the larger overlap in NO_2^+ than in NO_2 or NO_2^-. The structure is retained in linear NO_2^+ but the bonds are then equivalent. This description of the α and β localized orbitals of NO_2 makes clear why the structure is intermediate between those of NO_2^- and NO_2^+.

The localized orbitals for N_2O_4 Φ_1 were obtained in two ways. The value of D, the quantity which is maximized on localization according to the method in Appendix V, had the value 90.127 for the canonical MO's. When all twenty-three orbitals were simultaneously localized D rose to 250.220.

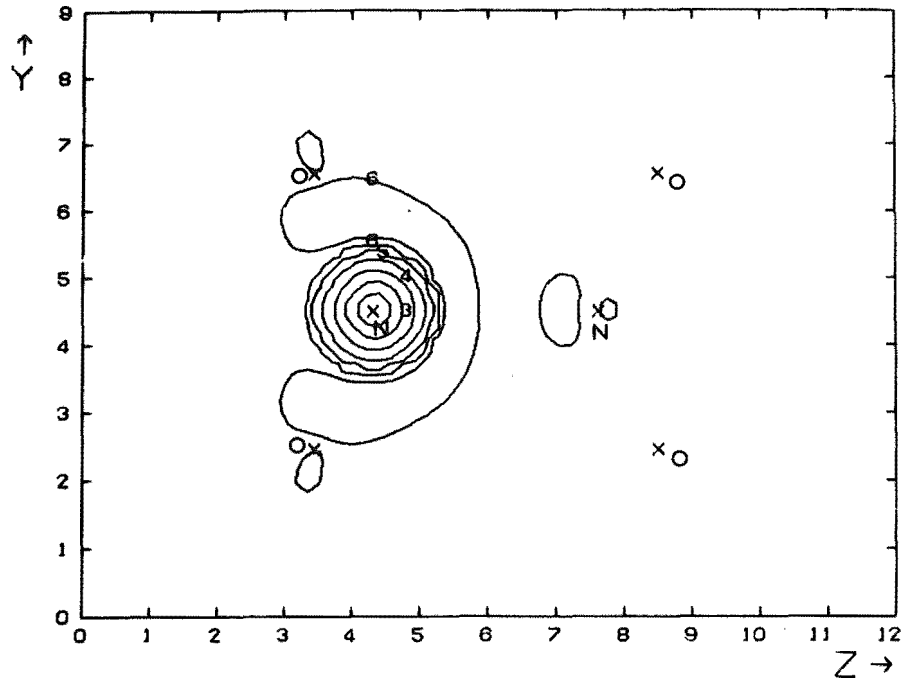

Fig. 6.17 Localized Orbitals N_2O_4

(a) Max Dens. 44.3

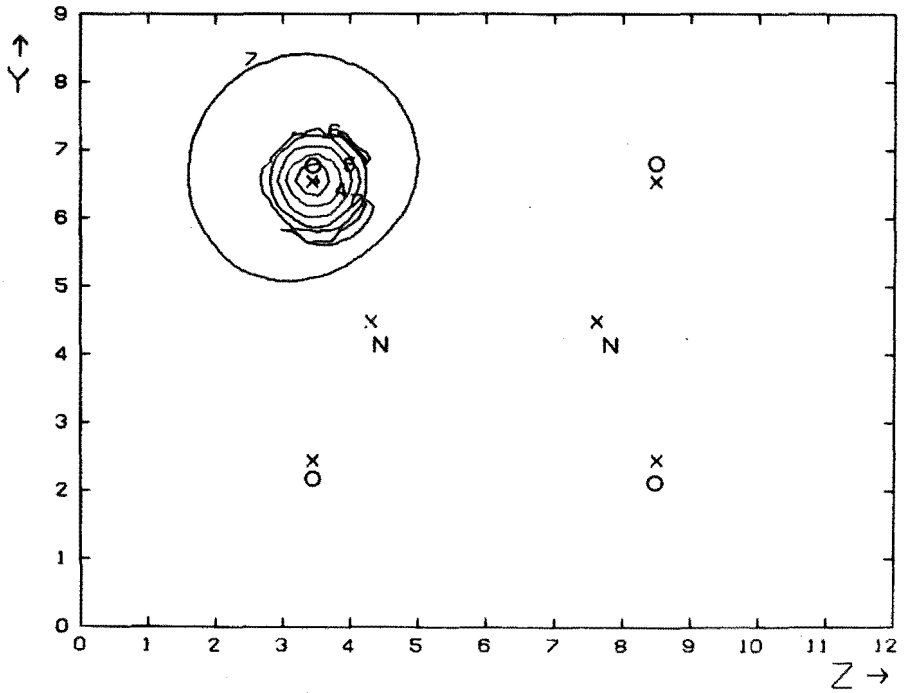

(b) Max Dens. 111.

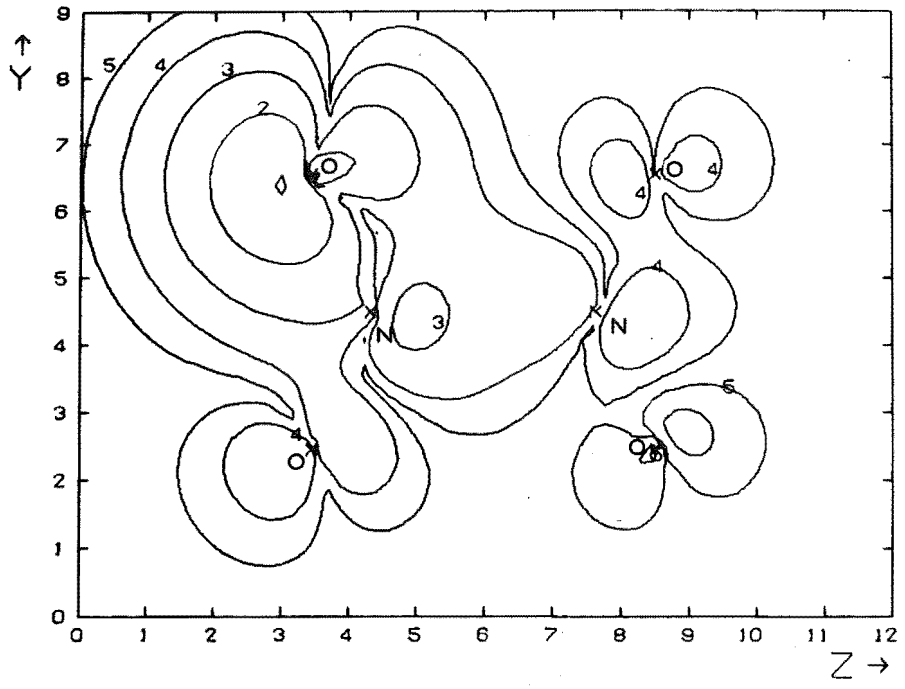

(c) Max Dens. 1.14

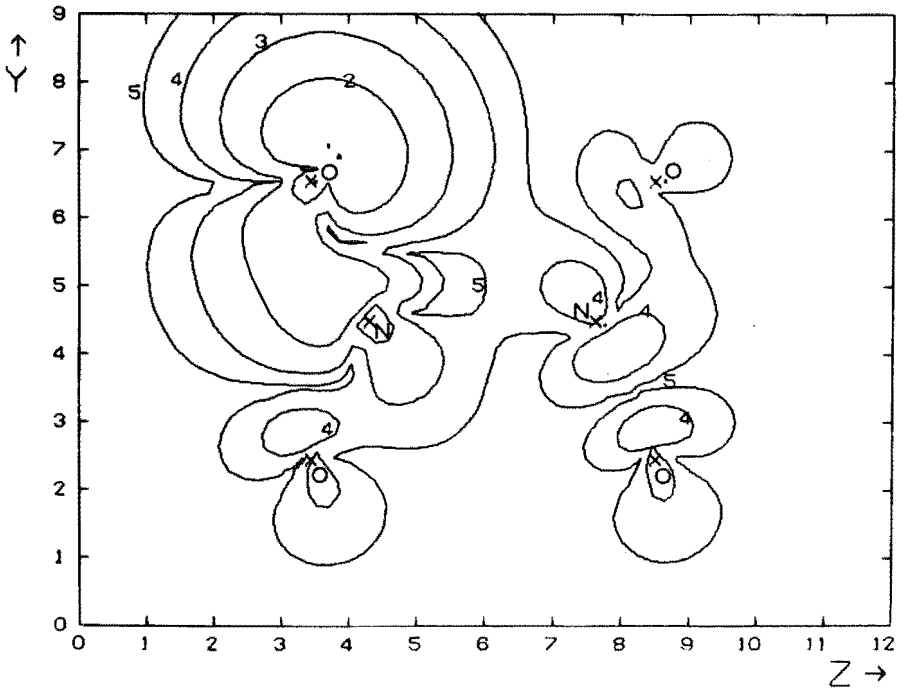

(d) Max Dens. 1.08

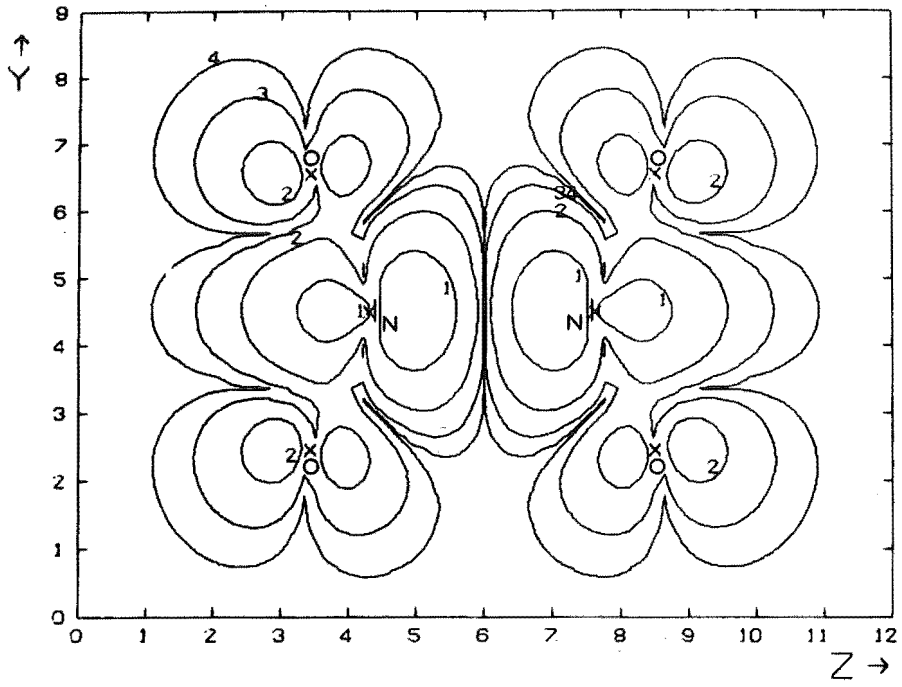

(e) Max Dens. 0.518

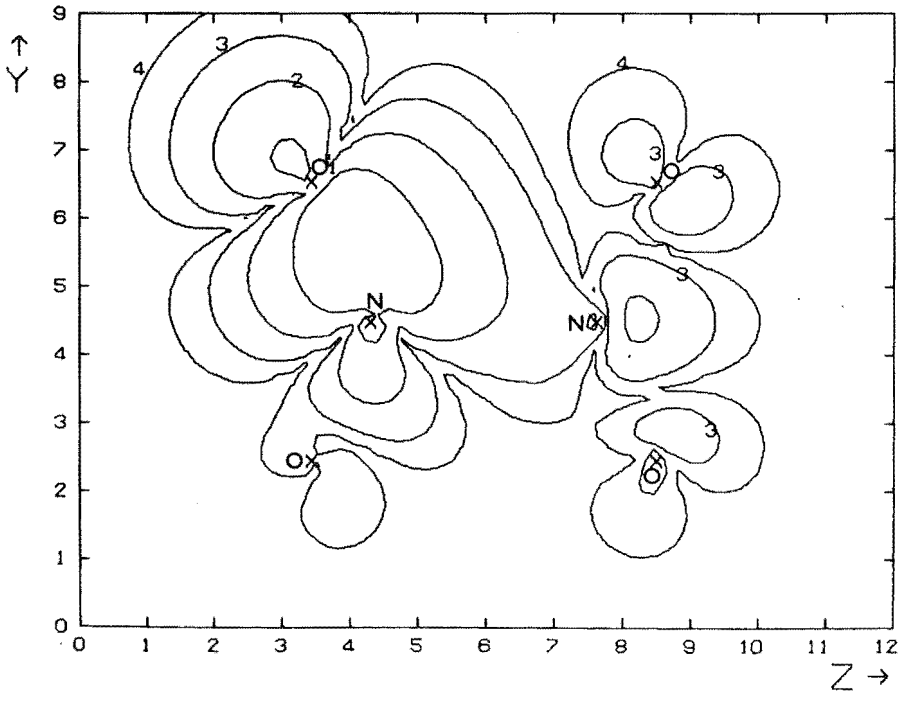

(f) Max Dens. 0.496

There were then three banana bonds from each nitrogen atom to each oxygen atom. Two of these, however, were largely localized on the oxygen atom and the third had large 2sN and $2p_yN$ contributions. In addition there was in the molecular plane a lone pair orbital on each oxygen atom. The N - N antibonding $6b_{1u}$ orbital remained virtually unchanged by the localization. The alternative treatment was to localize the sigma and pi MO's separately. This gave a value for D of 250.014 (sigma 207.652, pi 42.362) so that while these orbitals are not maximally localized they should lead to a similar description of the amount of bonding in N_2O_4. The pi orbitals localized into four N - O bonds with the oxygen coefficient about twice that of the nitrogen atom. One of each type of the sigma orbitals is shown in Figure 6.17. There are two lone pairs on each oxygen atom and, of the inner shell orbitals, that on the oxygen atom is more tightly bound owing to oxygen's larger nuclear charge. The N - O sigma bonding orbital, while not as symmetrical as the one in N_2O, is very similar in that it has a much larger contribution from the nitrogen atom than from the oxygen. The N - O sigma overlap in N_2O_4 Φ_1 has the small value 0.063. Another factor that is responsible for this low value is the N - O antibonding character present in the localized MO shown in Figure 6.17e. The strong N - N antibonding of this orbital is clearly evident.

6.7 Comment on the "Pi-Only" Model for N_2O_4

As described in Sections 2.6 and 2.7 the "pi-only" model has no N - N sigma bond and only six pi electrons. Its configuration, N_2O_4 Φ_3, is given in Table 6.11. Coulson & Duchesne[62] suggested that it was formed by pi bonding between

two NO_2 $^2A_2$ moieties. A comparison between NO_2 $^2A_2$ at the N_2O_4 geometry and N_2O_4 Φ_3 is therefore given in Table 6.19. The subtotal atomic populations clearly show the similarity between these two wave functions and this may be compared with the correlation between N_2O_4 Φ_1 and NO_2 $^2A_1$ which are included in the same table. The subtotal overlap populations, however, do not help in distinguishing Φ_1 and Φ_3 with regard to their component monomers because the values for sigma orbitals are so much reduced for N_2O_4 compared with NO_2. Since the la_2 orbital of NO_2, which is singly filled in the $^2A_2$ state and doubly occupied in $^2A_1$, is N - O non-bonding the pi N - O overlap is about the same in all four cases. Also because this orbital has no nitrogen atom contribution N - N pi overlap is about 0.02 for both Φ_1 and Φ_3. Although the la_u orbital is vacant in N_2O_4 Φ_3 01-03 pi bonding is still very small at 0.002. The N - O overlap in Φ_3 is larger than that in Φ_1 as the result of small changes in several MO's; as expected from earlier discussions in Section 6.6 this difference is paralleled by a similar change in the N - O two centre bond energy.

6.8 Conclusions

The method of combining the conjugate gradients technique with Roothaan's diagonalization procedure for minimizing the energy of a closed shell system has proved to be computationally most effective. For both closed and open shell calculations, and in particular for those on N_2O_4, the advantage of using a symmetry basis was demonstrated. A description of the bonding in N_2O_4 and NO_2 using the Simplified Ab Initio method led to problems of interpretation caused by poor results obtained from the Mulliken analysis for overlap populations.

Table 6.19

Comparison of the "π-only" wavefunction for N_2O_4, Φ_3

	N_2O_4 Φ_1	N_2O_4 Φ_3	NO_2 $^2A_1$	NO_2 $^2A_2$
Subtotal Atomic Populations				
Oσ	6.586	6.989	6.616	7.002
Oπ	1.564	1.083	1.527	1.036
O total	8.150	8.072	8.143	8.038
Nσ	5.828	6.022	5.767	5.996
Nπ	0.872	0.834	0.945	0.928
N total	6.700	6.856	6.712	6.924
Subtotal Overlap Populations				
(N-O)σ	0.063	0.166	0.265	0.247
(N-O)π	0.215	0.212	0.222	0.222
(N-O) total	0.278	0.378	0.487	0.469
(N-O) Two centre energy	-0.3399	-0.4683	-0.6997	-0.5905

An investigation using the 2G/S method, in which most two electron repulsion integrals were calculated by expanding each Slater basis function in terms of two Gaussian orbitals, suggested an explanation for the weakness of the N - N bond of N_2O_4. The ground state wave function, Φ_1, had an occupied antibonding orbital between the nitrogen atoms while the expected sigma bonding orbital $6a_g$ was vacant. This state accounted for over 95% of a CI wave function which included six doubly-excited configurations. In particular, the "pi-only" structure of Coulson & Duchesne[62] was found to have a higher energy and a negligible contribution to the CI wave function. The major difficulty with the state Φ_1 was to explain why N_2O_4 is stable at all. All covalent bonding was reduced and indeed the dissociation energy was calculated to be negative (-0.0422 a.u. using the CI wave function for N_2O_4 and the RHF wave function at the experimental geometry for NO_2). Electron correlation effects become more important in larger systems and as noted by Clark & Stewart[5] are known to be responsible even at the Hartree-Fock limit for reducing calculated values for dissociation energies. A well-known example is the fluorine molecule where the Hartree-Fock wave function produces a nonbonded state[178]. For the calculated state N_2O_4 Φ_1 long range O1-O3 interactions were negligible and N - N π bonding was small.

In order to understand why the N - N nonbonded state had the lowest energy of those considered a bond energy analysis was implemented. The state Φ_1 had small net atomic charges on the nitrogen atoms, and appeared to be stabilized by N1-O3 long range interactions and three centre interactions of the

type N - N - O. These three effects have been suggested by Harcourt[133] to be important factors in the increased valence description of N_2O_4. As discussed in Section 2.8 the increased valence formula for N_2O_4 represents resonance amongst several covalent and ionic structures. In this regard it is interesting to note that Larcher & Linnett[179] from a study of pentaborane-9 suggested that ionic B - B bonding could result from migration of charge out of the bonding region to give a more favourable charge location.

Although N_2O_4 was correctly predicted to be intermediate between NO_2^+ and NO_2^- the decrease in sigma bonding in N_2O_4 made a comparison between it and these smaller species difficult. An electron density difference map clearly showed the increase in electron charge around the nitrogen atoms as compared with NO_2. It is possible that calculations carried out with the more accurate but far more time consuming 3G/S method would lead to better comparisons here.

APPENDIX I

CHARACTER TABLES FOR POINT GROUPS C_{2v} and D_{2h}

C_{2v}	I	$C_2(z)$	$\sigma_v(xz)$	$\sigma_v(yz)$
A_1	1	1	1	1
A_2	1	1	-1	-1
B_1	1	-1	1	-1
B_2	1	-1	-1	1

D_{2h}	I	$\sigma(xy)$	$\sigma(xz)$	$\sigma(yz)$	i	$C_2(z)$	$C_2(y)$	$C_2(x)$
A_g	1	1	1	1	1	1	1	1
A_u	1	-1	-1	-1	-1	1	1	1
B_{1g}	1	1	-1	-1	1	1	-1	-1
B_{1u}	1	-1	1	1	-1	1	-1	-1
B_{2g}	1	-1	1	-1	1	-1	1	-1
B_{2u}	1	1	-1	1	-1	-1	1	-1
B_{3g}	1	-1	-1	1	1	-1	-1	1
B_{3u}	1	1	1	-1	-1	-1	-1	1
Γ*	30	0	6	18	0	2	0	0

* Γ is the reducible representation for which the thirty atomic orbitals of N_2O_4 form a basis.

APPENDIX II

GEOMETRIES

The following values for the Cartesian coordinates of the atoms were used for the calculations of this project.

Dinitrogen Tetroxide[89], N_2O_4

	x	y	z
O1	0.0	2.0500	-2.5305
O2	0.0	-2.0500	-2.5305
N1	0.0	0.0	-1.6535
N2	0.0	0.0	1.6535
O3	0.0	2.0500	2.5305
O4	0.0	-2.0500	2.5305

Nitrogen Dioxide[48], NO_2

	x	y	z
O1	0.0	-2.0835	0.8790
O2	0.0	-2.0835	0.8790
N	0.0	0.0	0.0

Nitrite Ion[175]

	x	y	z
O1	0.0	-1.96860	1.25414
O2	0.0	1.96860	1.25414
N	0.0	0.0	0.0

Nitronium Ion[51] NO_2^+

	x	y	z
O1	0.0	-2.1730	0.0
O2	0.0	2.1730	0.0
N	0.0	0.0	0.0

Nitrogen[51], N_2

	x	y	z
N1	0.0	-1.034	0.0
N2	0.0	1.034	0.0

Hydrazine[180], N_2H_4

	x	y	z
H1	1.52902	2.08733	0.90172
H2	-1.52902	2.08733	0.90172
N1	0.0	1.37007	0.0
H3	0.90172	-2.08733	1.52902
H4	0.90172	-2.08733	-1.52902
N2	0.0	-1.37007	0.0

Nitrous Oxide[181], N_2O

	x	y	z
N1	0.0	-2.1273	0.0
N2	0.0	0.0	0.0
O	0.0	2.2418	0.0

HNO[108]

	x	y	z
O	0.0	-2.2884	0.0
N	0.0	0.0	0.0
H	0.0	0.6368	1.9030

NO_2,NO_2^-,NO_2^+ with geometry of N_2O_4

	x	y	z
01	0.0	-2.0500	0.8770
02	0.0	2.0500	0.8770
N	0.0	0.0	0.0

N_2 with identical bond length to N_2O_4

	x	y	z
N1	0.0	-1.6535	0.0
N2	0.0	1.6535	0.0

HNO with NO bond length identical to that in N_2O_4

	x	y	z
O	0.0	-2.2298	0.0
N	0.0	0.0	0.0
H	0.0	0.6368	1.903

APPENDIX III

SYMMETRY ORBITALS

As described in Chapter Three the computations are simplified by forming from the atomic basis functions linear combinations which transform as irreducible representations of the molecular point group. The unnormalized symmetry orbitals are given as follows:

N_2O_4 (Point Group D_{2h})

$$\sigma_1(a_g) = 1s01 + 1s02 + 1s03 + 1s04$$
$$\sigma_2(a_g) = 2s01 + 2s02 + 2s03 + 2s04$$
$$\sigma_3(a_g) = 2p_y01 - 2p_y02 + 2p_y03 - 2p_y04$$
$$\sigma_4(a_g) = 2p_z01 + 2p_z02 - 2p_z03 - 2p_z04$$
$$\sigma_5(a_g) = 1sN1 + 1sN2$$
$$\sigma_6(a_g) = 2sN1 + 2sN2$$
$$\sigma_7(a_g) = 2p_zN1 - 2p_zN2$$

$$\sigma_8(a_u) = 2p_x01 - 2p_x02 - 2p_x03 + 2p_x04$$

$$\sigma_9(b_{3g}) = 1s01 - 1s02 - 1s03 + 1s04$$
$$\sigma_{10}(b_{3g}) = 2s01 - 2s02 - 2s03 + 2s04$$
$$\sigma_{11}(b_{3g}) = 2p_y01 + 2p_y02 - 2p_y03 - 2p_y04$$
$$\sigma_{12}(b_{3g}) = 2p_z01 - 2p_z02 + 2p_z03 - 2p_z04$$
$$\sigma_{13}(b_{3g}) = 2p_yN1 - 2p_yN2$$

$$\sigma_{14}(b_{3u}) = 2p_x01 + 2p_x02 + 2p_x03 + 2p_x04$$
$$\sigma_{15}(b_{3u}) = 2p_xN1 + 2p_xN2$$

$$\sigma_{16}(b_{2g}) = 2p_x01 + 2p_x02 - 2p_x03 - 2p_x04$$
$$\sigma_{17}(b_{2g}) = 2p_xN1 - 2p_xN2$$

$\sigma_{18}(b_{2u}) = 1s01 - 1s02 + 1s03 - 1s04$

$\sigma_{19}(b_{2u}) = 2s01 - 2s02 + 2s03 - 2s04$

$\sigma_{20}(b_{2u}) = 2p_y01 + 2p_y02 + 2p_y03 + 2p_y04$

$\sigma_{21}(b_{2u}) = 2p_z01 - 2p_z02 - 2p_z03 + 2p_z04$

$\sigma_{22}(b_{2u}) = 2p_yN1 + 2p_yN2$

$\sigma_{23}(b_{1g}) = 2p_x01 - 2p_x02 + 2p_x03 - 2p_x04$

$\sigma_{24}(b_{1u}) = 1s01 + 1s02 - 1s03 - 1s04$

$\sigma_{25}(b_{1u}) = 2s01 + 2s02 - 2s03 - 2s04$

$\sigma_{26}(b_{1u}) = 2p_y01 - 2p_y02 - 2p_y03 + 2p_y04$

$\sigma_{27}(b_{1u}) = 2p_z01 + 2p_z02 + 2p_z03 + 2p_z04$

$\sigma_{28}(b_{1u}) = 1sN1 - 1sN2$

$\sigma_{29}(b_{1u}) = 2sN1 - 2sN2$

$\sigma_{30}(b_{1u}) = 2p_zN1 + 2p_zN2$

NO_2 (Point Group C_{2v})

$\sigma_1(a_1) = 1s01 + 1s02$

$\sigma_2(a_1) = 2s01 + 2s02$

$\sigma_3(a_1) = 2p_y01 - 2p_y02$

$\sigma_4(a_1) = 2p_z01 + 2p_z02$

$\sigma_5(a_1) = 1sN$

$\sigma_6(a_1) = 2sN$

$\sigma_7(a_1) = 2p_zN$

$\sigma_8(a_2) = 2p_x01 - 2p_x02$

$\sigma_9(b_1) = 2p_x01 + 2p_x02$

$\sigma_{10}(b_1) = 2p_xN$

$\sigma_{11}(b_2)$ = 1s01 - 1s02

$\sigma_{12}(b_2)$ = 2s01 - 2s02

$\sigma_{13}(b_2)$ = $2p_y$01 + $2p_y$02

$\sigma_{14}(b_2)$ = $2p_z$01 - $2p_z$02

$\sigma_{15}(b_2)$ = $2p_y$N

N_2H_4 (Point Group C_2)

$\sigma_1(a)$ = 1sH1 + 1sH3

$\sigma_2(a)$ = 1sH2 + 1sH4

$\sigma_3(a)$ = 1sN1 + 1sN2

$\sigma_4(a)$ = 2sN1 + 2sN2

$\sigma_5(a)$ = $2p_x$N1 + $2p_z$N2

$\sigma_6(a)$ = $2p_z$N1 + $2p_x$N2

$\sigma_7(a)$ = $2p_y$N1 - $2p_y$N2

$\sigma_8(b)$ = 1sH1 - 1sH3

$\sigma_9(b)$ = 1sH2 - 1sH4

$\sigma_{10}(b)$ = 1sN1 - 1sN2

$\sigma_{11}(b)$ = 2sN1 - 2sN2

$\sigma_{12}(b)$ = $2p_x$N1 - $2p_z$N2

$\sigma_{13}(b)$ = $2p_z$N1 - $2p_x$N2

$\sigma_{14}(b)$ = $2p_y$N1 + $2p_y$N2

NO_2^+ (Point Group $D_{\infty h}$)

$\sigma_1(\sigma_g)$ = 1s01 + 1s02

$\sigma_2(\sigma_g)$ = 2s01 + 2s02

$\sigma_3(\sigma_g)$ = $2p_y$01 - $2p_y$02

$\sigma_4(\sigma_g)$ = 1sN

$\sigma_5(\sigma_g)$ = 2sN

$\sigma_6(\sigma_u) = 1s01 - 1s02$

$\sigma_7(\sigma_u) = 2s01 - 2s02$

$\sigma_8(\sigma_u) = 2p_y01 + 2p_y02$

$\sigma_9(\sigma_u) = 2p_yN$

$\sigma_{10}(\pi_g) = 2p_x01 - 2p_x02$

$\sigma_{11}(\pi_g) = 2p_z01 - 2p_z02$

$\sigma_{12}(\pi_u) = 2p_x01 + 2p_x02$

$\sigma_{13}(\pi_u) = 2p_z01 + 2p_z02$

$\sigma_{14}(\pi_u) = 2p_xN$

$\sigma_{15}(\pi_u) = 2p_zN$

N_2 (Point Group $D_{\infty h}$)

$\sigma_1(\sigma_g) = 1sN1 + 1sN2$

$\sigma_2(\sigma_g) = 2sN1 + 2sN2$

$\sigma_3(\sigma_g) = 2p_yN1 - 2p_yN2$

$\sigma_4(\sigma_u) = 1sN1 - 1sN2$

$\sigma_5(\sigma_u) = 2sN1 - 2sN2$

$\sigma_6(\sigma_u) = 2p_yN1 + 2p_yN2$

$\sigma_7(\pi_u) = 2p_xN1 + 2p_xN2$

$\sigma_8(\pi_u) = 2p_zN1 + 2p_zN2$

$\sigma_9(\pi_g) = 2p_xN1 - 2p_xN2$

$\sigma_{10}(\pi_g) = 2p_zN1 - 2p_zN2$

APPENDIX IV

THE METHOD OF CONJUGATE GRADIENTS

Solution of Linear Equations

The basic algorithm for the conjugate gradients method was constructed by Hestenes & Stiefel[182] for the solution of a system of linear algebraic equations. Beckman's[183] description of the method will be given, and later the connection with the minimization problem will be shown.

Let $\underline{A}\ \underline{x} = \underline{k}$ be a system of N linear equations in the N unknowns $\underline{x}$. $\underline{A}$ is an N x N positive definite symmetric matrix and the components of the vector $\underline{k}$ are constants. Let $\underline{x}_0$ be an arbitrary starting approximation to the required solution $\underline{h}$, and take

$$\underline{p}_0 = \underline{r}_0 = \underline{k} - \underline{A}\ \underline{x}_0. \tag{IV.1}$$

$(\underline{p},\underline{q})$ represents the inner product of vectors $\underline{p}$ and $\underline{q}$. If $(\underline{A}\ \underline{p},\underline{q}) = 0$ for $\underline{p} \neq \underline{q}$ then $\underline{p}$ and $\underline{q}$ are said to be $\underline{A}$-orthogonal or $\underline{A}$-conjugate. We simultaneously derive a sequence of orthogonal residual vectors $\{\underline{r}_i\}$ and a sequence of $\underline{A}$-orthogonal direction vectors $\{\underline{p}_i\}$.

The $\{\underline{r}_i\}$ are formed by Gram-Schmidt orthogonalization of $\underline{r}_0$, $\underline{A}\ \underline{p}_0$, $\underline{A}\ \underline{p}_1,\ldots,\underline{A}\ \underline{p}_{N-2}$, while the $\{\underline{p}_i\}$ are formed by Gram-Schmidt $\underline{A}$-orthogonalization of $\underline{r}_0$, $\underline{r}_1,\ldots,\underline{r}_{N-1}$. The $\underline{A}$-orthogonalization is performed as follows. Let $\{\underline{v}_i\}$ be linearly independent and construct $\{\underline{t}_i\}$ $\underline{A}$-orthogonal.

$$\underline{t}_1 = \underline{v}_1 \tag{IV.2}$$

$$\underline{t}_{k+1} = \underline{v}_{k+1} + \alpha_{k+1,1}\underline{t}_1 + \alpha_{k+1,2}\underline{t}_2 + \cdots + \alpha_{k+1,k}\underline{t}_k \qquad \text{(IV.3)}$$

This is $\underline{A}$-orthogonal to $\underline{t}_r$ for $r \leqslant k$ if

$$(\underline{A}\ \underline{t}_{k+1}, \underline{t}_r) = (\underline{A}\ \underline{v}_{k+1}, \underline{t}_r) + \alpha_{k+1,r}(\underline{A}\ \underline{t}_t, \underline{t}_r) = 0 \qquad \text{(IV.4)}$$

This implies

$$\alpha_{k+1,r} = -(\underline{A}\ \underline{v}_{k+1}, \underline{t}_r)/(\underline{A}\ \underline{t}_r, \underline{t}_r) \qquad \text{(IV.5)}$$

so that

$$\underline{t}_{k+1} = \underline{v}_{k+1} - \left[\frac{(\underline{A}\ \underline{v}_{k+1}, \underline{t}_1)}{(\underline{A}\ \underline{t}_1, \underline{t}_1)}\underline{t}_1 + \frac{(\underline{A}\ \underline{v}_{k+1}, \underline{t}_2)}{(\underline{A}\ \underline{t}_2, \underline{t}_2)}\underline{t}_2 + \cdots + \frac{(\underline{A}\ \underline{v}_{k+1}, \underline{t}_k)}{(\underline{A}\ \underline{t}_k, \underline{t}_k)}\underline{t}_k\right] \qquad \text{(IV.6)}$$

From this $\underline{v}_k$ can be expressed as a linear combination of $\underline{t}_1, \ldots, \underline{t}_k$ so that

$$(\underline{v}_k, \underline{A}\ \underline{t}_i) = 0 \qquad \text{for } i > k \qquad \text{(IV.7)}$$

An orthogonal set $\{\underline{t}_i^*\}$ may be constructed from the $\{\underline{v}_i\}$ as follows.

$$\underline{t}_1^* = \underline{v}_1 \qquad \text{(IV.8)}$$

$$\underline{t}_{k+1}^* = \underline{t}_k^* + \beta_{k+1,1}\underline{t}_1^* + \beta_{k+1,2}\underline{t}_2^* + \cdots + \beta_{k+1,k-1}\underline{t}_{k-1}^* + \beta_{k+1,k}\underline{v}_{k+1} \qquad \text{(IV.9)}$$

This is orthogonal to $\underline{t}_k^*$ if

$$(\underline{t}_{k+1}^*, \underline{t}_k^*) = (\underline{t}_k^*, \underline{t}_k^*) + \beta_{k+1,k}(\underline{v}_{k+1}, \underline{t}_k^*) = 0 \qquad \text{(IV.10)}$$

which implies

$$\beta_{k+1,k} = -(\underline{t}_k^*, \underline{t}_k^*)/(\underline{v}_{k+1}, \underline{t}_k^*) \quad \text{if } (\underline{v}_{k+1}, \underline{t}_k^*) \neq 0 \qquad \text{(IV.11)}$$

and to $\underline{t}_r^*$, $r < k$ if

$$(\underline{t}_{k+1}^*, \underline{t}_r^*) = \beta_{k+1,r}(\underline{t}_r^*, \underline{t}_r^*) + \beta_{k+1,k}(\underline{v}_{k+1}, \underline{t}_r^*) = 0 \qquad \text{(IV.12)}$$

which implies

$$\beta_{k+1,r} = -\beta_{k+1,k}(\underline{v}_{k+1}, \underline{t}_r^*)/(\underline{t}_r^*, \underline{t}_r^*) \qquad \text{(IV.13)}$$

so that

$$\underline{t}_{k+1}^* = \underline{t}_k^* + \frac{(\underline{t}_k^*, \underline{t}_k^*)}{(\underline{v}_{k+1}, \underline{t}_k^*)} \left[\frac{(\underline{v}_{k+1}, \underline{t}_1^*)}{(\underline{t}_1^*, \underline{t}_1^*)} \underline{t}_1^* + \cdots + \frac{(\underline{v}_{k+1}, \underline{t}_{k-1}^*)}{(\underline{t}_{k-1}^*, \underline{t}_{k-1}^*)} \underline{t}_{k-1}^* - \underline{v}_{k+1} \right] \qquad \text{(IV.14)}$$

Since from this $\underline{v}_k$ can be expressed as a linear combination of $\underline{t}_1^*, \ldots, \underline{t}_k^*$ we have

$$(\underline{v}_k, \underline{t}_i^*) = 0 \qquad \text{for} \qquad i > k \qquad \text{(IV.15)}$$

Now when $\underline{r}_{i+1}$ is formed by orthogonalizing $\underline{r}_0$, $\underline{A}\ \underline{p}_0$, $\underline{A}\ \underline{p}_1$, ... $\underline{A}\ \underline{p}_i$ we already have $\underline{p}_0, \ldots, \underline{p}_i$ formed by $\underline{A}$ orthogonalization of $\underline{r}_0, \ldots, \underline{r}_i$ so that Equation IV.7 implies

$$(\underline{r}_k, \underline{A}\ \underline{p}_i) = 0 \qquad \text{for} \qquad i > k \qquad \text{(IV.16)}$$

When, on the other hand, $\underline{p}_{i+1}$ is formed by $\underline{A}$-orthogonalization of $\underline{r}_0, \ldots, \underline{r}_{i+1}$, this set has been formed by orthogonalization of $\underline{r}_0$, $\underline{A}\ \underline{p}_0$, ..., $\underline{A}\ \underline{p}_i$ so that Equation IV.15 implies that

$$(\underline{A}\ \underline{p}_k, \underline{r}_i) = 0 \qquad \text{for} \qquad i > k+1 \qquad \text{(IV.17)}$$

Hence using Equation IV.14

$$\underline{r}_{i+1} = \underline{r}_i + \frac{(\underline{r}_i,\underline{r}_i)}{(\underline{A}\ \underline{p}_i,\underline{r}_i)}\left[\frac{(\underline{A}\ \underline{p}_i,\underline{r}_0)}{(\underline{r}_0,\underline{r}_0)}\ \underline{r}_0 + \cdots + \frac{(\underline{A}\ \underline{p}_i,\underline{r}_{i-1})}{(\underline{r}_{i-1},\underline{r}_{i-1})}\ \underline{r}_{i-1} - \underline{A}\ \underline{p}_i\right]$$

$$= \underline{r}_i - \frac{|\underline{r}_i|^2}{(\underline{A}\ \underline{p}_i,\underline{r}_i)}\ \underline{A}\ \underline{p}_i \qquad \text{(IV.18)}$$

using Equation IV.16.

Similarly using Equation IV.6

$$\underline{p}_{i+1} = \underline{r}_{i+1} - \left[\frac{(\underline{A}\ \underline{r}_{i+1},\underline{p}_0)}{(\underline{A}\ \underline{p}_0,\underline{p}_0)}\ \underline{p}_0 + \frac{(\underline{A}\ \underline{r}_{i+1},\underline{p}_1)}{(\underline{A}\ \underline{p}_1,\underline{p}_1)}\ \underline{p}_1 + \cdots + \frac{(\underline{A}\ \underline{r}_{i+1},\underline{p}_i)}{(\underline{A}\ \underline{p}_i,\underline{p}_i)}\ \underline{p}_i\right]$$

$$= \underline{r}_{i+1} - \frac{(\underline{A}\ \underline{r}_{i+1},\underline{p}_i)}{(\underline{A}\ \underline{p}_i,\underline{p}_i)}\ \underline{p}_i \qquad \text{(IV.19)}$$

using Equation IV.17. Thus

$$\underline{p}_{i+1} = \underline{r}_{i+1} + \beta_i \underline{p}_i \qquad \text{(IV.20)}$$

with

$$\beta_i = \frac{-(\underline{A}\ \underline{r}_{i+1},\underline{p}_i)}{(\underline{A}\ \underline{p}_i,\underline{p}_i)} \qquad \text{(IV.21)}$$

and

$$\underline{r}_{i+1} = \underline{r}_i - \alpha_i\ \underline{A}\ \underline{p}_i \qquad \text{(IV.22)}$$

with

$$\alpha_i = \frac{|\underline{r}_i|^2}{(\underline{A}\ \underline{p}_i,\underline{r}_i)}$$

$$= |\underline{r}_i|^2/(\underline{p}_i,\underline{A}\ \underline{p}_i) \qquad \text{(IV.23)}$$

since

$$\underline{p}_i = \underline{r}_i + \beta_{i-1}\underline{p}_{i-1} \qquad \text{from (IV.20)}$$

implies

$$(\underline{p}_i, \underline{A}\ \underline{p}_i) = (\underline{r}_i, \underline{A}\ \underline{p}_i) \tag{IV.24}$$

These are the formulae for generating the sequences $\{\underline{r}_i\}$ and $\{\underline{p}_i\}$. The expressions for α_i and β_i may be put in a different form as follows. Since by using Equation IV.19 $\underline{p}_i$ can be expressed as a linear combination of $\underline{r}_0, \ldots, \underline{r}_i$ it follows that

$$(\underline{p}_i, \underline{r}_{i+1}) = 0 \tag{IV.25}$$

Therefore, from Equation IV.22

$$(\underline{p}_i, \underline{r}_i) - \alpha_i(\underline{p}_i, \underline{A}\ \underline{p}_i) = 0 \tag{IV.26}$$

so that

$$\alpha_i = (\underline{p}_i, \underline{r}_i)/(\underline{p}_i, \underline{A}\ \underline{p}_i) \tag{IV.27}$$

and we note from Equation IV.23 that

$$(\underline{p}_i, \underline{r}_i) = |\underline{r}_i|^2 \geq 0 \tag{IV.28}$$

Furthermore

$$\underline{r}_{i+1} = \underline{r}_i - |\underline{r}_i|^2/(\underline{p}_i, \underline{A}\ \underline{p}_i).\underline{A}\ \underline{p}_i \tag{IV.29}$$

implies

$$|\underline{r}_{i+1}|^2 = -\frac{|\underline{r}_i|^2}{(\underline{p}_i, \underline{A}\ \underline{p}_i)}\ (\underline{r}_{i+1}, \underline{A}\ \underline{p}_i) \tag{IV.30}$$

so that

$$\beta_i = |\underline{r}_{i+1}|^2/|\underline{r}_i|^2 \tag{IV.31}$$

Finally we take $\underline{x}_{i+1} = \underline{x}_i + \alpha_i \underline{p}_i$ and show by induction that $\underline{r}_i$ represents the residual vector $\underline{k} - \underline{A}\,\underline{x}_i$. Certainly $\underline{r}_0 = \underline{k} - \underline{A}\,\underline{x}_0$ by definition and if

$$\underline{r}_i = \underline{k} - \underline{A}\,\underline{x}_i \tag{IV.32}$$

then

$$\begin{aligned}\underline{r}_{i+1} &= \underline{r}_i - \alpha_i \underline{A}\,\underline{p}_i \\ &= \underline{k} - (\underline{A}\,\underline{x}_i + \alpha_i \underline{A}\,\underline{p}_i) \\ &= \underline{k} - \underline{A}\,\underline{x}_{i+1}\end{aligned} \tag{IV.33}$$

The method will converge to the solution in at most N iterations for $\underline{r}_N$ if calculated from $\underline{A}\,\underline{p}_{N-1}$ would be orthogonal to all the N orthogonal vectors $\underline{r}_0,\ldots,\underline{r}_{N-1}$ and must therefore be zero. Thus the method produces a solution $\underline{h} = \underline{x}_M$ for $M \leqslant N$.

The value of α_i also arises by minimizing $H(\underline{x}) = (\underline{A}(\underline{h}-\underline{x}),\underline{h}-\underline{x}) \geqslant 0$ over all $\underline{x} = \underline{x}_i + \lambda_i \underline{p}_i$. The proof of this is as follows.

$$\begin{aligned}H(\underline{x}_i + \lambda_i \underline{p}_i) &= (\underline{A}(\underline{h}-\underline{x}_i-\lambda_i \underline{p}_i),\underline{h}-\underline{x}_i-\lambda_i \underline{p}_i) \\ &= H(\underline{x}_i) - 2\lambda_i(\underline{r}_i,\underline{p}_i) + \lambda_i^2(\underline{A}\,\underline{p}_i,\underline{p}_i)\end{aligned} \tag{IV.34}$$

which implies

$$\frac{\partial H}{\partial \lambda_i} = -2(\underline{r}_i,\underline{p}_i) + 2\lambda_i(\underline{A}\,\underline{p}_i,\underline{p}_i) \tag{IV.35}$$

so that

$$\begin{aligned}\lambda_i &= \frac{(\underline{r}_i,\underline{p}_i)}{(\underline{A}\,\underline{p}_i,\underline{p}_i)} \\ &= \alpha_i\end{aligned} \tag{IV.36}$$

In summary, the algorithm for solution, $\underline{h}$, of simultaneous equations $\underline{A}\ \underline{x} = \underline{k}$ is

$$\underline{p}_0 = \underline{r}_0 = \underline{k} - \underline{A}\ \underline{x}_0 \qquad \text{from (IV.1)}$$

$$\underline{r}_{i+1} = \underline{r}_i - \alpha_i\ \underline{A}\ \underline{p}_i \qquad \text{(IV.37)}$$

where

$$\alpha_i = \frac{(\underline{p}_i, \underline{r}_i)}{(\underline{p}_i, \underline{A}\ \underline{p}_i)}$$

minimizes $H(\underline{x}) = (\underline{A}(\underline{h}-\underline{x}), \underline{h}-\underline{x})$ over all $\underline{x} = \underline{x}_i + \lambda_i \underline{p}_i$

$$\underline{p}_{i+1} = \underline{r}_{i+1} + \beta_i \underline{p}_i \qquad \text{(IV.38)}$$

where $\beta_i = |\underline{r}_{i+1}|^2 / |\underline{r}_i|^2$

and $$\underline{x}_{i+1} = \underline{x}_i + \alpha_i \underline{p}_i \qquad \text{(IV.39)}$$

Application of the Conjugate Gradients Method to Function Minimization

The following description has been given by Fletcher & Reeves[184]. Suppose a function f of many variables $\underline{x}$ can be expanded near its minimum $\underline{h}$ as

$$f(\underline{x}) = f(\underline{h}) + \tfrac{1}{2} \sum_{ij} A_{ij} (x_i - h_i)(x_j - h_j) + \text{higher terms} \qquad \text{(IV.40)}$$

where $\underline{A}$ is the symmetric positive definite matrix of second order partial derivatives. Then

$$\frac{\partial f}{\partial x_k} = \sum_i A_{ki} (x_i - h_i) \qquad \text{(IV.41)}$$

which implies that the gradient $\underline{g}(\underline{x}) = \underline{A}(\underline{x}-\underline{h})$. Hence for the gradient to vanish we seek the numerical solution of $\underline{A}\ \underline{x} = \underline{A}\ \underline{h}$ where $\underline{A}$ is not given but $\underline{g}(\underline{x}) = \underline{A}(\underline{x}-\underline{h})$ is available. If we identify

$$\underline{r}_i = \underline{k} - \underline{\underline{A}}\,\underline{x}_i$$

with

$$-\underline{g}_i = \underline{\underline{A}}\,\underline{h} - \underline{\underline{A}}\,\underline{x}_i \qquad \text{(IV.42)}$$

the previous algorithm becomes:

take $\underline{x}_0$ arbitrary

$$\underline{g}_0 = \underline{g}(\underline{x}_0); \qquad \underline{p}_0 = -\underline{g}_0 \qquad \text{(IV.43)}$$

$$\underline{x}_{i+1} = \underline{x}_i + \alpha_i \underline{p}_i \qquad \text{(IV.44)}$$

where α_i is chosen to minimize $(\underline{\underline{A}}(\underline{h}-\underline{x}),\underline{h}-\underline{x})$ over all $\underline{x} = \underline{x}_i + \lambda_i \underline{p}_i$

$$\underline{g}_{i+1} = \underline{g}(\underline{x}_{i+1}) \qquad \text{(IV.45)}$$

$$\underline{p}_{i+1} = -\underline{g}_{i+1} + \beta_i \underline{p}_i \qquad \text{(IV.46)}$$

where $\beta_i = |\underline{g}_{i+1}|^2/|\underline{g}_i|^2$.

The minimization is performed by the method used by Davidon[185] and Fletcher & Powell[186]. We determine λ_m such that $y'(\lambda_m) = 0$ where

$$y(\lambda) = f(\underline{x}_i + \lambda \underline{p}_i) \qquad \text{(IV.47)}$$

and therefore

$$y'(\lambda) = (\underline{p}_i, \underline{g}(\underline{x}_i + \lambda \underline{p}_i)) \qquad \text{(IV.48)}$$

Thus $y(\lambda)$ and $y'(\lambda)$ can be calculated for any λ and in particular $y(0) = f_i$ and $y'(0) = (\underline{p}_i, \underline{g}_i) \leqslant 0$ from Equation IV.28. Let "est" be an estimate of the unconstrained minimum of f. Take as a tentative step length

$$t = \ell \quad \text{if } 0 < \ell < |\underline{p}_i|^{-1}$$

$$= |\underline{p}_i|^{-1} \text{ otherwise} \qquad \text{(IV.49)}$$

where $\ell = 2(est - f_i)/(\underline{p}_i, \underline{g}_i)$. Then examine y' at the points $\lambda = 0, t, 2t, 4t, \ldots, a, b$ where λ is doubled each time and b is the first of these values at which y' becomes non-negative. Then

$$a < \lambda_m \leqslant b \tag{IV.50}$$

Define

$$z = 3 . \frac{y(a)-y(b)}{b-a} + y'(a) + y'(b) \tag{IV.51}$$

and

$$w = (z^2 - y'(a)y'(b))^{\frac{1}{2}} \tag{IV.52}$$

The estimate λ_e of λ_m is

$$\lambda_e = b - \left(\frac{y'(b) + w - z}{y'(b) - y'(a) + 2w}\right) (b-a) \tag{IV.52}$$

If neither y(a) nor y(b) is less than $y(\lambda_e)$ then λ_e is taken as the estimate of λ_m. Otherwise according as $y'(\lambda_e)$ is positive or negative, the interpolation is repeated over (a,λ_e) or (λ_e,b) respectively.

Application of Conjugate Gradients Method to SCF LCAO Wave Functions

An expression for the gradient of the energy is found by the method due to Fletcher[146]. The electronic energy is given by

$$E = 2\ \underline{H} : \underline{R} + \underline{R} : \underline{B} : \underline{R} \tag{IV.54}$$

where the symbols are defined in Section 3.6. We vary E as a function of an m x n matrix $\underline{Y}$.

$$\delta E = \sum_{ij} \frac{\partial E}{\partial Y_{ij}} \delta Y_{ij} + O(\delta Y^2)$$

$$= \nabla E : \delta \underline{Y} \text{ to first order.} \qquad \text{(IV.55)}$$

For non-orthonormal basis functions $\underline{C}^T \underline{S}\, \underline{C} = \underline{I}$ is satisfied by

$$\underline{C} = \underline{Y}(\underline{Y}^T \underline{S}\, \underline{Y})^{-\frac{1}{2}} \qquad \text{(IV.56)}$$

so that

$$\underline{R} = \underline{C}\, \underline{C}^T$$

$$= \underline{Y}\, \underline{M}\, \underline{Y}^T \qquad \text{(IV.57)}$$

where

$$\underline{M} = (\underline{Y}^T \underline{S}\, \underline{Y})^{-1}$$

Consider a variation $\underline{Y} \rightarrow \underline{Y} + \delta \underline{Y}$. Then

$$\underline{M} + \delta \underline{M} = [\,(\underline{Y}^T + \delta \underline{Y}^T)\underline{S}(\underline{Y} + \delta \underline{Y})\,]^{-1}$$

$$= [\underline{Y}^T \underline{S}\, \underline{Y} + \delta \underline{Y}^T \underline{S}\, \underline{Y} + \underline{Y}^T \underline{S}\, \delta \underline{Y}]^{-1} \quad \text{to first order}$$

$$= (\underline{I} + \underline{M}\, \underline{\varepsilon})^{-1} \underline{M}$$

where $\underline{\varepsilon} = \delta \underline{Y}^T \underline{S}\, \underline{Y} + \underline{Y}^T \underline{S}\, \delta \underline{Y}$

$$= (\underline{I} - \underline{M}\, \underline{\varepsilon})\, \underline{M} \quad \text{to first order} \qquad \text{(IV.58)}$$

from which $\delta \underline{M} = -\underline{M}\, \underline{\varepsilon}\, \underline{M}$.

Also

$$\underline{R} + \delta \underline{R} = (\underline{Y} + \delta \underline{Y})\,(\underline{M} + \delta \underline{M})\,(\underline{Y}^T + \delta \underline{Y}^T) \qquad \text{(IV.59)}$$

leads to

$$\delta\underline{R} = \underline{Y}\,\underline{M}\,\delta\underline{Y}^T + \underline{Y}\,\delta\underline{M}\,\underline{Y}^T + \delta\underline{Y}\,\underline{M}\,\underline{Y}^T$$

$$= \underline{Y}\,\underline{M}\,\delta\underline{Y}^T - \underline{Y}\,\underline{M}(\delta\underline{Y}^T\,\underline{S}\,\underline{Y} + \underline{Y}^T\,\underline{S}\,\delta\underline{Y})\,\underline{M}\,\underline{Y}^T + \delta\underline{Y}\,\underline{M}\,\underline{Y}^T$$

$$= \underline{Y}\,\underline{M}\,\delta\underline{Y}^T(\underline{I} - \underline{S}\underline{R}) + (\underline{I} - \underline{S}\underline{R})^T\delta\underline{Y}\,\underline{M}\,\underline{Y}^T \qquad \text{(IV.60)}$$

The energy changes to

$$E+\delta E = 2\underline{H} : (\underline{R}+\delta\underline{R}) + (\underline{R}+\delta\underline{R}) : \underline{B} : (\underline{R}+\delta\underline{R}) \qquad \text{(IV.61)}$$

so that

$$\delta E = 2\underline{H} : \delta\underline{R} + 2\underline{R} : \underline{B} : \delta\underline{R}$$

$$= 2\underline{F} : \delta\underline{R} \qquad \text{where } \underline{F} = \underline{H} + \underline{B} : \underline{R}$$

$$= 2 \text{ tr } \underline{F}\,\delta\underline{R}$$

$$= 4 \text{ tr } \underline{F}\,\underline{Y}\,\underline{M}\,\delta\underline{Y}^T\,(\underline{I} - \underline{S}\,\underline{R}) \quad \text{using invariance of the trace of a product under cyclic rearrangement of the factors}$$

$$= 4[(\underline{I} - \underline{S}\,\underline{R})\,\underline{F}\,\underline{Y}\,\underline{M}] : \delta\underline{Y}^T \qquad \text{(IV.62)}$$

from which finally

$$\nabla E = 4(\underline{I} - \underline{S}\,\underline{R})\,\underline{F}\,\underline{Y}\,\underline{M} \qquad \text{(IV.63)}$$

For an orthonormal basis set $\underline{R} = \underline{Y}(\underline{Y}^T\underline{Y})^{-1}\,\underline{Y}^T$ and a recurrence formula given by Fletcher[187] was used to calculate $(\underline{Y}^T\underline{Y})^{-1}\underline{Y}^T$. Define

$$\underline{A}_k^+ = (\underline{A}_k^T\,\underline{A}_k)^{-1}\,\underline{A}_k^T \qquad \text{(IV.64)}$$

where $\underline{A}_k$ is an (m x k) matrix of k linearly independent vectors $\{\underline{a}_i\}$. Then

$$\underline{v} = (\underline{I} - \underline{A}_k\underline{A}_k^+)\underline{a}_{k+1} \qquad \text{(IV.65)}$$

is the component of $\underline{a}_{k+1}$ which is orthogonal to $\underline{a}_1,\ldots,\underline{a}_k$. The recurrence formula is

$$\underline{A}^+_{k+1} = \begin{bmatrix} \underline{A}^+_k \\ \underline{0}^T \end{bmatrix} + \begin{bmatrix} -\underline{A}^+_k \, \underline{a}_{k+1} \\ 1 \end{bmatrix} \underline{v}^T \Big/ \underline{v}^T \underline{a}_{k+1} \qquad \text{(IV.66)}$$

with for $k = 0$, $\underline{A}^+_1 = \underline{a}^T_1/(\underline{a}^T_1 \cdot \underline{a}_1)$ (IV.67)

APPENDIX V

LOCALIZED ORBITALS

The exclusive orbitals of Boys[168] and Foster & Boys[167] are found by maximizing $\sum_a R_a^2$, where $\underline{R}_a = \langle\phi_a|\underline{r}|\phi_a\rangle$. The method used is similar to a maximization scheme proposed by Edmiston & Ruedenberg[169].

Consider first the general unitary transformation for two functions given by $(\phi_1,\phi_2) \rightarrow (u_1,u_2)$ where

$$u_1 = \phi_1 \cos\gamma + \phi_2 \sin\gamma$$

$$\text{and} \quad u_2 = -\phi_1 \sin\gamma + \phi_2 \cos\gamma \qquad \text{(V.1)}$$

The notation is simplified by taking $\underline{r} = (x_1,x_2,x_3)$ and $\langle a,i,b\rangle = \langle\phi_a|x_i|\phi_b\rangle$. Let

$$D(\phi) = \sum_a R_a^2$$

$$= \sum_{i=1}^{3} \sum_a \langle a,i,b\rangle. \qquad \text{(V.2)}$$

Then

$$D(u) = \sum_{i=1}^{3} \sum_a \langle u_a|x_i|u_a\rangle$$

$$= \sum_{i=1}^{3} [\langle\phi_1\cos\gamma + \phi_2\sin\gamma|x_i|\phi_1\cos\gamma + \phi_2\sin\gamma\rangle^2$$

$$+ \langle-\phi_1\sin\gamma + \phi_2\cos\gamma|x_i|-\phi_1\sin\gamma + \phi_2\cos\gamma\rangle^2]$$

$$= \sum_{i=1}^{3} ([\cos^2\gamma\langle1,i,1\rangle+2\sin\gamma\cos\gamma\langle1,i,2\rangle$$

$$+ \sin^2\gamma\langle2,i,2\rangle]^2 + [\sin^2\gamma\langle1,i,1\rangle$$

$$- 2\sin\gamma\cos\gamma\langle1,i,2\rangle + \cos^2\gamma\langle2,i,2\rangle]^2) \qquad \text{(V.3)}$$

Using the identities

$$\cos^4\gamma + \sin^4\gamma = 1 - 2\sin^2\gamma\cos^2\gamma$$

and

$$\cos 4\gamma = 1 - 8\sin^2\gamma\cos^2\gamma \qquad \text{(V.4)}$$

$$D(u) = D(\phi) + \sum_{i=1}^{3} \{(1-\cos 4\gamma)[\langle 1,i,2\rangle^2 - \tfrac{1}{4}(\langle 1,i,1\rangle - \langle 2,i,2\rangle)^2$$

$$\pm \sin 4\gamma \langle 1,i,2\rangle[\langle 1,i,1\rangle - \langle 2,i,2\rangle]\}$$

$$= D(\phi) + A_{12} - A_{12}\cos 4\gamma + B_{12}\sin 4\gamma \qquad \text{(V.5)}$$

where

$$A_{12} = \sum_{i=1}^{3} [\langle 1,i,2\rangle^2 - \tfrac{1}{4}(\langle 1,i,1\rangle - \langle 2,i,2\rangle)^2]$$

and

$$B_{12} = \sum_{i=1}^{3} \langle 1,i,2\rangle[\langle 1,i,1\rangle - \langle 2,i,2\rangle] \qquad \text{(V.6)}$$

Let $C \cos 4(\gamma-\alpha) = -A_{12}\cos 4\gamma + B_{12}\sin 4\gamma.$ (V.7)

A solution of this equation is

$$C \cos 4\alpha = -A_{12}$$

$$C \sin 4\alpha = B_{12}$$

$$C = (A_{12}^2 + B_{12}^2)^{\frac{1}{2}} \qquad \text{(V.8)}$$

Thus $\sin 4\alpha = B_{12}/(A_{12}^2+B_{12}^2)^{\frac{1}{2}}$

$$\cos 4\alpha = -A_{12}/(A_{12}^2+B_{12}^2)^{\frac{1}{2}} \qquad \text{(V.9)}$$

and

$$D(u) = D(\phi) + A_{12} + (A_{12}^2+B_{12}^2)^{\frac{1}{2}} \cos 4(\gamma-\alpha). \qquad \text{(V.10)}$$

D(u) will have a maximum increase of $A_{12}+(A_{12}^2+B_{12}^2)^{\frac{1}{2}}$ when γ has value $\gamma_{max} = \alpha, \alpha+\frac{1}{2}\pi, \alpha+\pi, \ldots$. The exclusive orbitals are then given by

$$\lambda_1 = \phi_1 \cos \alpha_0 + \phi_2 \sin \alpha_0$$

$$\lambda_2 = -\phi_1 \sin \alpha_0 + \phi_2 \cos \alpha_0 \qquad \text{(V.11)}$$

where α_0 is the value of γ_{max} lying between 0 and $\pi/2$.

Sin α_0 and cos α_0 are both non-negative and may be found as follows.

Since

$$\cos^2\alpha = \tfrac{1}{2}\{1 \pm [1 - \tfrac{1}{2}(1 - \cos 4\alpha)]^{\frac{1}{2}}\}$$

and

$$\sin 4\alpha = 4 \sin \alpha \cos \alpha (\cos^2\alpha - \sin^2\alpha) \qquad \text{(V.12)}$$

calculate cos $4\alpha_0$ and sin $4\alpha_0$ from A_{12} and B_{12} using Equations V.6. Then find

$$x^2 = \tfrac{1}{2}\{1 \pm [1 - \tfrac{1}{2}(1 - \cos 4\alpha_0)]^{\frac{1}{2}}\}$$

and

$$x = +(x^2)^{\frac{1}{2}}$$

and

$$y = +(1 - x^2)^{\frac{1}{2}} \qquad \text{(V.13)}$$

which yield two solutions (x_1,y_1) and (x_2,y_2). Then

$$\cos \alpha_0 = x_k \qquad \text{and} \qquad \sin \alpha_0 = y_k \qquad \text{(V.14)}$$

where (x_k,y_k) is that pair which satisfies

$$4x_k y_k (x_k^2 - y_k^2) = \sin 4\alpha_0. \qquad \text{(V.15)}$$

For the general case of n molecular orbitals the 2 x 2 transformation is applied to each pair of orbitals in turn. Convergence is attained when $A_{ij} + (A_{ij}^2+B_{ij}^2)^{\frac{1}{2}}$ is less than some tolerance value for all pairs (i,j).

APPENDIX VI

COMPUTER PROGRAMS

The computer programs described here have been modified or written for use on the University of Canterbury IBM 360/44 computer, which has 128K bytes of core storage and two small disk cartridge drives for peripheral storage. A number of the programs were initially obtained as listings from the Chemistry Department of Monash University (M.U.) and this basic set was modified and augmented during the course of study described in this thesis. The contour maps given in Chapter Six were drawn on an IBM 1627 X-Y plotter which is controlled by a PDP-11 computer. Some of the programs were too large for the high speed core storage and were therefore constructed as multiphase. Programs were written in Fortran IV language except for a few isolated subroutines which were written in IBM 360 assembler language in order to increase execution efficiency. Except where otherwise stated, all programs were written or modified by the author.

Program INTS

This is a multiphase program structure comprising FORH, NUATTN and REPMAT. These are programs obtained from M.U. and require as basic input atomic Cartesian coordinates, orbital classification (i.e. 1s, 2s, $2p_x$, $2p_y$ or $2p_z$) and orbital exponents.

FORH calculates overlap, kinetic energy and x-, y- and z-moment integrals for a general Slater basis set.

NUATTN calculates all nuclear attraction integrals for the Slater basis set.

REPMAT calculates all NDDO two-electron repulsion integrals in the Slater basis.

Program NDDO

This is a multiphase program comprising TRANS, HMATRX, GMATRX and FMATRX. The original versions were obtained from M.U. The program is executed after INTS to calculate SCF wave functions by the SAI method.

TRANS computes the matrices required for the transformations between the Slater basis and the orthonormal Löwdin basis. Some of the routines were rewritten to increase execution speed.

HMATRIX calculates the Hamiltonian core matrix and transforms it to the Löwdin basis.

GMATRIX calculates the NDDO repulsion integrals from the Slater NDDO set. The subroutine incorporating the Ruedenberg expansion method was rewritten in assembler language.

FMATRIX solves the SCF equations by Roothaan's iterative procedure. The section which constructs the G matrix from the repulsion integrals was rewritten in assembler language.

Program MULLIK

This program, obtained from M.U., performs a Mulliken population analysis. It was extended to give overlap populations.

Program NEWMUL

This calculates the full set of two electron repulsion integrals for a Slater basis using the multi-Gaussian expansion technique. It was obtained from M.U. and made operational for the IBM 360 by Mr P.B. Morgan. It requires, in addition to the usual orbital information, an input symmetry number for each orbital depending on whether the

orbital is of pi or sigma type. The program was extensively modified to incorporate the use of molecular symmetry in the reduction of the number of unique integrals actually calculated. Some of the Fortran was rewritten by Dr R.G.A.R. Maclagan to increase execution efficiency.

Program UHF

This does the Unrestricted Hartree Fock calculations using the results of INTS and NEWMUL. It was obtained from M.U. and was modified to make it compatible with the improved version of NEWMUL.

Program STEEP

This program solves the closed shell SCF equations by McWeeny's Steepest Descent method, as described in Section 3.5. It is executed after INTS and NEWMUL.

Program SYMTA

This program calculates the transformation matrices relating the Slater, Löwdin, and Löwdin symmetry bases. It requires as input the Slater overlap matrix and the transformation matrix from the Slater basis to the symmetry basis.

Program CGRAD

This solves the closed shell SCF equations by the method of conjugate gradients, Section 3.6. The calculations are done in the Löwdin symmetry basis. Two similar versions are used:

CGRAD1 is for the SAI method and is executed after INTS, SYMTA, TRANS, HMATRX AND GMATRX.

CGRAD2 is used for the multi-Gaussian expansion method and is executed after INTS, SYMTA and NEWMUL.

Program FMAT

This solves the closed shell SCF equations by Roothaan's diagonalization method using the Löwdin symmetry basis. Two versions are again in use.

FMAT1 is a modified version of FMATRX and is executed after the same chain as CGRAD1.

FMAT2 is a modified version of UHF and is executed after the same chain as CGRAD2.

Program COMBIN

This is a multiphase program which permits solution of the closed shell SCF equations by successive iterations of conjugate gradients or matrix diagonalization methods. Thus two versions are used.

COMBI1 composed of CGRAD1 and FMAT1.

COMBI2 composed of CGRAD2 and FMAT2.

Program RHF

This calculates the open shell wavefunctions by McWeeny's method of Section 4.2. A Löwdin symmetry basis is used. The diagonalization routine was DGIVEN, a program obtained from the Quantum Chemistry Program Exchange, Indiana University. There are two versions of RHF corresponding to the closed shell SAI and MGE methods.

RHF1 is executed after the same program chain as CGRAD1.

RHF2 is executed after the same program chain as CGRAD2.

Program LOCAL

This calculates the localized molecular orbitals described in Section 5.4. It requires as input the canonical orbitals from COMBIN or UHF and the x-, y- and z-matrices from FORH.

Program MAP

This produces the data, as punched card output for the PDP-11 computer, for drawing contour maps on the X-Y plotter. A program obtained from M.U. calculated the electron density values at each point on a grid. Routines were written to draw smooth contours by linear interpolation between these grid points. MAP requires as input the coefficients of the orbitals to be plotted as well as specifications of map size and orientation and contour values.

Program CI

This program was written specifically to perform the configuration interaction calculations for N_2O_4. It requires as input the canonical orbitals obtained from COMBI2 and integrals from FORH, NUATTN and NEWMUL.

Program BOND

This performs the bond energy analysis of Section 5.5 for the MGE approximation. Slightly different versions are required for open and closed shell wavefunctions. Both require integrals from FORH, NUATTN and NEW MUL.

BONDC is for closed shells and uses canonical coefficients from COMBI2.

BONDO is for open shells and uses the coefficients from RHF2.

APPENDIX VII

2G/S WAVE FUNCTION FOR N_2O_4 Φ_1

	$1a_g$	$2a_g$	$3a_g$	$4a_g$	$5a_g$
1s01	0.49875	-0.00137	-0.07539	0.07894	-0.06546
2s01	0.00524	0.00408	0.27526	-0.34788	0.33879
$2p_z$01	0.00018	0.00136	0.09786	0.25314	0.20793
$2p_y$01	-0.00100	-0.00382	-0.18255	0.02736	0.26158
$2p_x$01	0.00000	0.00000	-0.00000	-0.00000	-0.00000
1s02	0.49875	-0.00137	-0.07539	0.07894	-0.06546
2s02	0.00524	0.00408	0.27526	-0.34788	0.33879
$2p_z$02	0.00018	0.00136	0.09786	0.25314	0.20793
$2p_y$02	0.00100	0.00382	0.18255	-0.02736	-0.26158
$2p_x$02	-0.00000	-0.00000	0.00000	0.00000	0.00000
1sN1	-0.00011	0.70563	-0.11283	-0.04920	0.05967
2sN1	0.00051	0.00270	0.25683	0.25294	-0.28400
$2p_z$N1	0.00043	0.00348	0.11001	0.21821	0.17892
$2p_y$N1	-0.00000	0.00000	-0.00000	-0.00000	-0.00000
$2p_x$N1	0.00000	-0.00000	0.00000	0.00000	-0.00000
1sN2	-0.00011	0.70563	-0.11283	-0.04920	0.05967
2sN2	0.00051	0.00270	0.25683	0.25294	-0.28400
$2p_z$N2	-0.00043	-0.00348	-0.11001	-0.21821	-0.17892
$2p_y$N2	0.00000	-0.00000	0.00000	0.00000	0.00000
$2p_x$N2	-0.00000	-0.00000	-0.00000	-0.00000	-0.00000
1s03	0.49875	-0.00137	-0.07539	0.07894	-0.06546
2s03	0.00524	0.00408	0.27526	-0.34788	0.33879
$2p_z$03	-0.00018	-0.00136	-0.09786	-0.25314	-0.20793
$2p_y$03	-0.00100	-0.00382	-0.18255	0.02736	0.26158
$2p_x$03	-0.00000	0.00000	0.00000	0.00000	0.00000
1s04	0.49875	-0.00137	-0.07539	0.07894	-0.06546
2s04	0.00524	0.00408	0.27526	-0.34788	0.33879
$2p_z$04	-0.00018	-0.00136	-0.09786	-0.25314	-0.20793
$2p_y$04	0.00100	0.00382	0.18255	-0.02736	-0.26158
$2p_x$04	-0.00000	0.00000	-0.00000	-0.00000	-0.00000
Orbital energy	-20.69396	-15.87034	-1.73802	-1.04079	-0.81311

	$6a_g$*	$1b_{1u}$	$2b_{1u}$	$3b_{1u}$	$4b_{1u}$
1s01	0.00267	-0.49881	0.00128	-0.08220	-0.09076
2s01	-0.05359	-0.00458	-0.00282	0.26768	0.45979
$2p_z$01	0.36408	-0.00013	-0.00124	0.00755	-0.03884
$2p_y$01	-0.01098	0.00033	0.00196	-0.12670	0.18600
$2p_x$01	0.0	-0.00000	-0.00000	0.00000	-0.00000
1s02	0.00267	-0.49881	0.00128	-0.08220	-0.09076
2s02	-0.05359	-0.00458	-0.00282	0.26768	0.45979
$2p_z$02	0.36408	-0.00013	-0.00124	0.00755	-0.03884
$2p_y$02	0.01098	-0.00033	-0.00196	0.12670	-0.18600
$2p_x$02	-0.0	0.00000	0.00000	-0.00000	-0.00000
1sN1	0.00964	0.00027	-0.70576	-0.10432	0.10196
2sN1	-0.06273	-0.00183	-0.00373	0.28636	-0.50583
$2p_z$N1	-0.53301	0.00142	0.00353	-0.20619	0.00018
$2p_y$N1	0.0	-0.00000	0.00000	-0.00000	-0.00000
$2p_x$N1	0.0	-0.00000	0.00000	-0.00000	0.00000
1sN2	0.00964	-0.00027	0.70576	0.10432	-0.10196
2sN2	-0.06273	0.00183	0.00373	-0.28636	0.50583
$2p_z$N2	0.53301	0.00142	0.00353	-0.20619	0.00018
$2p_y$N2	-0.0	0.00000	-0.00000	0.00000	0.00000
$2p_x$N2	-0.0	0.00000	0.00000	0.00000	-0.00000
1s03	0.00267	0.49881	-0.00128	0.08220	0.09076
2s03	-0.05359	0.00458	0.00282	-0.26768	-0.45979
$2p_z$03	-0.36408	-0.00013	-0.00124	0.00755	-0.03884
$2p_y$03	-0.01098	-0.00033	-0.00196	0.12670	-0.18600
$2p_x$03	-0.0	0.00000	0.00000	-0.00000	0.00000
1s04	0.00267	0.49881	-0.00128	0.08220	0.09076
2s04	-0.05359	0.00458	0.00282	-0.26768	-0.45979
$2p_z$04	-0.36408	-0.00013	-0.00124	0.00755	-0.03884
$2p_y$04	0.01098	0.00033	0.00196	-0.12670	0.18600
$2p_x$04	0.0	-0.00000	0.00000	0.00000	0.00000
Orbital energy	0.27333	-20.69401	-15.86964	-1.69026	-0.79944

	$5b_{1u}$	$6b_{1u}$	$1b_{1g}$	$1a_u$	$1b_{3u}$
1s01	-0.01793	-0.01386	0.00000	0.00000	0.00000
2s01	0.07094	0.10085	0.00000	-0.00000	-0.00000
$2p_z$01	0.24264	-0.40741	-0.00000	0.00000	0.00000
$2p_y$01	0.15084	-0.14446	0.00000	-0.00000	0.00000
$2p_x$01	-0.00000	0.00000	0.50210	0.50305	0.29759
1s02	-0.01793	-0.01386	-0.00000	-0.00000	-0.00000
2s02	0.07094	0.10085	-0.00000	0.00000	0.00000
$2p_z$02	0.24264	-0.40741	0.00000	-0.00000	-0.00000
$2p_y$02	-0.15084	0.14446	0.00000	-0.00000	0.00000
$2p_x$02	-0.00000	0.00000	-0.50210	-0.50305	0.29759
1sN1	-0.07749	-0.03002	0.00000	0.00000	-0.00000
2sN1	0.39264	0.17132	-0.00000	-0.00000	-0.00000
$2p_z$N1	0.49915	0.63666	0.00000	-0.00000	-0.00000
$2p_y$N1	-0.00000	-0.00000	-0.00000	-0.00000	-0.00000
$2p_x$N1	0.00000	-0.00000	0.00000	0.00000	0.44240
1sN2	0.07749	0.03002	-0.00000	-0.00000	0.00000
2sN2	-0.39264	-0.17132	0.00000	0.00000	0.00000
$2p_z$N2	0.49915	0.63666	0.00000	-0.00000	-0.00000
$2p_y$N2	0.00000	0.00000	-0.00000	-0.00000	-0.00000
$2p_x$N2	-0.00000	0.00000	0.00000	-0.00000	0.44240
1s03	0.01793	0.01386	0.00000	0.00000	0.00000
2s03	-0.07094	-0.10085	0.00000	-0.00000	-0.00000
$2p_z$03	0.24264	-0.40741	0.00000	-0.00000	-0.00000
$2p_y$03	-0.15084	0.14446	0.00000	-0.00000	0.00000
$2p_x$03	0.00000	-0.00000	0.50210	-0.50305	0.29759
1s04	0.01793	0.01386	-0.00000	-0.00000	-0.00000
2s04	-0.07094	-0.10085	-0.00000	0.00000	0.00000
$2p_z$04	0.24264	-0.40741	-0.00000	0.00000	0.00000
$2p_y$04	0.15084	-0.14446	0.00000	-0.00000	0.00000
$2p_x$04	0.00000	-0.00000	-0.50210	0.50305	0.29759
Orbital energy	-0.50788	-0.33345	-0.38167	-0.34574	-0.90065

	$2b_{3u}$*	$1b_{2g}$	$1b_{2u}$	$2b_{2u}$	$3b_{2u}$
1s01	0.0	0.00000	0.49877	0.10076	0.06118
2s01	0.0	0.00000	0.00473	-0.33691	-0.34458
$2p_z$01	0.0	-0.00000	-0.00011	-0.05666	0.32400
$2p_y$01	0.0	0.00000	0.00037	-0.03210	-0.05648
$2p_x$01	0.42476	0.37077	0.00000	0.00000	0.00000
1s02	0.0	-0.00000	-0.49877	-0.10076	-0.06118
2s02	0.0	-0.00000	-0.00473	0.33691	0.34458
$2p_z$02	0.0	0.00000	0.00011	0.05666	-0.32400
$2p_y$02	0.0	0.00000	0.00037	-0.03210	-0.05648
$2p_x$02	0.42476	0.37077	0.00000	0.00000	0.00000
1sN1	0.0	0.00000	0.00000	-0.00000	0.00000
2sN1	0.0	-0.00000	0.00000	-0.00000	-0.00000
$2p_z$N1	0.0	0.00000	-0.00000	-0.00000	0.00000
$2p_y$N1	0.0	-0.00000	0.00202	-0.32203	0.35095
$2p_x$N1	-0.55916	0.35745	0.00000	0.00000	0.00000
1sN2	0.0	-0.00000	-0.00000	0.00000	-0.00000
2sN2	0.0	0.00000	-0.00000	0.00000	0.00000
$2p_z$N2	0.0	0.00000	-0.00000	-0.00000	0.00000
$2p_y$N2	0.0	-0.00000	0.00202	-0.32203	0.35095
$2p_x$N2	-0.55916	-0.35745	0.00000	0.00000	0.00000
1s03	0.0	0.00000	0.49877	0.10076	0.06118
2s03	0.0	0.00000	0.00473	-0.33691	-0.34458
$2p_z$03	0.0	0.00000	0.00011	0.05666	-0.32400
$2p_y$03	0.0	0.00000	0.00037	-0.03210	-0.05648
$2p_x$03	0.42476	-0.37077	0.00000	0.00000	0.00000
1s04	0.0	-0.00000	-0.49877	-0.10076	-0.06118
2s04	0.0	-0.00000	-0.00473	0.33691	0.34458
$2p_z$04	0.0	-0.00000	-0.00011	-0.05666	0.32400
$2p_y$04	0.0	0.00000	0.00037	-0.03210	-0.05648
$2p_x$04	0.42476	-0.37077	0.00000	0.00000	0.00000
Orbital energy	0.20595	-0.66100	-20.69402	-1.49630	-0.64599

	$4b_{2u}$	$1b_{3g}$	$2b_{3g}$	$3b_{3g}$	$4b_{3g}$
1s01	-0.01441	0.49871	-0.11602	0.03906	0.00123
2s01	0.12118	0.00527	0.43332	-0.29901	-0.00566
$2p_z$01	0.28699	0.00004	-0.01808	0.02216	0.48421
$2p_y$01	0.36171	0.00005	0.01164	-0.25266	0.15200
$2p_x$01	0.00000	0.00000	0.00000	-0.00000	0.00000
1s02	0.01441	-0.49871	0.11602	-0.03906	-0.00123
2s02	-0.12118	-0.00527	-0.43332	0.29901	0.00566
$2p_z$02	-0.28699	-0.00004	0.01808	-0.02216	-0.48421
$2p_y$02	0.36171	0.00005	0.01164	-0.25266	0.15200
$2p_x$02	0.00000	-0.00000	-0.00000	-0.00000	0.00000
1sN1	0.00000	0.00000	-0.00000	0.00000	0.00000
2sN1	-0.00000	0.00000	-0.00000	0.00000	0.00000
$2p_z$N1	0.00000	-0.00000	0.00000	-0.00000	-0.00000
$2p_y$N1	-0.25413	0.00085	0.20310	0.56185	-0.00239
$2p_x$N1	0.00000	-0.00000	-0.00000	0.00000	-0.00000
1sN2	-0.00000	-0.00000	0.00000	-0.00000	-0.00000
2sN2	0.00000	-0.00000	0.00000	-0.00000	-0.00000
$2p_z$N2	0.00000	-0.00000	0.00000	-0.00000	-0.00000
$2p_y$N2	-0.25413	-0.00085	-0.20310	-0.56185	0.00239
$2p_x$N2	0.00000	-0.00000	0.00000	0.00000	-0.00000
1s03	-0.01441	-0.49871	0.11602	-0.03906	-0.00123
2s03	0.12118	-0.00527	-0.43332	0.29901	0.00566
$2p_z$03	-0.28699	0.00004	-0.01808	0.02216	0.48421
$2p_y$03	0.36171	-0.00005	-0.01164	0.25266	-0.15200
$2p_x$03	0.00000	-0.00000	-0.00000	0.00000	0.00000
1s04	0.01441	0.49871	-0.11602	0.03906	0.00123
2s04	-0.12118	0.00527	0.43332	-0.29901	-0.00566
$2p_z$04	0.28699	-0.00004	0.01808	-0.02216	-0.48421
$2p_y$04	0.36171	-0.00005	-0.01164	0.25266	-0.15200
$2p_x$04	0.00000	0.00000	0.00000	-0.00000	0.00000
Orbital energy	-0.36974	-20.69388	-1.35493	-0.47054	-0.26964

* Virtual orbital

2G/S WAVE FUNCTION FOR NO_2 $^2A_1$ (N_2O_4 GEOMETRY)

	$1a_1$	$2a_1$	$3a_1$	$4a_1$
1s01	0.70547	-0.00147	0.11882	0.12224
2s01	0.00675	0.00365	-0.40999	-0.60326
$2p_x$01	0.0	0.0	0.0	0.0
$2p_y$01	0.00109	0.00325	-0.19835	0.19199
$2p_z$01	-0.00030	-0.00135	0.04273	-0.19044
1sN	-0.00017	0.99825	0.15678	-0.14039
2sN	0.00077	0.00475	-0.43556	0.66181
$2p_x$N	0.0	0.0	0.0	0.0
$2p_y$N	0.0	0.0	0.0	0.0
$2p_z$N	0.00024	-0.00055	-0.08219	-0.13381
1s02	0.70547	-0.00147	0.11882	0.12224
2s02	0.00675	0.00365	-0.40999	-0.60326
$2p_x$02	0.0	0.0	0.0	0.0
$2p_y$02	-0.00109	-0.00325	0.19835	-0.19199
$2p_z$02	-0.00030	-0.00135	0.04273	-0.19044
Orbital energy	-20.68577	-15.92091	-1.62607	-0.86277

	$5a_1$	$6a_1$*	$1a_2$	$1b_1$
1s01	0.04547	-0.00274	0.0	0.0
2s01	-0.24411	0.04645	0.0	0.0
$2p_x$01	0.0	0.0	0.71075	0.45389
$2p_y$01	0.28854	0.02187	0.0	0.0
$2p_z$01	0.40764	0.54844	0.0	0.0
1sN	0.00549	-0.04764	0.0	0.0
2sN	-0.00371	0.29476	0.0	0.0
$2p_x$N	0.0	0.0	0.0	0.60120
$2p_y$N	0.0	0.0	0.0	0.0
$2p_z$N	0.49918	-0.77850	0.0	0.0
1s02	0.04547	-0.00274	0.0	0.0
2s02	-0.24411	0.04645	0.0	0.0
$2p_x$02	0.0	0.0	-0.71075	0.45389
$2p_y$02	-0.28854	-0.02187	0.0	0.0
$2p_z$02	0.40764	0.54844	0.0	0.0
Orbital energy	-0.72139	-0.34642	-0.36215	-0.73341

	$1b_2$	$2b_2$	$3b_2$	$4b_2$
1s01	0.70539	0.15513	0.07196	-0.00352
2s01	0.00712	-0.55973	-0.45443	0.04801
$2p_x$01	0.0	0.0	0.0	0.0
$2p_y$01	0.00043	-0.01278	0.28299	-0.41886
$2p_z$01	-0.00021	0.03196	-0.28733	-0.57550
1sN	0.0	0.0	0.0	0.0
2sN	0.0	0.0	0.0	0.0
$2p_x$N	0.0	0.0	0.0	0.0
$2p_y$N	-0.00079	0.35336	-0.62326	0.14592
$2p_z$N	0.0	0.0	0.0	0.0
1s02	-0.70539	-0.15513	-0.07196	0.00352
2s02	-0.00712	0.55973	0.45443	-0.04801
$2p_x$02	0.0	0.0	0.0	0.0
$2p_y$02	0.00043	-0.01278	0.28299	-0.41886
$2p_z$02	0.00021	-0.03196	0.28733	0.57550
Orbital energy	-20.68588	-1.39500	-0.58222	-0.36098

* Singly occupied

REFERENCES

1. E.R. Cohen & J.W.M. DuMond - Revs Mod. Phys. 37, 537 (1965).
2. "Molecular Orbitals in Chemistry, Physics and Biology", Edited by P.O. Löwdin and B. Pullman (Academic Press, New York, 1964).
3. E. Clementi - Chem. Revs 68, 341 (1968).
4. J. Gerratt - Ann. Reports Chem. Soc. 65A, 3 (1968).
5. R.G. Clark & E.T. Stewart - Quart. Rev. 24, 95 (1970).
6. E. Steiner - Ann. Reports Chem. Soc. 67A, 2 (1970).
7. B.J. Duke - Ann. Reports Chem. Soc. 68A, 3 (1971).
8. G.R.J. Williams - Ph.D. Thesis, Monash University (1971).
9. C.E. Eckart - Phys. Rev. 36, 878 (1930).
10. F.L. Pilar - "Elementary Quantum Chemistry" (McGraw-Hill, New York, 1968).
11. M. Born & J.R. Oppenheimer - Ann. Phys. 84, 457 (1927).
12. J.C. Slater - "Quantum Theory of Molecules and Solids" Vol. 1, Chapter 3 (McGraw-Hill, New York, 1963).
13. W. Pauli - Phys. Rev. 58, 716 (1940).
14. R. McWeeny & B.T. Sutcliffe - "Methods of Molecular Quantum Mechanics", Chapter 4 (Academic Press, New York 1969).
15. D.R. Hartree - Proc. Camb. Phil. Soc. 24, 328 (1928).
16. V.A. Fock - Z. Physik 61, 126 (1930).
17. R. McWeeny & B.J. Sutcliffe - Chapter 5 of ref. 14.
18. C.C.J. Roothaan - Revs Mod. Phys. 23, 69 (1951).
19. P.O. Löwdin - J. Chem. Phys. 18, 365 (1950).
20. B.C. Carlson & J.M. Keller - Phys. Rev. 105, 102 (1957).

21. J.H. Wilkinson - "The Algebraic Eigenvalue Problem" (Clarendon Press, 1965).

22. Advances in Chemical Physics - Vol. 14 (1969).

23. R. McWeeny & B.T. Sutcliffe - Chapter 3 of ref. 14.

24. J.C. Slater - "Quantum Theory of Atomic Structure" Vol 1, p.291 (McGraw-Hill, 1960).

25. L. Brillouin - Act. Sci. et Ind., Nos 71,159,160 (1933-4).

26. C. Møller & M.S. Plesset - Phys. Rev. 46, 618 (1934).

27. E. Clementi - J. Chem. Phys. 46, 3842 (1967).

28. N.G. Mukherjee & R. McWeeny - Intern. J. Quantum Chem. 4, 97 (1970).

29. R.D. Brown, F.R. Burden & G.R. Williams - Theoret. Chim. Acta 18, 98 (1970).

30. R.D. Brown, F.R. Burden, G.R. Williams & L.F. Phillips - Theoret. Chim. Acta 21, 205 (1971).

31. C.C.J. Roothaan - J. Chem. Phys. 19, 1445 (1951).

32. A.C. Wahl, P.E. Cade, C.C.J. Roothaan - J. Chem. Phys. 41, 2578 (1964).

33. S. Fraga - Canad. J. Chem. 42, 2509 (1964).

34. J.A. Pople, D.P. Santry & G.A. Segal - J. Chem. Phys. S129, S136 (1965).

35. K. Ruedenberg, C.C.J. Roothaan & W. Jaunzemis - J. Chem. Phys. 24, 201 (1956).

36. N.M. Klimenko & M.E. Dyatkina - Zh. Strukt. Khimii 6, 604, 714 (1965)

37. K. Ruedenberg - J. Chem. Phys. 19, 1433 (1951).

38. H. Taketa, S. Huzinaga & K.O-ohata - J. Phys. Soc. Japan 21, 2313 (1966).

39. S.F. Boys - Proc. Roy. Soc. (London) A201, 125 (1950).

40. S. Huzinaga - Suppl. Prog. Theoret. Phys. 40, 52 (1967).

41. D.B. Cook & P. Palmieri - Mol. Phys. 17, 271 (1969).

42. R.F. Stewart - J. Chem. Phys. 52, 431 (1970).

43. J.W. Mellor - Supplement to the Comprehensive Treatise on Inorganic and Theoretical Chemistry. Vol. 8, Supplement II, 'N' part II p246 (1967).

44. C.F. Bell - "Synthesis and Physical Studies of Inorganic Compounds", p35 (Pergamon Press 1972).

45. S. Claesson, J. Donohue & V. Schomaker - J. Chem. Phys. 16, 207 (1948).

46. G.E. Moore - J. Opt. Soc. Amer. 43, 1045 (1953).

47. G.R. Bird - J. Chem. Phys. 25, 1040 (1956).

48. V.W. Laurie & D. Herschbach - J. Chem. Phys. 37, 1687 (1962).

49. G.R. Bird, J.C. Baird, A.W. Jache, J.A. Hodgeson, R.F. Curl Jr, A.C. Kunkle, J.W. Bransford, J. Rastrup-Anderson, J. Rosenthal - J. Chem. Phys. 40, 3378 (1964).

50. A.D. Walsh - J. Chem. Soc. 2266 (1953).

51. L.E. Sutton - "Tables of Interatomic Distances and Configurations in Molecules and Ions" - Chemical Society London (1958, 1965).

52. R.S. Mulliken - Revs Mod. Phys. 14, 204 (1942).

53. R.S. Mulliken - Canad. J. Chem. 36, 10 (1958).

54. S.D. Peyerimhoff & R.J. Buenker - J. Chem. Phys. 47, 1953 (1967).

55. R.J. Buenker & S.D. Peyerimhoff - J. Chem. Phys. 45, 3682 (1966).

56. S.D. Peyerimhoff, R.J. Buenker & L.C. Allen - J. Chem. Phys. 45, 734 (1966)

57. L. Burnelle, P. Beaudouin & L.J. Schaad - J. Phys. Chem. 71, 2240 (1967).

58. C.A. Coulson & B.M. Deb - Intern. J. Quantum Chem. 5, 411 (1971).

59. M. Green & J.W. Linnett - J. Chem. Soc. 163, 4959 (1960).

60. L. Pauling - "The Nature of the Chemical Bond" (Cornell U.P., Ithaca, N.Y., 1960).

61. J.W. Linnett - J. Amer. Chem. Soc. 83, 2643 (1961).

62. C.A. Coulson & Duchesne - Bull. Classe Sci. Acad. Roy. Belg. 43, 522 (1957).

63. K.L. McEwen - J. Chem. Phys. 32, 1801 (1960).

64. T.J. Schaafsma & J. Kommandeur - Mol. Phys. 14, 517 (1968).

65. P.W. Atkins, N. Keen & M.C.R. Symons - J. Chem. Soc. 2873 (1962).

66. G.R. Bird, J.C. Baird & R.B. Williams - J. Chem. Phys. 28, 738 (1958).

67. M. Green & J.W. Linnett - Trans. Faraday Soc. 57, 1 (1961).

68. C.R. Brundle, D. Newmann, W. Price, D. Evans, A.W. Potts, D.G. Streets - J. Chem. Phys. 53, 705 (1970).

69. H.F. Schaefer III & S. Rothenberg - J. Chem. Phys. 54, 1423 (1971).

70. J. Serre - Mol. Phys. 4, 269 (1961).

71. H. Kato, T. Yonezawa, K. Morokuma & K. Fukui - Bull. Chem. Soc. Japan 37, 1710 (1964).

72. R. Hoffmann - J. Chem. Phys. 39, 1397 (1963).

73. J. Tanaka - J. Chem. Soc. Japan, Pure Chem. Sec. 78, 1643 (1957).

74. J.A. Pople & G.A. Segal - J. Chem. Phys. 44, 3289 (1966).

75. V.K. Kelkar, K.C. Bhalla & P.G. Khubchandani - J. Mol. Struct. 9, 383 (1971).

76. T. Yonezawa, H. Nakatsuji, T. Kawamura & H. Kato - Bull. Chem. Soc. Japan 40, 2211 (1967).

77. K. Watanabe - J. Chem. Phys. 26, 542 (1957).

78. M.I. Al-Joboury & D.W. Turner - J. Chem. Soc. 4434 (1964).

79. L. Burnelle, A.M. May & R.A. Gangi - J. Chem. Phys. 49, 561 (1968).

80. C.C.J. Roothaan - Revs Mod. Phys. 32, 179 (1960).

81. S. Huzinaga - Phys. Rev. 120, 866 (1960).

82. R. McWeeny - p305 of ref. 2.

83. W.H. Fink - J. Chem. Phys. 49, 5054 (1968).

84. L. Burnelle & K.P. Dressler - J. Chem. Phys. 51, 2758 (1969).

85. J.E. DelBene - J. Chem. Phys. 54, 3487 (1971).

86. W.J. Hunt, T.H. Dunning Jr, W.A. Goddard III - Chem. Phys. Lett. 3, 606 (1969).

87. R.A. Gangi & L. Burnelle - J. Chem. Phys. 55, 843 (1971).

88. J.S. Broadley & J.M. Robertson - Nature 164, 915 (1949).

89. D.W. Smith & K. Hedberg - J. Chem. Phys. 25, 1282 (1956).

90. R.G. Snyder & I.C. Hisatsune - J. Mol. Spectry 1, 139 (1957).

91. R.N. Wiener & E.R. Nixon - J. Chem. Phys. 26, 906 (1957).

92. G.M. Begun & W.H. Fletcher - J. Mol. Spectry 4, 388 (1960).

93. W.G. Fateley, H.A. Bent, B. Crawford Jr - J. Chem. Phys. 31, 204 (1959).

94. I.C. Hisatsune & J.P. Devlin - J. Chem. Phys. 31, 1130 (1959).

95. I.C. Hisatsune, J.P. Devlin & Y. Wada - J. Chem. Phys. 33, 714 (1960).

96. P. Groth & O. Hassel - Proc. Chem. Soc. 379 (1962).

97. P. Groth - Nature 198, 1081 (1963).

98. P. Groth - Acta Chem. Scand. 17, 2419 (1963).

99. B.S. Cartwright & J.H. Robertson - Chem. Commun. 82 (1966).

100. B.W. McClelland, G. Gundersen & K. Hedberg - J. Chem. Phys. 56, 4541 (1972).

101. P.A. Giguère & V. Schomaker - J. Amer. Chem. Soc. 65, 2025 (1943).

102. A. Yamaguchi, I. Ichishima, T. Shimanouchi & S. Mizushima - J. Chem. Phys. 31, 843 (1959).

103. M.M. Gilbert, G. Gundersen & K. Hedberg - J. Chem. Phys. 56, 1691 (1972).

104. I.C. Hisatsune - J. Phys. Chem. 65, 2249 (1961).

105. A. Guttman & S.S. Penner - J. Chem. Phys. 36, 98 (1962).

106. W.F. Giauque & J.D. Kemp - J. Chem. Phys. 6, 40 (1938).

107. M. Szwarc - Proc. Roy. Soc. (London) A 198, 267 (1949).

108. F.W. Dalby - Canad. J. Phys. 36, 1336 (1958).

109. G.G. Havens - Phys. Rev. 41, 337 (1932).

110. O. Chalvet & R. Daudel - Comptes Rendus Acad. Sci. Paris 231, 855 (1950).

111. O. Chalvet & R. Daudel - J. Phys. Chem. 56, 365 (1952).

112. J. Mason - J. Chem. Soc. 162, 1288 (1959).

113. A.H. Brittain, A.P. Cox & R.L. Kuczkowski - Trans. Faraday Soc. 65, 1963 (1969).

114. G. Herzberg - "Molecular Spectra and Molecular Structure, III, Electronic Spectra and Electronic Structure of

Polyatomic Molecules" p325 (D. van Nostrand Co. Inc. Princeton, N.J., 1966).

115. M. Green & J.W. Linnett - Trans. Faraday Soc. 57, 10 (1961).

116. R. Le Goff & J. Serre - Theoret. Chim. Acta 1, 66 (1962).

117. G. Leroy, M. van Meersche & G. Germain - J. Chim. Phys. 1282 (1963).

118. H.A. Bent - Inorg. Chem. 2, 747 (1963).

119. E.B. Moore Jr - J. Chem. Phys. 43, 503 (1965).

120. E.B. Moore Jr - Theoret. Chim. Acta 7, 144 (1967).

121. R.D. Brown & R.D. Harcourt - Proc. Chem. Soc. 216 (1961).

122. R.D. Brown & R.D. Harcourt - Aust. J. Chem. 16, 737 (1963).

123. R.D. Brown & R.D. Harcourt - Aust. J. Chem. 18, 1115 (1965).

124. R.D. Brown & R.D. Harcourt - Aust. J. Chem. 18, 1885 (1965).

125. T.H. Redmond & B.B. Wayland - J. Phys. Chem. 72, 3038 (1968).

126. R.D. Harcourt - Theoret. Chim. Acta 2, 437 (1964).

127. R.D. Harcourt - Theoret. Chim. Acta 6, 131 (1966).

128. R.D. Harcourt - Intern. J. Quantum Chem. 4, 173 (1970).

129. R.D. Harcourt - Aust. Sci. Teachers J. 14, 55 (1968).

130. R.D. Harcourt - J. Chem. Ed. 45, 779 (1968).

131. R.D. Harcourt - Aust. J. Chem. 22, 279 (1969).

132. R.D. Harcourt - J. Mol. Struct. 8, 11 (1971).

133. R.D. Harcourt - J. Mol. Struct. 9, 221 (1971).

134. R.D. Brown & M.L. Heffernan - Trans. Faraday Soc. 54, 757 (1958).

135. C.A. Coulson - "Valence" p187 (Oxford Univ. Press:

London, 1961).

136. G.R.J. Williams - Private Communication.

137. F.A. Cotton - "Chemical Applications of Group Theory" (Interscience, New York, 1963).

138. A.L.H. Chung & G.L. Goodman - J. Chem. Phys. 56, 4125 (1972).

139. F.P. Billingsley II - Intern. J. Quantum Chem. 6, 617 (1972).

140. D.H. Sleeman - Theoret. Chim. Acta 11, 135 (1968).

141. J. Koutecky & V. Bonacic-Koutecky - J. Chem. Phys. 55, 2408 (1971).

142. J. Koutecky & V. Bonacic-Koutecky - Chem. Phys. Lett. 15, 558 (1972).

143. R. McWeeny - Proc. Roy. Soc. A 235, 496 (1956).

144. M. Simonetta & Gianinetti - p83 of ref.2.

145. J. Kowalik & M.R. Osborne - "Methods for Unconstrained Optimization Problems" (Amer. Elsevier Pub. Coy. New York, 1968).

146. R. Fletcher - Mol. Phys. 19, 55 (1970).

147. T.A. Claxton & N.A. Smith - Theoret. Chim. Acta 22, 399 (1971).

148. T.E.H. Walker - Chem. Phys. Lett. 9, 174 (1971).

149. T.E.H. Walker - Theoret. Chim. Acta 25, 1 (1972).

150. R. McWeeny - Proc. Roy. Soc. (London) A 241, 239 (1957).

151. G. Berthier & P. Millie - Intern. J. Quantum Chem. 25, 67 (1968).

152. J.L. Dodds & R. McWeeny - Chem. Phys. Lett. 13, 9 (1972).

153. T.A. Koopmans - Physica 1, 104 (1933).

154. W.G. Richards - J. Mass Spectrometry and Ion Physics 2, 419 (1969).

155. L.L. Shipman & R.E. Christoffersen - Chem. Phys. Lett. 15, 469 (1972).

156. R. Kari & B.T. Sutcliffe - Chem. Phys. Lett. 7, 149 (1970).

157. C.C.J. Roothaan & P.S. Bagus - "Methods in Computational Physics" 2, 62 (1963).

158. J.A. Pople & R.K. Nesbet - J. Chem. Phys. 22, 571 (1954).

159. A.T. Amos & G.G. Hall - Proc. Roy. Soc. (London) A 263, 483 (1961).

160. G. Berthier - p.57 of ref.2.

161. J. Goodisman & W. Klemperer - J. Chem. Phys. 38, 721 (1963).

162. R.S. Mulliken - J. Chem. Phys. 23, 1833,1841,2338,2343 (1955).

163. S. Fraga & G. Malli - "Many Electron Systems: Properties and Interactions", p71 (W.B. Saunders Coy, 1968).

164. P. Politzer & R.S. Mulliken - J. Chem. Phys. 55, 5135 (1971).

165. H. Weinstein, R. Pauncz & M. Cohen - Advances in Atomic and Molecular Physics 7, 97 (1971).

166. W. England, L.S. Salmon & K. Ruedenberg - Fortschr. Chem. Forsch 23, 31 (1971).

167. J.M. Foster & S.F. Boys - Revs Mod. Phys. 32, 300 (1960).

168. S.F. Boys - "Quantum Theory of Atoms, Molecules and the Solid State" - Ed. P.O. Löwdin, p253 (1966).

169. C. Edmiston & K. Ruedenberg - Revs Mod. Phys. 35, 457 (1963).

170. E. Clementi - Intern. J. Quantum Chem. 3S, 179 (1969).

171. E. Clementi & W. von Niessen - J. Chem. Phys. 54, 521 (1971).

172. E. Clementi & A. Routh - Intern. J. Quantum Chem. 6, 525 (1972).

173. E. Clementi & H. Popkie - J. Amer. Chem. Soc. 94, 4057 (1972).

174. C.C.J. Roothaan - Lab. of Molecular Structure and Spectra, Univ. of Chicago, Tech. report 24 (1955).

175. C. Petrongolo, E. Scrocco & J. Tomasi - J. Chem. Phys. 48, 407 (1968).

176. R. Bonaccorsi, C. Petrongolo, E. Scrocco & J. Tomasi - J. Chem. Phys. 48, 1497 (1968).

177. J.D. Hinchen - "Practical Statistics for Chemical Research" (Science Paperbacks, 1969).

178. A.C. Wahl - J. Chem. Phys. 41, 2600 (1964).

179. J.F. Larcher & J.W. Linnett - Theoret. Chim. Acta 12, 127 (1968).

180. W.H. Fink, D.C. Pan & L.C. Allen - J. Chem. Phys. 47, 895 (1967).

181. S.D. Peyerimhoff & R.J. Buenker - J. Chem. Phys. 49, 2473 (1968).

182. M.R. Hestenes & E. Stiefel - J. Res. N.B.S. 49, 409 (1952).

183. F.S. Beckman - "Mathematical Methods for Digital Computers" p62, Eds A. Ralston & H.S. Wilf (Wiley, 1960).

184. R. Fletcher & C.M. Reeves - Computer J. 7, 149 (1964).

185. W.C. Davidon - "Variable Metric Method for Minimization" - A.E.C. Research and Development Report ANL - 5990 (rev.), (1959).

186. R. Fletcher & M.J.D. Powell - Computer J. 6, 163 (1963).

187. R. Fletcher - J. Inst. Maths Applics 5, 162 (1969).